

**Improved Mathematical Model for Sheet Reheat  
Phase in Thermoforming Process**

**Sohail Akbar Khan**

**A Thesis  
in  
The Department  
of  
Mechanical and Industrial Engineering**

**Presented in Partial Fulfillment of the Requirements  
for the Degree of Master of Applied Science (Industrial Engineering)  
at  
Concordia University  
Montreal, Quebec, Canada**

**August 2009**

© Sohail Akbar Khan, 2009



Library and Archives  
Canada

Published Heritage  
Branch

395 Wellington Street  
Ottawa ON K1A 0N4  
Canada

Bibliothèque et  
Archives Canada

Direction du  
Patrimoine de l'édition

395, rue Wellington  
Ottawa ON K1A 0N4  
Canada

*Your file* *Votre référence*  
*ISBN: 978-0-494-63122-5*  
*Our file* *Notre référence*  
*ISBN: 978-0-494-63122-5*

**NOTICE:**

The author has granted a non-exclusive license allowing Library and Archives Canada to reproduce, publish, archive, preserve, conserve, communicate to the public by telecommunication or on the Internet, loan, distribute and sell theses worldwide, for commercial or non-commercial purposes, in microform, paper, electronic and/or any other formats.

The author retains copyright ownership and moral rights in this thesis. Neither the thesis nor substantial extracts from it may be printed or otherwise reproduced without the author's permission.

---

In compliance with the Canadian Privacy Act some supporting forms may have been removed from this thesis.

While these forms may be included in the document page count, their removal does not represent any loss of content from the thesis.

**AVIS:**

L'auteur a accordé une licence non exclusive permettant à la Bibliothèque et Archives Canada de reproduire, publier, archiver, sauvegarder, conserver, transmettre au public par télécommunication ou par l'Internet, prêter, distribuer et vendre des thèses partout dans le monde, à des fins commerciales ou autres, sur support microforme, papier, électronique et/ou autres formats.

L'auteur conserve la propriété du droit d'auteur et des droits moraux qui protègent cette thèse. Ni la thèse ni des extraits substantiels de celle-ci ne doivent être imprimés ou autrement reproduits sans son autorisation.

---

Conformément à la loi canadienne sur la protection de la vie privée, quelques formulaires secondaires ont été enlevés de cette thèse.

Bien que ces formulaires aient inclus dans la pagination, il n'y aura aucun contenu manquant.

  
**Canada**

## **Abstract**

### **Improved Mathematical Model for Sheet Reheat Phase in Thermoforming Process**

**Sohail Akbar Khan**

Thermoforming is widely used industrial manufacturing process in which tub-shaped components are manufactured by heating a plastic sheet in the oven and formed to the desired shape through vacuum or pressure. Heating of the sheet is the most important phase which determines product quality and process efficiency. In order to automate the process to improve the product quality and process efficiency, the development of a mathematical model of heat propagation to the sheet and inside the sheet is imperative. Heat transfer takes place through the combination of convection, conduction and radiation energy, which conducts and absorbed inside the sheet and greatly depends on material properties, oven air temperature and velocity and sheet color. A mathematical model based on variable material properties including density, specific heat and thermal conductivity is developed and validated against experimental data. The effect of both oven air temperature and velocity is studied by simulating the already developed and validated variable properties mathematical model for different values of oven air velocity and temperature. The sheet color effect is also studied by considering two extreme cases of black color sheet and white color sheet and validated by simulating the models and comparing the results against experimental data. The sheet heating model based on exact solution to conduction equation with constant material properties and convection heat as boundary condition is also developed and validated against experimental data.

## **Résumé**

### **Improved Mathematical Model for Sheet Reheat Phase in Thermoforming Process**

**Sohail Akbar Khan**

Le thermoformage est largement utilisé dans les processus de fabrication industrielle dans lequel les composants qui ont la forme d'une baignoire sont fabriqués par réchauffement d'une feuille de plastique dans un four, puis mis en formes désirées par l'application du vide ou pression.

Le chauffage de la feuille est la phase la plus importante qui détermine la qualité du produit et l'efficacité du processus. Dans le but d'automatiser le processus afin d'améliorer la qualité du produit et l'efficacité du processus, le développement d'un modèle mathématique de la propagation de chaleur à la feuille et son intérieur est impératif.

Le transfert de chaleur s'effectue à travers la combinaison de la convection, la conduction, et la radiation d'énergie, ce qui résulte sa conduction et absorption dans la feuille, tout en dépendant des propriétés matérielles, la température de l'air du four, la vitesse et la couleur de la feuille. Un modèle mathématique basé sur des propriétés des matériaux variables, y compris la densité, la chaleur spécifique, et la conductivité thermique, est développé et validé avec des données expérimentales.

L'effet de la température du four et la vitesse, est étudié par la simulation des propriétés variables du modèle mathématique, déjà développées et validées, pour des différentes valeurs de température et vitesse. L'effet de la couleur de la feuille est aussi étudié en considérant deux cas extrêmes ; la couleur noire et couleur blanche, et validé par la simulation de ces modèles avec des données expérimentales.

Le modèle de chauffage de la feuille qui est basé sur la solution exacte de l'équation de conduction avec des propriétés du matériel et convections de chaleur constantes comme condition limites, est aussi développé et validé avec des données expérimentales.

## Acknowledgments

I would like to thank my supervisors, Dr. Nadia Bhuiyan Department of Mechanical and Industrial Engineering, Concordia University and Dr. Vince Thomson, Department of Mechanical Engineering, McGill University, for their admirable supervision during my research years. I would like to express my gratitude for the technical and non-technical advice and support during my M.A.Sc. I would also like to thank Mr. Patrick Girard, Industrial Material Institute-NRC, for his continuous guidance, creative suggestions and help during experimental work. I am pleased to thank Dr. Benoit Boulet, Department of Electrical, McGill University, Montreal, Canada for his guidance during my research.

I would like to thank Mr. Mark Andre Rainville at IMI-NRC for his constant and tireless help during experimental work. I wish to acknowledge the cooperation offered by Industrial Material Institute (IMI), National Research Council Canada (NRC). I would like to recognize the help and support offered by the research officers in IMI, the professors, staffs, and peers at Concordia and McGill University.

I am pleased to thank Mr. Salman Saeed at McGill University for consistent help in computer programming and simulation. I thank my family and friends outside university for moral support throughout my master's degree.

## **Dedication**

This work is dedicated to my family, parents and friends for their continuous support at every step during my studies.

# TABLE OF CONTENTS

<b>LIST OF FIGURES.....</b>	<b>xi</b>
<b>LIST OF TABLES.....</b>	<b>xvi</b>
<b>CHAPTER 1 INTRODUCTION .....</b>	<b>1</b>
1.1 MOTIVATION.....	1
1.2 ORGANIZATION OF THESIS .....	3
<b>CHAPTER 2 PROBLEM DEFINITION .....</b>	<b>4</b>
2.1 PROBLEM DEFINITION .....	5
2.2 THESIS OBJECTIVE .....	8
2.2.1 <i>Sheet Color Based Model</i> .....	8
2.2.2 <i>Sheet Heating Model with Variable Material Properties</i> .....	9
2.2.3 <i>Sheet Heating Model with Exact Solution to the Conduction Equation</i> .....	9
2.2.4 <i>Effect of Convection Coefficient on Heating Process</i> .....	10
<b>CHAPTER 3 THERMOFORMING PROCESS .....</b>	<b>11</b>
3.1 HISTORY .....	11
3.2 ADVANTAGES OF THERMOFORMING .....	14
3.2.1 <i>Cost</i> .....	15
3.2.2 <i>New Product Development</i> .....	15
3.3 <i>Limitations of Thermoforming</i> .....	16
3.3.1 <i>Design Limitation</i> .....	16
3.3.2 <i>Process Limitations</i> .....	16
3.4 THERMOFORMING PROCESS DESCRIPTION .....	16
3.4.1 <i>Clamping</i> .....	17
3.4.2 <i>Heating</i> .....	18
3.4.3 <i>Forming</i> .....	21
3.4.4 <i>Trimming</i> .....	21

3.5 THERMOFORMING MATERIALS.....	21
3.6 THERMAL BEHAVIOR OF POLYMERS .....	23
<b>CHAPTER 4 HEAT TRANSFER THEORY.....</b>	<b>25</b>
4.1 CONDUCTION .....	25
4.1.1 <i>General Differential Equation of Conduction Heat Transfer</i> .....	27
4.1.2 <i>Transient Conduction</i> .....	29
4.1.3 <i>Thermal Conductivity</i> .....	31
4.2 CONVECTION.....	32
4.3 RADIATION.....	34
4.3.1 <i>Gray Body</i> .....	36
4.3.2 <i>Real Body</i> .....	36
4.3.3 <i>Radiation Shape Factor</i> .....	37
<b>CHAPTER 5 SHEET HEATING MODEL.....</b>	<b>40</b>
5.1 ANALYTICAL MODEL OF THE SHEET REHEAT PHASE.....	42
5.1.1 <i>Oven</i> .....	42
5.1.2 <i>Sheet</i> .....	44
5.1.3 <i>Methodology</i> .....	44
5.1.4 <i>Assumptions</i> .....	46
5.1.5 <i>Equations</i> .....	48
5.2 BASIC STEADY STATE MODEL .....	49
5.3 ABSORPTIVITY BASED STEADY STATE MODEL.....	52
5.4 SHEET COLOR BASED MODEL.....	56
5.4.1 <i>Heating Model for White Sheet</i> .....	57
5.4.2 <i>Heating Model for Colored Sheet</i> .....	57
5.5 SHEET HEATING MODEL WITH VARIABLE MATERIAL PROPERTIES .....	58
5.5.1 <i>Heat Capacity</i> .....	58
5.5.2 <i>Density</i> .....	63
5.5.3 <i>Thermal Conductivity</i> .....	63

5.5.4 Thermal Diffusivity.....	66
5.6 NUMERICAL MODELING .....	68
5.6.1 Model When Sheet Surface Temperature is known .....	69
5.6.2 Model When Sheet Surface Temperature is Not Known.....	70
5.7 SHEET HEATING MODEL WITH EXACT SOLUTION TO CONDUCTION EQUATION .....	71
5.8 CONVECTION HEAT COEFFICIENT AND ITS EFFECT ON THERMOFORMING .....	76
<b>CHAPTER 6 EXPERIMENTAL SETUP AND RESULTS .....</b>	<b>78</b>
6.1 IMI THERMOFORMING MACHINE.....	79
6.2 THERMOCOUPLES AND INFRARED SENSORS .....	81
6.3 EXPERIMENTS .....	81
6.3.1 White Sheet Experiments.....	81
6.3.2 Black Sheet Experiment.....	85
6.4 OVEN AIR TEMPERATURE .....	87
6.5 RESULTS AND DISCUSSION.....	88
6.5.1 Variable Material Properties Model.....	89
6.5.2 Sheet Heating Model with Exact Solution to the Heating Equation.....	92
6.5.3 Sheet Color Based Model.....	94
6.5.4 Effect of Convection Heating Coefficient on Sheet Reheat Phase.....	97
<b>CHAPTER 7 CONCLUSION .....</b>	<b>100</b>
7.1 FUTURE WORK.....	103
<b>REFERENCES .....</b>	<b>104</b>
<b>APPENDIX A: LIST OF SYMBOLS .....</b>	<b>107</b>
<b>APPENDIX B: MATLAB CODES FOR SIMULATION.....</b>	<b>108</b>
<b>APPENDIX C: EXPERIMENTAL RESULTS.....</b>	<b>122</b>

## List of Figures

Figure 2-1: Forming window .....	6
Figure 2-2: Sheet reheat with high heating .....	7
Figure 3-1: Brief outline of the history of thermoforming (Moore, 2002) .....	12
Figure 3- 2: Stages of Thermoforming Process (Kumar, 2005) .....	17
Figure 3- 3: Pneumatic Clamping Mechanism (Kumar, 2005).....	18
Figure 3- 4: IR Heating elements used in the Oven (Kumar, 2005).....	19
Figure 3- 5: Temperature effect on polymers (Groover, 1996) .....	23
Figure 4- 1: Nomenclature for one dimensional heat conduction analysis.....	27
Figure 4- 2: Nomenclature for Transient Heat Flow .....	30
Figure 4- 3: Convection heat transfer from wall (Holman, 1997) .....	34
Figure 4- 4: Radiation behavior of bodies, (Holman, 1997).....	36
Figure 4- 5: Radiation Shape Factor (Holman, 1997).....	37
Figure 4- 6: View Factor between two flat surfaces and the related solution, (Walter 2002). .....	39
Figure 5- 1: Heat energy distribution for thermoforming with double side heating of sheet. Concept derived from (Brinken, 1980).....	41
Figure 5- 2: Discretization of sheet.....	45
Figure 5- 3: Sheet Nodes.....	46
Figure 5- 4: Oven Zones .....	46
Figure 5- 5: Result for heating of HDPE sheet (Kumar, 2005). .....	48
Figure 5-6: Schematic presentation of the absorption terms in sheet model (Gauthier, 2005) .....	55
Figure 5- 7: Experimental heat capacity curves determined by different cooling rates obtained by varying fan speed and unadjusted Reynolds number (for bottom heating at 280°C) (Zhang, 2004) .....	60

Figure 5- 8: Experimental heat capacity curves determined by different cooling rates obtained by varying fan speed and unadjusted Reynolds number (for bottom heating at 320°C) (Zhang, 2004) .....	61
Figure 5- 9: Experimental heat capacity curves determined by different cooling rates obtained by varying fan speed and unadjusted Reynolds number (for bottom heating at 420°C) (Zhang, 2004) .....	61
Figure 5- 10: Experimental heat capacity curves by using Matlab program for the top .....	62
Figure 5- 11: HDPE thermal conductivity variation with temperature (Santos, 2005). .....	64
Figure 5- 12: HDPE fit for thermal conductivity.....	65
Figure 5- 13: Variation in Thermal Diffusivity with temperature for HDPE (Santos, 2005). .....	66
Figure 5-14: Fit for variation in thermal diffusivity with temperature .....	67
Figure 5-15: Sheet model for transient heating with neutral plane at the center .....	74
Figure 5-16: Transient heat transfer coefficient for the lower side of the sheet for transient and constant air temperature (Yousefi, 2002). .....	74
Figure 5-17: Transient heat transfer coefficient for the upper side of the sheet for transient and constant air temperature (Yousefi, 2002). .....	75
Figure 6- 1: AAA thermoforming machine at IMI (Benqiang, 2003) .....	79
Figure 6- 2: Ceramic heater elements of AAA machine (Benqiang, 2003).....	80
Figure 6- 3: Oven layout for AAA model MBE-2438 M thermoforming machine (Benqiang, 2003).....	80
Figure 6-4: Experimental setup of a HDPE BA 50 sheet (Benqiang, 2003) .....	83
Figure 6-5: Sheet after heating implanted with five thermocouples (Benqiang, 2003) .....	83
Figure 6-6: Length and depth of hole for thermocouple insertion (Benqiang, 2003). .....	84
Figure 6-7: Colored Sheet experimental setup.....	87

Figure 6-8: Comparison of simulation model results against experimental result. ....	90
Figure 6-9: Comparison of simulation model temperature against experimental result. .....	91
Figure 6-10: Comparison of simulation model and experimental results at different oven temperatures. ....	91
Figure 6-11: Difference of variable properties model and constant properties model at different oven temperatures. ....	92
Figure 6-12: Exact model simulation vs. experimental data.....	93
Figure 6-13: Colored Sheet combined models simulation vs. experimental data.....	95
Figure 6-14: Colored Sheet models simulation vs. experimental data .....	96
Figure 6-15: Average Temperature Difference at 8mm .....	96
Figure 6-16: Temperature difference for 100 °C oven temperature.....	97
Figure 6-17: Variation in sheet temperature for different values of convection Coefficient.....	98
Figure 6-18: Effect of convection coefficient on sheet temperature for different values of Oven temperatures. ....	99
Figure C-1: Comparison of simulation model temperature against experimental result at 11mm depth.....	122
Figure C-2: Comparison of simulation model temperature against experimental result at 9mm depth.....	122
Figure C-3: Comparison of simulation model temperature against experimental result at 6mm depth.....	123
Figure C-4: Comparison of simulation model temperature against experimental result at 3mm depth.....	123
Figure C-5: Comparison of simulation model temperature against experimental result at 1mm depth.....	124
Figure C-6: Comparison of simulation model temperature against experimental result at 1mm depth.....	124

Figure C-7: Comparison of simulation model temperature against experimental result at 3mm depth.....	125
Figure C-8: Comparison of simulation model temperature against experimental result 6mm depth .....	125
Figure C-9: Comparison of simulation model temperature against experimental result 9mm depth. ....	126
Figure C-10: Comparison of simulation model temperature against experimental result at 11mm depth.....	126
Figure C-11: Difference between variable properties model and experimental result .....	127
Figure C-12: Difference between variable properties model and experimental result .....	127
Figure C-13: Difference between variable properties model and experimental result .....	128
Figure C-14: <i>Difference between variable properties model and constant properties model.....</i>	128
Figure C-15: <i>Difference between variable properties model and constant properties model.....</i>	129
Figure C-16: Comparison of simulation model temperature against experimental result.....	129
Figure C-17: Comparison of simulation model temperature against experimental result.....	130
Figure C-18: Comparison of simulation model temperature against experimental result.....	130
Figure C-19: Comparison of simulation model and experimental results at different oven temperatures .....	131
Figure C- 20: Comparison of simulation model and experimental results at different oven temperatures .....	131
Figure C-21: Comparison of simulation model and experimental results at different oven temperatures .....	132

Figure C-22: Difference of variable properties model and constant properties model at different oven temperatures .....	132
Figure C-23: Difference of variable properties model and constant properties model at different oven temperatures .....	133
Figure C-24: Difference of variable properties model and constant properties model at different oven temperatures .....	133
Figure C-25: Exact model simulation vs. experimental data.....	134
Figure C- 26: Exact model simulation vs. experimental data.....	134
Figure C-27: Colored Sheet models simulation vs. experimental data.....	135
Figure C-28: Colored sheet models simulation vs. experimental data .....	135
Figure C-29: Colored Sheet models simulation vs. experimental data.....	136
Figure C-30: Colored Sheet models simulation vs. experimental data.....	136
Figure C- 31: Temperature difference for 100 °C oven temperature .....	137
Figure C-32:Variation in sheet temperature for different values of convection coefficient .....	137
Figure C-33:Variation in sheet temperature for different values of convection coefficient .....	138
Figure C-34: Effect of convection coefficient on sheet temperature for different values of Oven temperatures.....	138
Figure C-35: Effect of convection coefficient on sheet temperature for different values of Oven temperatures.....	139

## List of Tables

Table 3-1: Thermoforming Applications .....	13
Table 3- 2: Heating elements .....	20
Table 3-3:Characteristic temperatures of polymers used in thermoforming .....	24
Table 6-1: Material properties of HDPE BA-50.....	82
Table 6-2: Experimental design .....	85
Table 6-3: Material properties of HDPE for Black Sheet.....	86
Table 6-4: Experimental Oven air temperatures .....	88

# **Chapter 1 Introduction**

Thermoforming is a term generally used for the process in which tub-shaped plastic parts are manufactured from a flat plastic sheet. The thermoforming process can be divided into three main stages: 1) sheet heating, 2) forming, and 3) cooling. In the heating stage, a flat plastic sheet is heated in an oven until the material is soft and pliable. In the second stage, the sheet is formed to a mold using pressure and/or vacuum forces to achieve the desired shape. In the third and final stage, the formed part is left in mold to cool down and become rigid enough to be removed from the mold.

## **1.1 Motivation**

The thermoforming process is important for many industries, including the automotive industry, residential building construction, appliances, the marine industry, recreational vehicles and watercraft, signs and displays for the retail sector, and this list is growing. Despite the fact that the thermoforming process is one of the most widely used industrial processes, not much work has been done in terms of its automation and control. The Industrial Material Institute in Montréal took an initiative in 2001 and formed a research group with McGill University in order to study the thermoforming process with specific emphasis on the sheet heating stage. A series of experiments have been performed to understand the dynamics of the process and to develop a controller for the thermoforming sheet heating phase in order to improve process control. The motivation for better control is to improve the product quality and process efficiency.

The material distribution during the forming stage can be manipulated through better control of temperature distribution in depth and across the surface of the sheet during the reheat stage. This results not only in improved quality of the part in terms of surface finish and tolerance limits but also results in a reduction in the number of rejected parts for a given production cycle. The reduction in rejected parts means improvement in production efficiency and a decrease in material costs. This is particularly important for products manufactured from very expensive plastic materials. Also, a better understanding of the reheat phase will allow for more aggressive sheet temperature trajectories and thus shorter heating time to make each part. This also contributes positively to production efficiency.

Another motivation for developing a control system for the sheet reheat stage is to decrease energy consumption by generating optimal (in terms of energy) control signals that will achieve the desired sheet temperature profile. This aspect is important since thermoforming is generally an energy intensive process and energy, or heating costs, are often the most significant operating expense for a thermoforming operation.

Finally, real time control of the sheet reheat stage also provides an opportunity to reduce the machine maintenance. Naturally with the use of oven heating elements, their performance deteriorates as a whole and also individual heating elements deteriorate at different rates. The optimal use of heating elements will prolong the heating element's life by reducing unnecessary use of elements and hence reduce the maintenance cost.

## **1.2 Organization of Thesis**

In this thesis, Chapter 2 is dedicated to defining the problem and highlighting briefly previous works that are performed in this area. This sets the groundwork for objectives of this research which are then presented briefly. In Chapter 3, the thermoforming process is described in detail to understand the process dynamics and related issues. Also, the industrial scope, related materials and future prospects of the thermoforming process is discussed briefly. Chapter 4 describes the heat transfer theory which is the basis for understanding and developing the mathematical model of the thermoforming process. It was learned from experience that in order to improve the production rate and product quality and to develop a better control system, one has to understand and improve the existing mathematical model for sheet heating phase of the thermoforming process. Chapter 5 describes the detailed modeling of the heating process, the proposed models' development procedure and material properties that are prone to change with temperature during the heating of the sheet. Chapter 6 presents the details on the experimental setup, machines, equipments and results. Results of proposed models simulated in Matlab are compared against the experimental data that is collected from industrial standard thermoforming machines. Chapter 7 presents conclusion of thesis and the future work needed in this area.

## Chapter 2 Problem Definition

The appropriate mathematical model is the first step in developing a real time control system for any process. The most important step in developing a mathematical model for a process is to understand the parameters that govern the process. The basic governing parameters for the thermoforming process are heat energy transfer properties, sheet material properties and process conditions. Over the years, researchers have studied the different aspects of these parameters. Some of important works are summarized here. Brinken (1980) worked out the heat energy distribution in the heating phase for one side sheet heating. He also determined that the color of the sheet has no significant effect on sheet temperature distribution. Throne (1996) analyzed modeling of heat transfer in semitransparent polymers for thermoforming application by addressing the wave length dependency of sheet absorptivity and heater emissivity. Monteix *et al.* (2001) determined the spectral properties of infrared emitters that are important factors in determining the optimal heating rate. Chang (2005) applies neural networks to the thermoforming process with end product dimension as input and process parameters as output and found satisfactory results. Thomas (2005) developed a sheet heating cycle profile for different size, and thicknesses of material. Thomas (2005) also developed minimized cycle times for the different sheets and discussed different heater systems and found that quartz heaters give better results for cycle minimization then ceramic heaters.

Yousafi *et al.* (2002) for the first time carried out a sensitivity analysis and showed that the sensitivity of the sheet temperature to each processing parameter was dynamic in

nature during reheat. The parameter highly affecting the sheet surface temperature was the temperature of the radiant heater. The emissivity of the radiant heater, the view factor, and the polymer specific heat were the other parameters significantly affecting the reheat phase. His work demonstrated that the prediction of the sheet reheat phase could be significantly improved by implementing appropriate input parameters. Zhang (2004) developed the component libraries for the thermoforming process which contains materials and equipments used in the process. Kumar (2005) worked on the estimation of absorptivity of the sheet and heat fluxes between the heating elements and sheet during the thermoforming process. Benqiang (2003) developed a soft sensor system for the estimation of sheet internal temperature distribution in the thermoforming process. Moore (2002) developed the  $H_\infty$  control system for the sheet reheat phase but found that the results are not satisfactory due to slow heater elements response. Ajersch (2004) and Gauthier (2005) worked on developing a real time controller by using a state space model of the thermoforming process and found satisfactory results.

## **2.1 Problem Definition**

The forming of plastic sheets is only possible in a certain temperature range defined by the upper temperature limit,  $T_{upper}$  and the lower temperature limit,  $T_{lower}$ , and the difference between these two temperatures is called the forming window, as shown in Figure 2.1.

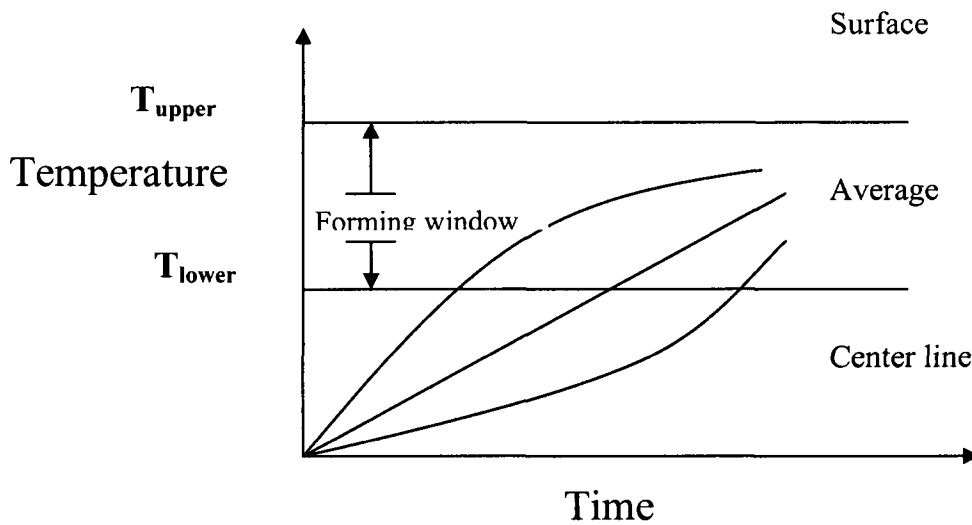


**Figure 2-1: Forming window**

The end product quality can be affected in terms of surface finish, color and tolerance limits if the polymer is heated above  $T_{upper}$  and then formed, while if formed when the sheet temperature is below  $T_{lower}$ , it will be too stiff to form and may develop surface cracks or spring back effects. Thus the lower and upper forming temperatures define the absolute boundaries of formability for the thermoforming process.

The mechanism for sheet heating is that the heat energy is absorbed by the sheet surface through both radiation and convection. This absorbed energy at the sheet surface is then propagated to the interior of the sheet through conduction which is a far slower process in terms of the rate of heat propagation than the radiation. It is due to slow thermal diffusive characteristics of plastic materials. Also a part of energy is absorbed by the interior of the sheet directly through radiation. The heating rate is determined by the fact that the difference between the sheet centerline temperature and surface temperature should

remain within the forming window and must be controlled to prevent deficient forming, material degradation and surface overheating. The effect of high heating rate is shown in Figure 2.2.

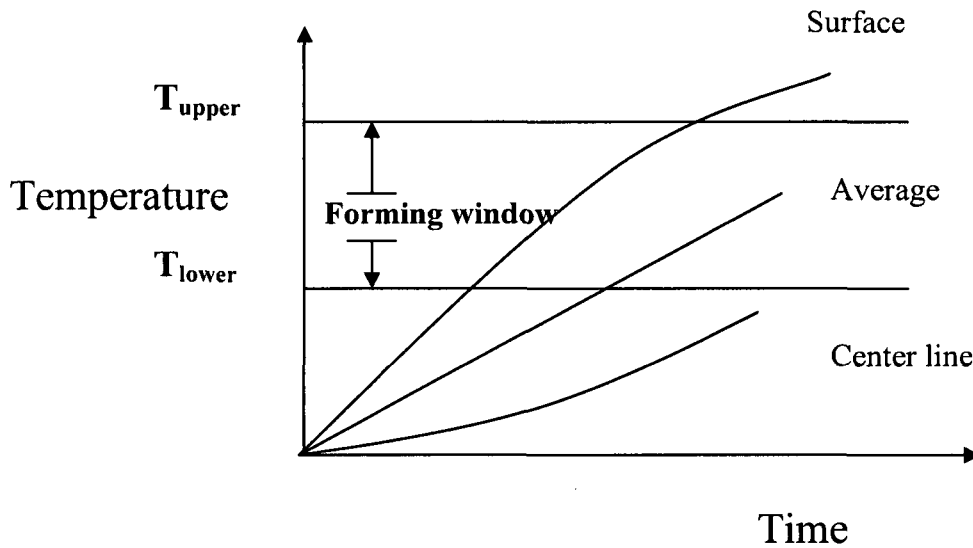


**Figure 2-2:** Sheet reheat with high heating

The desire of decreasing cycle time by increasing the heating rate is restricted by the fact that the conduction is a slower heat propagation process than radiation heating. In heating a thin sheet, the difference between the sheet surface and center temperature remains small enough to not cause any problems and can be considered the same for practical purposes. But the problem of maintaining the sheet temperature within the forming window escalates as the sheet thickness increases. The “slowness” of conduction restricts the heat energy to propagate to the interior at the same rate as it is received at the surface and the temperature difference increases between the surface and interior of the sheet. This problem can only be resolved by decreasing the sheet heating rate but it affects the production efficiency. In order to achieve the maximum production efficiency, it is

imperative to heat the sheet by using the optimum heating rate. The optimum heating rate can be found by understanding the heating process and developing an accurate mathematical model to get an insight into the process dynamics.

Sheet color is another factor that affects the sheet heating rate. The conduction becomes more and more dominant as the sheet color gets darker and the heating rate needs to be adjusted accordingly.

## **2.2 Thesis Objective**

The objective of this thesis is to develop mathematical models for the sheet reheat phase in order to predict optimum heating rates for different situations and to study the effect of the convection coefficient on the heating process. The following different cases are taken into consideration:

1. Sheet color based model.
2. Sheet heating model with variable material properties.
3. Sheet heating model with exact solution to the conduction equation.
4. Effect of convection coefficient on heating process.

### **2.2.1 Sheet Color Based Model**

The mathematical models developed to date are based on considering the sheet as transparent or semi-transparent. But in industry, many parts are made from colored sheets. As the color of the sheet becomes darker, it starts behaving more like opaque material and conduction becomes the dominant heat transfer method. As conduction is a “slower” process than the radiation, the heating rate needs to be adjusted accordingly. In

order to study the affect of color on heating rate, two extreme cases are considered. In first case, the sheet is considered as 100% transparent and a model is developed with only radiation as responsible for heating of the sheet interior, while in the second model, the sheet is considered as 100% opaque and a model is developed with only conduction as responsible for heating of the sheet interior. These two models are then simulated and compared with the experimental data to validate the model.

### **2.2.2 Sheet Heating Model with Variable Material Properties**

The sheet heating models developed to date are based on the assumption that the sheet material properties remain constant with temperature. In fact, the sheet material properties like density, thermal conductivity, diffusivity and heat capacity are all a function of temperature and vary with temperature. In this work a sheet heating model is developed with density, thermal conductivity, diffusivity and heat capacity as a function of temperature. This model is then simulated in Matlab and the results are compared with the experimental results in order to validate the model.

### **2.2.3 Sheet Heating Model with Exact Solution to the Conduction Equation**

The models that were developed before or described above all use numerical solution to the differential heat equation. This model is developed by considering the exact solution to the heat differential equation by assuming constant material properties and convection heating as boundary conditions. The results are then compared with the experimental data to validate the model.

#### **2.2.4 Effect of Convection Coefficient on Heating Process**

Convection heat transfer is one of the three main heating processes that are responsible for heat transfer to the sheet surface during heating phase in thermoforming process. The convection heat transfer largely depends on convection coefficient which is determined by air velocity in the thermoforming oven. Thermoforming ovens are open from both ends to facilitate sheet feeding to the oven and therefore are susceptible to any air movement in oven vicinity. In order to understand the impact, a study of effect of convection coefficient is performed by simulating the models for different values of convection coefficient.

## **Chapter 3 Thermoforming Process**

Thermoforming can be described as a process of molding thermoplastic sheets to form three-dimensional shapes. Thermoplastic sheets are clamped in a frame, heated to make them soft, and then under some kind of pressure, the sheet is molded to conform to the contours of a mold. When the polymer sheet is held against the surface of the mold, cold air is used to solidify the part. Finally, the mold is taken away and the excess plastic is trimmed away.

Thermoforming has two main divisions, thin gauge and thick gauge. Thin gauge sheets are used to produce low cost products like packaging, bottles, etc. These sheets are produced in rolls, whereas heavy gauge plastic sheets are used to produce equipment parts, automobile parts and housings, etc.

### **3.1 History**

The process of thermoforming is not new. It has been used in one form or another to satisfy various needs over time. Centuries ago, the ancient Egyptians heated tortoise shells in hot oil to form food containers and bowls while ancient Americans heated natural cellulose in hot water and produced canoes. In the mid 19<sup>th</sup> century, J.W. Hyatt developed celluloid. It was a plastic material used to commercially produce various items for daily use. However, the modern age of thermoforming began at the start of the Second World War with the development of synthetic rubber. The industrial boom in the early 50s saw the start of the packaging industry as shown in Figure 3.1.

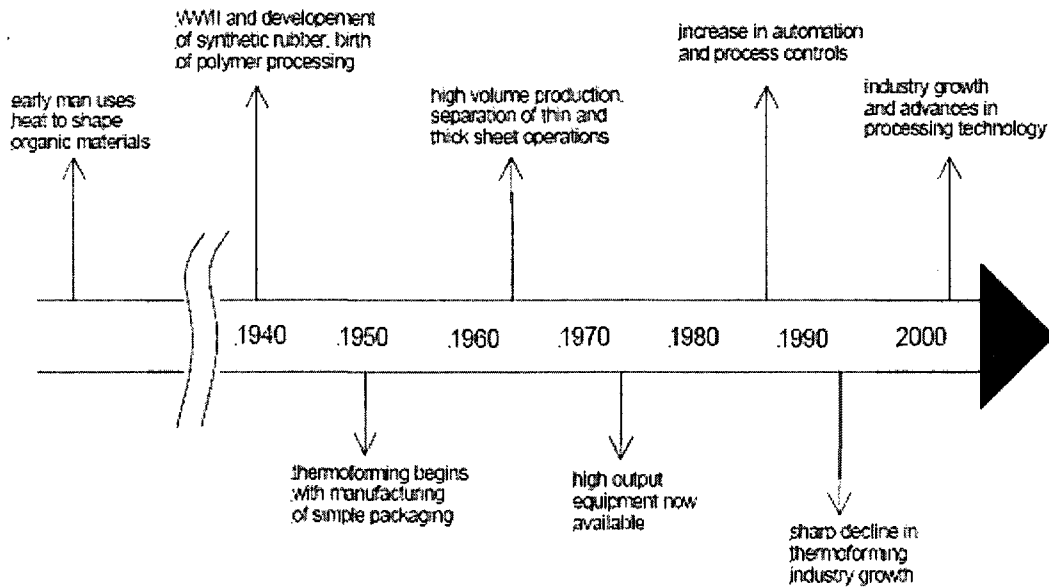


**Figure 3-1:** Brief outline of the history of thermoforming (Moore, 2002)

Hence, thermoforming got a boost and packaging became a growing industry. In the 60s, the thermoforming process lacked sophistication and plastic goods were considered junk. However, the development of technology and advances in material science helped the plastic industry to produce high quality products like thermoformed polymer shields used by astronauts. The success of thermoformed items compelled manufacturers to refine the process so as to cut cost and improve quality. At this time, more automated operations and techniques were introduced to reduce scrap.

Today, thermoforming is a rapidly growing processing method because of the variety and relatively low cost production of various items. Furthermore, tools and equipment required for thermoforming are less expensive compared to other processes. The range of thermoformed items is increasing day by day because thermoforming is more cost

effective compared to other processes involving higher upfront capital cost. Major areas of thermoformed products are industrial packaging, automobiles, electronics, medical and sports goods, food handling and wine transportation. A list of applications is presented in Table 3.1. Attempts are ongoing to make the process environmental friendly to address the related environmental issues.

**Table 3-1: Thermoforming Applications (Kumar, 2005)**

<p><b>Packaging and Related Items</b></p>	<p><i>Blister Packs, Point-of-Purchase</i>  <i>Bubble Packs, Slip Sleeve, Vacuum Carded</i>  <i>Electronics, Audio/Video Cassette Holders</i>  <i>Tools, Hand, Power</i>  <i>Cosmetics, Cases, Packages</i>  <i>Foams, Meat, Poultry Trays</i>  <i>Unit Serving, Foodstuffs</i>  <i>Convenience, Carryout, Cook-in-Box</i>  <i>Convertible-Oven Food Serving</i>  <i>Wide-Mouth Jars</i>  <i>Vending Machine Hot Cup</i>  <i>Egg Cartons, Wine Bottle Protectors</i>  <i>Produce Separators (Apples, Grapefruit)</i>  <i>Portion, Unit Dose Drugs</i>  <i>Form-Fill-Seal (Jelly, Crackers)</i></p>
<p><b>Vehicular</b></p>	<p><i>Automotive Door Inner Liners</i>  <i>Automotive Utility Shelves, Liners</i>  <i>Snow-Mobile Shrouds, Windshields</i>  <i>Motorcycle Windshields, Scooter Shrouds, Mudguards</i>  <i>All-Terrain Vehicle Exterior Components</i>  <i>Golf Cart Shrouds, Seats, Trays</i>  <i>Tractor Shrouds, Door Fascia</i></p>

	<i>Camper Hardtops, Interior Components (Doors, etc.)  Truck Cab Door Fascia, Instrument Cluster Fascia  Recreational Vehicle Interior Components, Window  Blisters</i>
<b>Industrial</b>	<i>Tote Bins  Pallets  Parts Trays, Transport Trays  Equipment Cases</i>
<b>Building Products</b>	<i>Shutters, Window Fascia  Skylights, Translucent Domes  Exterior Lighting Shrouds  Storage Modules, Bath, Kitchen, Pantry  Bath and Shower Surrounds (GR-UPE backed)  Soaking Tubs (GR-UPE Backed)  Retrofit Shower Components, Shower Trays</i>
<b>Miscellaneous</b>	<i>Exterior Signs  Advertising Signs, Lighted Indoor Signs  Swimming and Wading Pools  Trays, Baskets, Hampers, Carrying Cases  Luggage  Boat Hulls, Surf-Boards (with PUR Foams)  Animal Containers  Prototype Concepts for Other Plastic Processes</i>

### 3.2 Advantages of Thermoforming

In this manufacturing era which is categorized by high competition on price, time to market and product innovation, industry is looking for a process that can give them a

competitive advantage. Thermoforming is a good candidate to satisfy these needs due to the following attributes.

### **3.2.1 Cost**

Thermoforming is an efficient and cost effective process to produce plastic parts. The initial cost to set up a project is much lower if compared with other processes, e.g., injection molding. Due to high production rates approaching about 100,000 pieces per hour, low set up times, simple and few process steps and low tooling cost, the running cost is also comparatively low. A wide range of product sizes and specifications can be accommodated in a thermoforming process without considerable addition to cost in terms of tooling and process.

### **3.2.2 New Product Development**

In today's market, innovation and time to launch a new product are very important. The thermoforming process greatly facilitates new product development in two respects:

- First, it is easy to produce a new prototype as very few new tools are required. Only a new mold and clamping devices may be needed. The process can be easily and readily adapted to new sizes and new materials.
- Second, the time required to adapt the changes necessary for a new product is comparatively small. No tool path or process planning is required. Modern technology makes it very quick and cheap to get a new mold and other related devices. Also modern techniques and advances in the control of the thermoforming process enhance the accuracy and control of the process to ensure the required product quality level in fewer trials.

### **3.3 Limitations of Thermoforming**

Like every process, thermoforming has some limitations that can be summarized as follows.

#### **3.3.1 Design Limitation**

Thermoforming is only suitable for open parts, i.e., parts that can be molded in an open die. Closed parts like automobile fuel tanks can be thermoformed by forming two sides of the tank separately and then fusing them together to get a “closed” fuel tank, where thermoforming is the only option. Thermoforming is also limited in producing very fine details due to the fact that sheet viscosity at thermoforming temperatures is high. It is also not suitable for the parts with very tight tolerances. Materials also pose a limitation as very few from the plastic family can be thermoformed.

#### **3.3.2 Process Limitations**

The major process weakness is reproducibility. Dimensions from part to part vary and it is difficult to achieve very tight tolerances. Reworking a part is not possible in most cases and the whole part needs to be discarded which can considerably increase waste. This can be a major concern when thermoforming parts from expensive plastic sheets.

### **3.4 Thermoforming Process Description**

In the thermoforming process, the sheet is heated in an oven so that it becomes soft and is then formed to the desired shape by applying force as shown in Figure 3.2. Thermoforming consists of five phases: clamping, heating, forming, cooling and trimming.

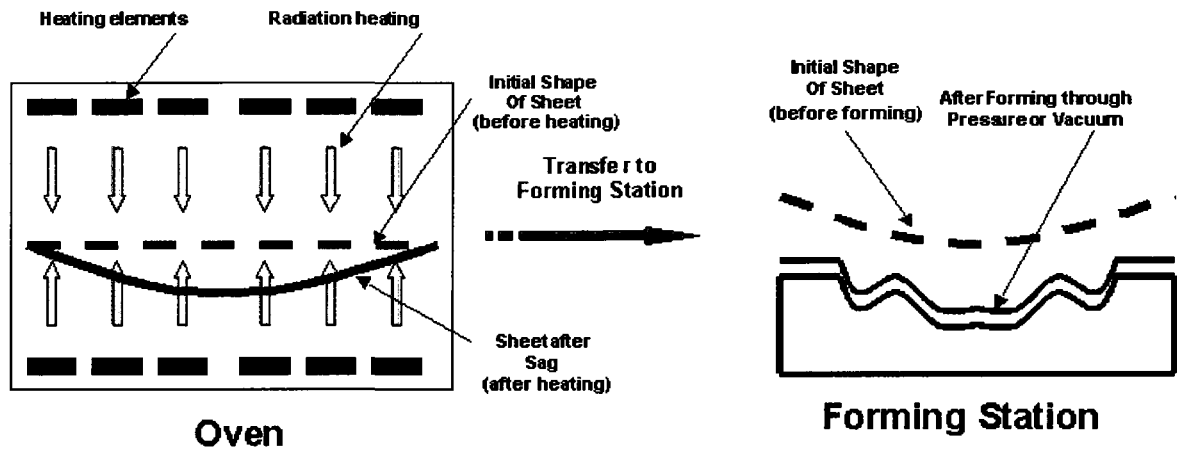


**Figure 3- 2: Stages of Thermoforming Process (Kumar, 2005)**

### 3.4.1 Clamping

In this phase a mechanism is used to hold the sheet to carry out the remaining four phases. It varies depending upon the gauge of the sheet. Thin gauge sheets are supplied in the form of rolls. Packaging items are produced through roll-fed machines. Parallel continuous loop pin chains are used for clamping. For thick sheets, clamping frames are used. It is a simpler mechanism as compared to thin gauge transport chains. The sheet is clamped between two frames. One is stationary and the other is hinged, which allows the sheet to be heated, formed and trimmed. A pneumatic clamping mechanism is shown in Figure 3.3.

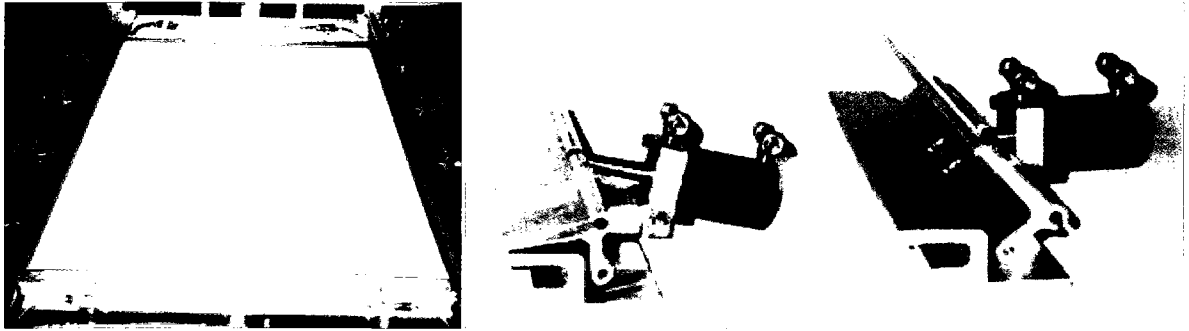
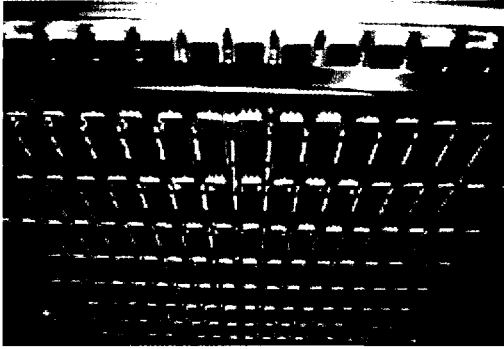


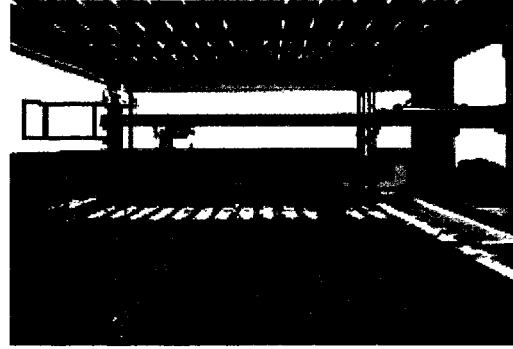
**Figure 3- 3: Pneumatic Clamping Mechanism (Kumar, 2005)**

### **3.4.2. Heating**

After clamping comes the next phase of heating the sheet. This phase is very critical because sheet needs to be heated evenly and properly. There are three ways to transfer heat to increase the sheet temperature: conduction, convection and radiation. Mostly radiant heat is used to increase the temperature of the plastic sheet properly to suit the forming. The plastic is heated through infrared radiation from one side or from both sides in a radiant heater. In one side heating, the sheet is heated either from top or bottom. The heat energy is received at the sheet surface facing heating elements through both radiation and convection. This energy then flows towards the other face of the sheet by combination of conduction and radiation. In both side of sheet heating, heater elements both at top and bottom faces of oven are used to heat the sheet. The heat flows from both faces towards the center of sheet. Heat transfer mechanism remains the same as that of one side heating. Either sides, or Sandwich heating, is recommended to accelerate the process of heating for sheets over 1/8 inches thick.



**Quartz Heating element**



**Ceramic Heating Element**

**Figure 3- 4:** IR Heating elements used in the Oven (Kumar, 2005)

During the early days of thermoforming, tubular heaters were used for heating, but they were not very efficient and had limited zoning possibilities. Therefore in newer machines this type of heating has been replaced by an array of small ceramic heating elements or an array of wide area radiant panels shown in Figure 3.4. The main advantage of ceramic elements over wide area radiant panels is their flexibility, which facilitates controlled differential heating. However, wide area radiant panels are widely used as they give excellent results in most of the cases. They are preferred due to their low cost as compared to zoned ceramic element arrays. In thermoforming, temperature control is essential to make the process efficient and to save the energy. To meet this purpose programmable logic controllers (PLC) are used. They are cost effective as compared to electrically controlled heaters. The various heating elements and their comparison are summarized in Table 3.2.

**Table 3- 2: Heating elements (Kumar, 2005)**

<p>Bare nichrome wire heaters</p>	<ul style="list-style-type: none"> <li>• Low initial cost.</li> <li>• Simple to repair and replace.</li> <li>• Limit the zoning capabilities.</li> <li>• Non-uniform heating.</li> <li>• Tend to age and degrade quickly</li> </ul>
<p>Metal tubular heaters (calrod)</p>	<ul style="list-style-type: none"> <li>• Require longer heat-up times.</li> <li>• Heat non-uniformly.</li> <li>• Limit the possibilities to highly zone an oven.</li> <li>• Very versatile and long lasting.</li> </ul>
<p>Ceramic</p>	<ul style="list-style-type: none"> <li>• Easily zoned and very effective for zone heating</li> <li>• Very efficient in production.</li> <li>• Moderate heat up times and slower response times when compared to quartz or halogen.</li> <li>• Best used in shuttle type machinery rather than rotaries due to their faster response times</li> <li>• Have excellent temperature control</li> </ul>
<p>Quartz and Halogen</p>	<ul style="list-style-type: none"> <li>• Easily zoned like the ceramic</li> <li>• Ability to incorporate heat steps within a cycle</li> <li>• Quick response times</li> <li>• Different controllable heat levels.</li> <li>• More fragile and easier to damage.</li> <li>• Life expectancy is slightly lower than ceramic.</li> <li>• More expensive than ceramic</li> </ul>

### **3.4.3 Forming**

In the third phase, the mold is driven into the hot plastic sheet. Here the sheet is stretched and is sealed against the mold's vacuum box. Vacuum valves are used to pull the air between sheet and mold, and the plastic sheet forms to the contour of the mold. Electric fans are used for cooling the thermoplastic sheet after forming. The cooled sheet becomes rigid when it is freed from the mold by blowing a jet of air through the mold. Now the mold is pulled from the formed part. The formed sheet is unclamped and removed from the machine to be trimmed.

### **3.4.4 Trimming**

The formed part is removed from the sheet through trimming. Trimming methods range from a hand-held razor knife to the most sophisticated computer controlled routers. The most widely used method for trimming is a hand-held router for thick gauge sheet and steel die cutting for thin gauge sheet.

## **3.5 Thermoforming Materials**

The thermoforming process was invented to shape polymers (plastics). Polymers can be divided into three different categories of 1) Thermoplastics 2) Thermo-sets and 3) Elastomers. The first two are generally called plastics while the last one is rubber.

### **1. Thermoplastics**

Thermoplastics are solid materials at room temperature, but become viscous liquids at a few hundred degrees centigrade of temperature and can be easily molded to any shape. They can be subjected to heating and cooling cycles without significantly losing their properties.

## **2. Thermosetting**

They have identical properties as thermoplastics with the only difference that they cannot tolerate repeated heating cycles and go through degradation of many of their properties.

## **3. Elastomers**

These polymers exhibit extreme elastic extensibility at mechanical stresses. They have very different mechanical and thermal properties than the plastics.

Thermoplastics are commercially most important, constituting about 70% of the total polymer market. The use of plastics is increasing rapidly due to its “fitness” for commercial use. Some of the important commercial properties include:

- a) Suitable for molding into intricate part geometries.
- b) Very compatible with “net shape” processes.
- c) Good strength to weight density and low density relative to metals.
- d) Requires less energy due to low working temperatures as compared to metals.
- e) Highly corrosion resistant and low thermal and electrical conductivity.

Along with their many strengths, plastics have some limitations:

- a) Low strength relative to metals.
- b) Low modulus of elasticity.
- c) Service temperatures are limited to a few hundred degree centigrade only.
- d) Visco-elastic properties can also limit their use in load bearing applications.

### 3.6 Thermal Behavior of Polymers

Polymers exist in both crystalline and amorphous structures. Both of these structures behave differently when heated. Figure 3.5 shows the difference in behavior on a specific volume versus temperature graph when both structures are subjected to temperature.

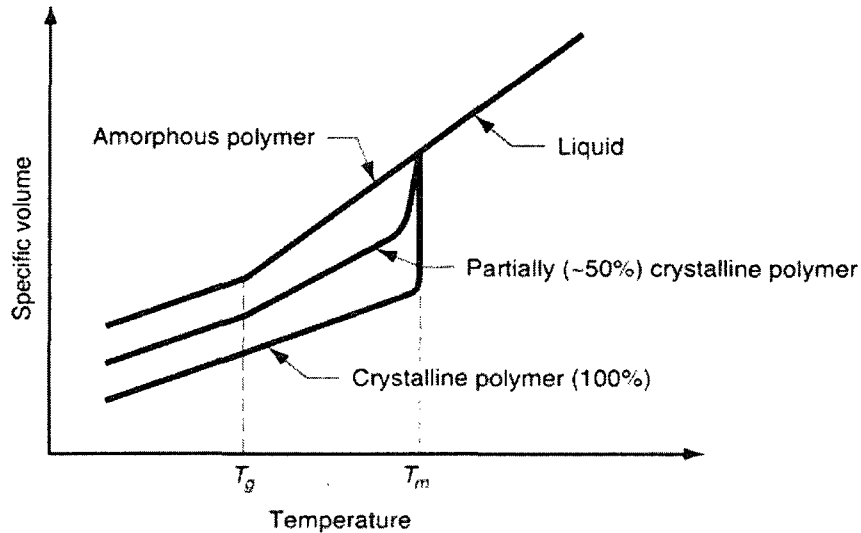


**Figure 3- 5:** Temperature effect on polymers (Groover, 1996)

Figure 3.5 shows three different polymers, 1) 100% crystalline 2) 100% amorphous and 3) Partially crystalline polymer. All three materials remain solid below the glass transition temperature,  $T_g$ . Between  $T_g$  and  $T_m$  (melting temperature) the materials assume a soft state in which they can be shaped. All plastic forming processes operate in this range of temperature. Above  $T_m$ , the polymers become liquid. It can also be inferred from Figure 3.5 that the change in volume is largest for crystalline polymers at  $T_m$  and smallest for amorphous polymers. A list of polymers typically used in thermoforming along with their characteristic temperatures is given as Table 3.3.

**Table 3-3:** Characteristic temperatures of polymers used in thermoforming (Zhang, 2004)

Polymer	Glass transition temperature (°C)	Melt temperature (°C)	Lower forming temperature (°C)	Upper forming temperature (°C)	Normal forming temperature (°C)
<b>Amorphous polymers</b>					
Polystyrene	94	-	127	182	149
PMMA	100	-	149	193	177
PMMA/PVA alloy	105	-	143	182	171
ABS	88-120	-	127	182	146
Polycarbonate	150	-	168	204	191
Rigid PVC	77	-	104	154	138
<b>Crystalline polymer</b>					
LDPE	-25	115	116	168	132
HDPE	-110	134	127	182	154
Cellulose acetate	70,100	230	127	182	146
Cellulose butyrate	120	140	127	182	146
Homo-Polypropylene	5	168	132	166	185
Co-Polypropylene	-20	150-175	143	193	204
GP PP	5	168	129	232	277
Polymethyl pentene	47	235	260	288	182
PVDC	0	245	163	199	149
PET	70	255	121	166	274
PBT	-80,70	245	260	288	224
Nylon 6	58	220	216	238	227
Nylon 66	78	255	249	288	274
<b>Foams</b>					
Polystyrene	70-85	158-185	88	113	220
Rigid PVC foam	70	158	110	171	290

## **Chapter 4 Heat Transfer Theory**

Heat transfer is defined as the transfer of energy from one region to another region by virtue of temperature difference. This heat transfer can take place within a body or from one body to another body through any one or more of the following methods:

1. conduction
2. convection
3. radiation

### **4.1 Conduction**

This mode of heat transfer is more dominant in solids where the molecules are packed tightly and can only vibrate about their mean position as explained by molecular theory. Due to close packing of molecules, electrons in the outer shell of an atom can become free from the influence of any atom and are called free electrons. These free electrons can move very easily in a body and when heat energy is supplied to the body, these electrons start moving inside the body and thus transport heat energy from one region to another region. Another but less dominant way of heat transfer in a solid is through vibration of molecules. When energy is supplied to a molecule, vibration increases and it starts colliding with the next molecule and thus transfers some of its energy to the next molecule. In this way heat energy is transferred from one molecule to the next. Heat transferred through free electron motion and molecular collision is called conduction heat transfer. Conduction can also be found in liquids and gases, but there, convection remains the dominant mode of heat transfer.

According to the second law of thermodynamics, heat can be exchanged between two systems if the two systems are at different temperatures. The heat will flow from the higher temperature to the lower temperature system, and the heat energy remains conserved along the flow path. Based on experimental evidence, Joseph Fourier was the first scientist who developed a mathematical model for conduction heat transfer called the “Fourier Law of Heat Conduction”. According to Fourier’s law, the heat transferred per unit area is proportional to the temperature gradient:

$$\frac{q}{A} \propto \frac{\partial T}{\partial x}$$

and with the introduction of proportionality constant k,

$$q = -kA \frac{\partial T}{\partial x} \quad (4.1)$$

where q is the heat transfer rate, A is the area through which heat transfer is occurring, k is the conductivity of the material,  $\partial T/\partial x$  is the heat gradient, and the negative sign is due to the fact the heat must flow downhill on the temperature scale. The Fourier equation can be simplified by solving for steady state conditions by separation of variables by assuming that conductivity k and area A remain constant along the heat flow path.

$$q \int_{x_1}^{x_2} dx = -kA \int_{T_2}^{T_1} dT = kA \int_{T_1}^{T_2} dT \quad (4.2)$$

If  $\Delta x (= x_2 - x_1)$  is the total heat flow path length then,

$$q = k \frac{A}{\Delta x} (T_1 - T_2)$$

The steady state equation can be used to approximate the amount of heat conducted in a very large number of situations where either the rate of heat conduction is very slow or precision is not the main issue.

#### 4.1.1 General Differential Equation of Conduction Heat Transfer

This basic equation can be extended to a more general form called the general conduction heat transfer equation that is applicable to any situation involving conduction heat transfer. Assuming a three dimensional homogenous solid as shown in Figure 4.1 which has a heat source or sink in the body such that the temperature of the body is changing with time.

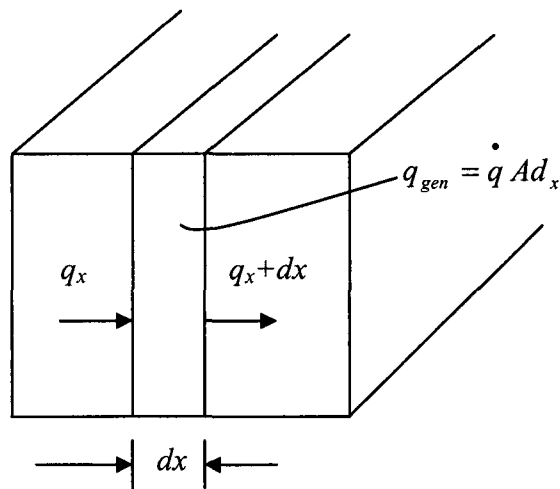


**Figure 4- 1:** Nomenclature for one dimensional heat conduction analysis

From the first law of thermodynamics, the energy balance for an element of thickness  $dx$  can be written as:

Energy conducted into the left face + heat generated within the element = change in internal energy + energy conducted out of the right face

where

$$\text{Energy into the left face} = q_x = -kA \frac{\partial T}{\partial x}$$

$$\text{Energy generated within the element} = q A dx$$

$$\text{Change in internal energy} = \rho C_p A \frac{\partial T}{\partial t} dx$$

$$\text{Energy out of the right face} = q_{x+dx} = -A \left[ k \frac{\partial T}{\partial x} + \frac{\partial}{\partial x} \left( k \frac{\partial T}{\partial x} \right) dx \right]$$

where  $q$  = energy generated per unit volume, W/m<sup>3</sup>

$C_p$  = specific heat of material, J/kg - °C

$\rho$  = density, kg/m<sup>3</sup>

Combing these terms into a single equation results in

$$-kA \frac{\partial T}{\partial x} + q A dx = \rho C_p A \frac{\partial T}{\partial t} dx - A \left[ k \frac{\partial T}{\partial x} + \frac{\partial}{\partial x} \left( k \frac{\partial T}{\partial x} \right) dx \right]$$

or

$$\frac{\partial}{\partial x} \left( k \frac{\partial T}{\partial x} \right) + q = \rho C_p \frac{\partial T}{\partial t} \quad (4.3)$$

The above equation is a one dimensional conduction heat equation. This equation can be easily extended to a three dimensional conduction heat equation:

$$\frac{\partial}{\partial x} \left( k \frac{\partial T}{\partial x} \right) + \frac{\partial}{\partial y} \left( k \frac{\partial T}{\partial y} \right) + \frac{\partial}{\partial z} \left( k \frac{\partial T}{\partial z} \right) + q_{in} = \rho C_p \frac{\partial T}{\partial t} \quad (4.4)$$

More details about the conduction heat equation can be found in (Holman, 1997).

### 4.1.2 Transient Conduction

In most cases, the quantity of heat energy entering and leaving a volume element of a body is not the same at any given instance and all such situations are categorized as transient conduction heat transfer. The lumped heat capacity method is one of the methods used to tackle transient heat transfer problems. This method is based on the assumption that the internal resistance of the body is negligible as compared to the external resistance. This assumption means that the temperature distribution in the body is uniform which is again not an exact real world situation. However, if the body size is small and the  $h(V/A)/k < 0.1$  condition is satisfied, the lumped capacity method gives an estimate of heat transfer within 5% of error limits (Holman, 1997).

Consider the semi-infinite solid body shown in figure 4.2. Let  $T_i$  be its initial temperature with the surface temperature decreased to  $T_o$ . For constant physical properties and no heat generation, the conduction equation temperature distribution becomes:

$$k \frac{\partial}{\partial x} \left( \frac{\partial T}{\partial x} \right) = \rho C_p \frac{\partial T}{\partial t}$$

Boundary and initial conditions are

$$T(x,0) = T_i$$

$$T(0,t) = T_o \quad \text{for } t > 0$$

The solution for this situation is given in (Holman, 1997) as:

$$\frac{T(x,t) - T_o}{T_i - T_o} = \text{erf} \frac{x}{2\sqrt{\alpha t}} \quad (4.5)$$

Now, if the boundary conditions are changed such that

$$T(x,0) = T_i$$

$$\frac{q_0}{A} = -k \frac{\partial T}{\partial x} \quad \text{at } x = 0 \text{ and } t > 0$$

The solution is given in (Holman, 1997) as:

$$T - T_i = \frac{2q_0 \sqrt{\alpha\tau} / \pi}{kA} \exp\left(\frac{-x^2}{4\alpha\tau}\right) - \frac{q_0 x}{kA} \left(1 - \operatorname{erf} \frac{x}{2\sqrt{\alpha\tau}}\right) \quad (4.6)$$

More sophisticated methods including numerical methods can be found in the literature for better estimation of conduction heat transfer, as required by the situation.

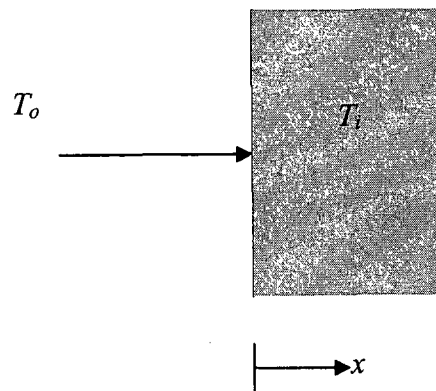


**Figure 4- 2:** Nomenclature for Transient Heat Flow

A practical situation that occurs frequently is when convection is the boundary condition at the surface of the solid. In such cases:

Heat convected into surface = heat conducted into surface

$$\text{or} \quad hA(T_\infty - T)_{x=0} = -kA \left. \frac{\partial T}{\partial x} \right|_{x=0}$$

The solution for this situation is given in (Holman, 1997) as:

$$\frac{T - T_i}{T_\infty - T_i} = 1 - \operatorname{erf} \frac{x}{2\sqrt{\alpha t}} - \left[ \exp\left(\frac{hx}{k} + \frac{h^2 \alpha t}{k^2}\right) \right] \times \left[ 1 - \operatorname{erf} \left( \frac{x}{2\sqrt{\alpha t}} + \frac{h\sqrt{\alpha t}}{k} \right) \right] \quad (4.7)$$

### 4.1.3 Thermal Conductivity

Thermal conductivity is a specific property of a heat conducting material. The numerical value of thermal conductivity varies over a large range depending on chemical composition, state of substance and physical structure. Crystalline materials exhibit high conductivities at low temperature while gases have very low values of conductivity. The variation in thermal conductivity for non homogeneous materials can be explained on the basis of porosity. Thermal conductivity for many materials has a large dependence on temperature. Assumption of linear dependence for thermal conductivity is a sufficient approximation in many cases. As compared to solids, the value of thermal conductivity for liquids and gases changes much more rapidly with the temperature. Also thermal conductivity changes substantially (drastically) with phase change for the same material. In most cases, this non-uniformity for thermal conductivity can be expressed as

$$k_t = k_0(1 \pm \beta T) \quad (4.8)$$

where  $k_0$  is the conductivity at reference temperature.

Thermal conductivity values for some common materials with reference to  $0^\circ\text{C}$  are tabulated in table 4.1.

Thermal capacity and thermal diffusivity are the two other important parameters used in conduction heat transfer. The thermal capacity,  $C$ , is the amount of heat required to raise the temperature of unit mass of a body by one degree. The thermal diffusivity,  $\alpha$ , gives interpretation in terms of heating time, i.e., it sets the rate at which heat can be added to a material. More detailed discussion about these material properties is presented in Chapter 6.

**Table 4- 1:** Thermal conductivity of various materials at 0°C (Holman, 1997)

Material	Thermal conductivity $k$	
	W/m °C	Btu/h ft F
<b>Metals:</b>		
Copper (pure)	385	223
Aluminum (pure)	202	117
Iron (pure)	73	42
Carbon steel, 1%C	43	25
<b>Nonmetallic solids:</b>		
Diamond	2300	1329
Quartz, parallel to axis	41.6	24
Glass, window	0.78	0.45
Glass wool	0.038	0.022
<b>Liquids:</b>		
Mercury	8.21	4.74
Water	0.556	0.327
Ammonia	0.540	0.312
<b>Gases:</b>		
Hydrogen	0.175	0.101
Helium	0.141	0.081
Air	0.024	0.0139

## 4.2 Convection

In convection, heat energy is transferred by the motion and mixing of macroscopic portions of a fluid. The term natural convection is used if this motion and mixing is caused by density variations due to differences of temperature within the fluid. The term forced convection is used if this motion and mixing is caused by an outside force, such as a fan or pump. Some of the factors that can affect convection heat transfer are:

- fluid velocity

- fluid viscosity
- heat flux
- surface roughness
- type of flow (laminar/turbulent).

The most general case in convection involves the transfer of heat between a surface at a given temperature,  $T_w$ , and fluid at a bulk temperature,  $T_\infty$ , as shown in Figure 4.3. The definition of the bulk temperature,  $T_\infty$ , depends on situation. For example, for flow adjacent to a hot or cold surface,  $T_\infty$  is the temperature of the fluid "far" from the surface while for flow in a pipe, it is the average temperature measured at a particular cross-section of the pipe. It is apparent from the fluid velocity profile in Figure 4.3 that the velocity of fluid near the surface is zero due to viscous action and heat is transferred only by conduction at the point of contact. The heat transfer rate,  $q$ , depends on temperature difference  $\Delta T$  between the fluid surface and the flat surface, and the area of contact and mathematically:

$$q = hA(T_w - T_\infty) \quad (4.9)$$

where  $h$  is the proportionality constant and called the convection heat transfer coefficient. It depends on the physical properties of the fluid and the physical situation. Typically, the convective heat transfer coefficient for laminar flow is relatively low compared to the convective heat transfer coefficient for turbulent flow. The reason is that the turbulent flow has a thinner stagnant fluid film layer than the heat transfer surface. The values of  $h$  have been measured experimentally and tabulated for different commonly used fluids and flow situations occurring during heat transfer by convection.

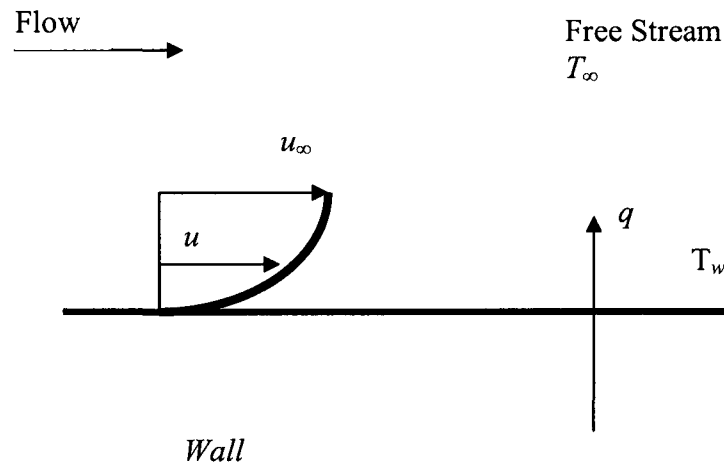


**Figure 4- 3:** Convection heat transfer from wall (Holman, 1997)

### 4.3 Radiation

All bodies emit electromagnetic radiation due to its temperature called thermal radiation. Thermal radiation transfers heat energy from one region to other depending on its wavelength. Thermal radiation needs no medium to carry heat and lies in the wavelength range from 0.1 to 100  $\mu\text{m}$  where the visible portion range is only from 0.35 to 0.75  $\mu\text{m}$ .

Stephan-Boltzmann law gives estimate of the energy radiated by a body due to its temperature and according to this law the total energy emitted by a body is proportional to the fourth power of the absolute temperature:

$$E_b = \sigma T^4 \quad (4.10)$$

where  $T$  is the absolute temperature of the body,  $\sigma$  is the Stephen-Boltzmann constant having a value equal to  $5.669 \times 10^{-8} \text{ W/m}^2 \cdot \text{K}^4$  and  $E_b$  is in  $\text{W/m}^2$ .  $E_b$  is the amount of

energy emitted per unit time per unit area by an idealized body called a black body. By definition it is a body that absorbs the entire radiations incident on it and the subscript “b” denotes that it is radiation from a black body.  $E_b$  is also called emissive power of a black body.

When radiation energy strikes a body, part of the radiation is absorbed, part is reflected and part is transmitted. The absorbed fraction is denoted by  $\alpha$  and called Absobtivity, reflected fraction is denoted by  $\rho$  and called reflectivity, transmitted fraction is denoted by  $\tau$  and called transmissivity. For anybody:

$$\alpha + \rho + \tau = 1 \quad (4.11)$$

For opaque bodies the transmissivity is very low and can be considered as zero for all practical purposes.

Another important term is the emissive power of a body  $E$  which is defined as the energy emitted by the body per unit area per unit time. The relation between emissive power of a body to the black body is established by a term called emissivity of the body and is denoted by  $\varepsilon$  where:

$$\varepsilon = \frac{E}{E_b} \quad (4.12)$$

The emissivity of substances varies widely with temperature, wavelength and surface conditions. The monochromatic emissivity  $\varepsilon_\lambda$  is also an important term used in radiation studies. It is defined as the ratio of the monochromatic emissive power of a body  $E_\lambda$  to the monochromatic emissive power of a black body  $E_{b\lambda}$  at the same wavelength and temperature. Mathematically,

$$\epsilon_{\lambda} = \frac{E_{\lambda}}{E_{b\lambda}} \quad (4.13)$$

### 4.3.1 Gray Body

A gray body is defined as the body whose monochromatic emissivity  $E_{\lambda}$  is independent of the wavelength. Mathematically,

$$\epsilon_{\lambda} = \text{const}$$

### 4.3.2 Real Body

Real bodies show considerable deviation from both black bodies and gray bodies. Among the deviations is that the intensity of emitted radiation is not constant over all directions, e.g., conductors emit more energy than the non-conductors in the large azimuth angle direction. The behavioral difference for all the three types of bodies can be seen in Figure 4.4.

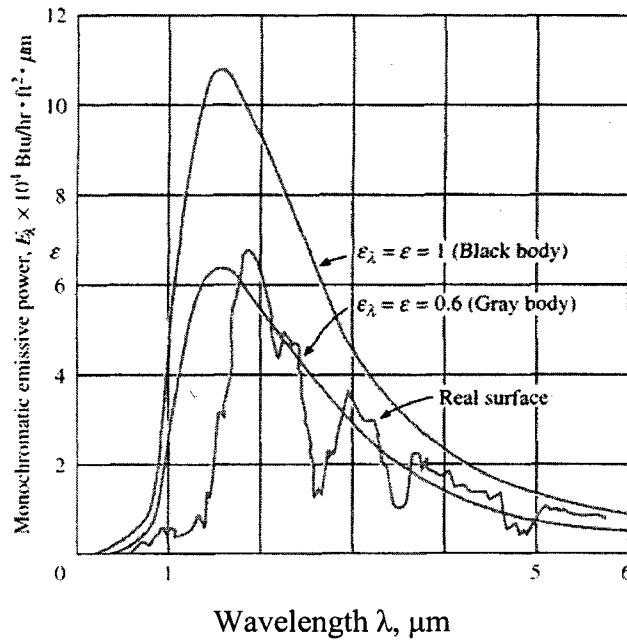


Figure 4- 4: Radiation behavior of bodies, (Holman, 1997)

Reflectance and absorptance of thermal radiation from real surfaces are a function of surface properties, direction and wavelength of the incident radiation as well as the surrounding surfaces, which makes analysis very complicated. To avoid these complications, surfaces are usually considered as gray bodies.

### 4.3.3 Radiation Shape Factor

The radiation shape factor is defined as the fraction of the area of the radiation emitting surface that can “see” the fraction of the area of the radiation receiving surface.

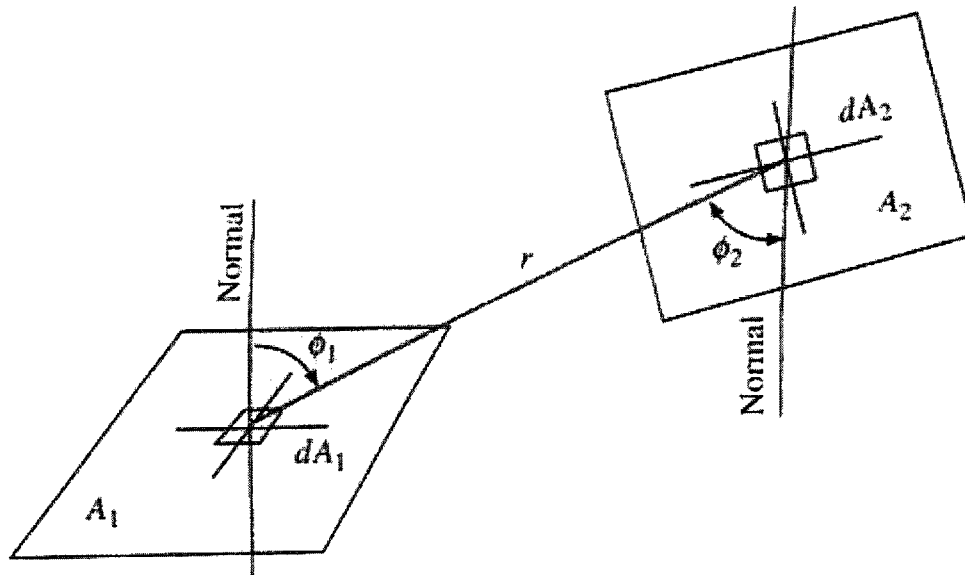


Figure 4- 5: Radiation Shape Factor (Holman, 1997)

In Figure 4.5, two black surfaces A<sub>1</sub> and A<sub>2</sub> are shown where

$F_{12}$  = fraction of energy leaving surface 1 which reaches surface 2

$F_{21}$  = fraction of energy leaving surface 2 which reaches surface 1

The energy leaving surface 1 and arriving at surface 2 is  $E_{b1} A_1 F_{12}$  and the energy leaving surface 2 and arriving at surface 1 is  $E_{b2} A_2 F_{21}$ . All the energy is absorbed as the surfaces are black and the net energy exchange is

$$Q_{12} = E_{b1} A_1 F_{12} - E_{b2} A_2 F_{21} \quad (4.14)$$

If the temperature of bodies is the same, then, there is no net transfer of energy and the above relation can be generalized for any two surfaces m and n as:

$$A_m F_{mn} = A_n F_{nm} \quad (4.15)$$

which is called reciprocity relation and holds for other surfaces as long as diffused radiation is involved.

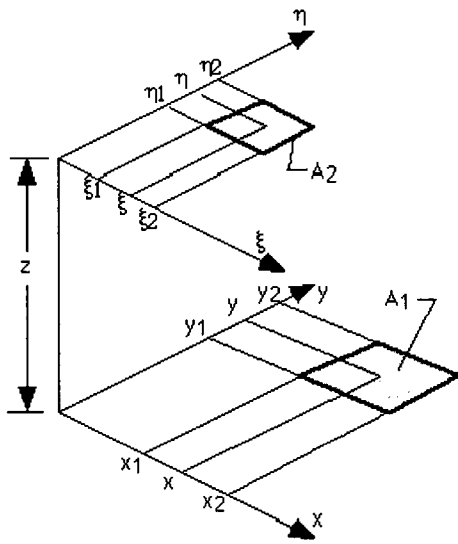
From Figure 4.5, it can be seen that the energy exchange between small areas  $dA_1$  and  $dA_2$  is:

$$dq_{12_{net}} = \cos \phi_1 \cos \phi_2 \frac{dA_1 dA_2}{\pi r^2} (E_1 - E_2) \quad (4.16)$$

The net energy exchange equation between two black bodies of area  $A_1$  and  $A_2$  can be generalized as:

$$q_{net_{12}} = (E_{b1} - E_{b2}) \int_{A_2} \int_{A_1} \cos \phi_1 \cos \phi_2 \frac{dA_1 dA_2}{\pi r^2} \quad (4.17)$$

This integral can be solved if the specific geometries of the surfaces are known. Solutions for some elementary geometric shapes are available in the literature. One of the solutions for two flat surfaces facing each other is used in estimating view factor between sheet and oven is presented in Figure 4.6.



$$F_{1-2} = \frac{1}{(x_2 - x_1)(y_2 - y_1)} \sum_{i=1}^2 \sum_{k=1}^2 \sum_{j=1}^2 \sum_{l=1}^2 (-1)^{(i+j+k+l)} G(x_i, y_j, \eta_k, \xi_l)$$

$$G = \frac{1}{2\pi} \left( \begin{aligned} & (y-\eta) \left[ (x-\xi)^2 + z^2 \right]^{1/2} \tan^{-1} \left\{ \frac{y-\eta}{\left[ (x-\xi)^2 + z^2 \right]^{1/2}} \right\} \\ & + (x-\xi) \left[ (y-\eta)^2 + z^2 \right]^{1/2} \tan^{-1} \left\{ \frac{x-\xi}{\left[ (y-\eta)^2 + z^2 \right]^{1/2}} \right\} \\ & - \frac{z^2}{2} \ln \left[ (x-\xi)^2 + (y-\eta)^2 + z^2 \right] \end{aligned} \right)$$

**Figure 4- 6:** View Factor between two flat surfaces and the related solution, (Walter 2002).

## Chapter 5 Sheet Heating Model

The three most commonly used methods in industry for sheet reheating are:

- 1- Gas Fired Convection Oven
- 2- Contact Heating Oven
- 3- Radiation Heating Oven

Among the above, radiation heating is the preferred and most widely used method due to superior controllability and efficiency. Sheet is inserted into heated oven at the middle between the upper and lower bank of heating elements as shown in Figure 5.1. The energy propagation from heater to sheet is through both radiation and convection with the radiation as a major carrier while both conduction and radiation absorption are responsible for the energy propagation inside the sheet (Kumar, 2005). When the thermal radiations from the heater element is incident on the sheet, a portion is absorbed in the sheet, while some are reflected back and some are transmitted through the sheet depending on the color and material of the sheet. The schematic presentation for sheet reheat energy model for double side heating is presented in Figure 5.1.

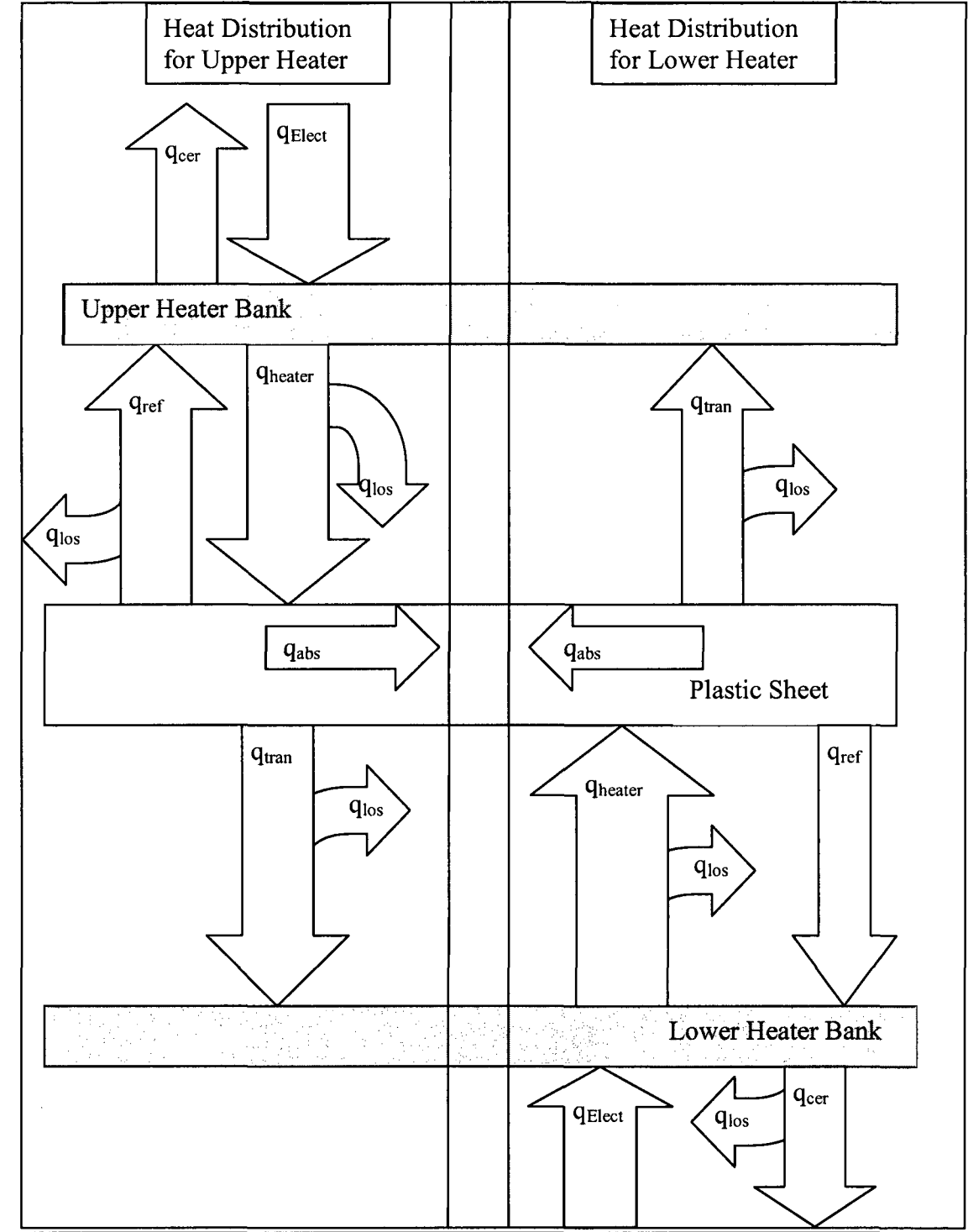


**Figure 5- 1:** Heat energy distribution for thermoforming with double side heating of sheet. Concept derived from (Brinken, 1980).

Where:

$q_{\text{elect}}$  = Electrical energy supplied to the heater

$q_{\text{cer}}$  = Energy lost due to ceramic elements efficiency

$q_{\text{heater}}$  = Heat Energy Released by Heater

$q_{\text{los}}$  = Heat Energy Lost to Environment

$q_{\text{ref}}$  = Heat Energy Reflected Back by Sheet Surface

$q_{\text{abs}}$  = Heat Energy Absorbed By the Sheet

$q_{\text{trans}}$  = Heat Energy Transmitted Through the Sheet

## 5.1 Analytical Model of the Sheet Reheat Phase

The sheet heating phase can be divided in to two subsystems that exchange energy, i.e., oven and sheet.

### 5.1.1 Oven

The oven consists of heating elements, arrangement to support the sheet and control devices. It can be seen from Figure 5.1 that the total energy supplied to the oven is  $q_{\text{elect}}$  but  $q_{\text{cer}}$  is the amount of energy lost due to ceramic heating elements efficiency and only  $q_{\text{heater}}$  is available at the heater's elements. Mathematically, this is:

$$q_{\text{heater}} = q_{\text{elect}} - q_{\text{cer}}$$

This  $q_{\text{heater}}$  starts propagation towards the sheet surface but it loses a portion  $q_{\text{los}}$  to the environment and the sheet surface receives only heat energy equal to  $q_{\text{heater}} - q_{\text{los}}$ . Furthermore, out of this remaining energy a portion of energy,  $q_{\text{ref}}$ , is reflected by the sheet surface, a portion  $q_{\text{trans}}$  is transmitted through the sheet while the rest of the energy is utilized to raise the sheet temperature. The  $q_{\text{trans}}$  and  $q_{\text{ref}}$  lose a portion to the

environment, while the rest is partly absorbed and partly reflected by furnace walls depending on the walls' temperature, color and material, and this process continues throughout the heating cycle.

The first step of this very work is to develop an analytical model for the above described system. Unfortunately this described system is very complicated and needs simplification in order to be modeled analytically. A reasonable simplification is to neglect  $q_{\text{los}}$  and  $q_{\text{ref}}$  as both comprise only 5% of total heat of the system (Ajersch, 2004). With this assumption  $q_{\text{heater}}$  become the total energy,  $q_{\text{tot}}$ , absorbed by the sheet surface through convection and radiation. The basic heat energy balance equation can now be written as:

Total energy,  $q_{\text{tot}}$ , propagated to the sheet surface per unit time = Energy received per unit time by the sheet surface through radiation,  $q_{\text{rad}}$  + Energy received per unit time through convection by sheet surface,  $q_{\text{conv}}$

In mathematical notation:

$$\dot{q}_{\text{tot}} = \dot{q}_{\text{rad}} + \dot{q}_{\text{conv}} \quad (5.1)$$

Where (5.2)

$$\dot{q}_{\text{rad}} = \sigma \varepsilon_{\text{eff}} F (T_h^4 - T_s^4) \quad (5.3)$$

$$\dot{q}_{\text{conv}} = h (T_{\infty} - T_s)$$

and

$$\varepsilon_{\text{eff}} = \left[ \frac{1}{\varepsilon_h} + \frac{1}{\varepsilon_s} - 1 \right]^{-1} \quad (5.4)$$

$T_h$  = Temperature of oven heating elements

$T_s$  = Temperature of sheet surface

$T_\infty$  = Temperature of ambient air

$\epsilon_h$  = Emissivity of oven heating elements

$\epsilon_s$  = Emissivity of sheet surface

$\sigma$  = Stefan Boltzmann's constant

F = View factor

h = Convection heat transfer coefficient

### 5.1.2 Sheet

As described earlier the portion of the heat energy,  $q_{tot}$  that reaches the sheet surface is utilized in increasing the sheet internal energy. Considering the sheet as a system then according to first law of thermodynamics the change in internal energy of the system (sheet) is equal to the heat entering the system plus heat generated inside the system (sheet) minus heat leaving the system (sheet) boundaries.

Mathematically:

$$\Delta E_{intrenal} = E_{entering} - E_{leaving} + E_{generated} \quad (5.5)$$

### 5.1.3 Methodology

The terms in the Equation 5.5 are continuous in nature and different for sheet surface and interior. Both these facts can be accommodated by discretizing the sheet in to M layers (M= 5 in this work) across its thickness as shown in Figure 5.2 (side view). Each layer is considered to be an isothermal entity and a node in the center of layer as per convention

represents that layer (Holman, 1997). The nodes and the distance between nodes are shown in Figure 5.3. The interaction between nodes constitutes the sheet heating model.

The sheet is also broken down into  $i$  zones ( $i = 6$  in this very work) in x-y plane (top view of Figure 5.2) in order to facilitate the design of real time control model of the sheet reheating phase which is the broader goal of this research activity. The oven heating elements are also divided into  $j$  zones ( $j = 6$  for this very work) on each side as shown in Figure 5.4.

The model is constructed by setting up an energy balance on each node which results in a set of finite dimension, ordinary differential equations. This set of ordinary differential equations is then simulated in computer and the results are verified against experimental results in order to validate the model. Before going into analytical model some assumption are discussed that are made to facilitate the analytical modeling process.

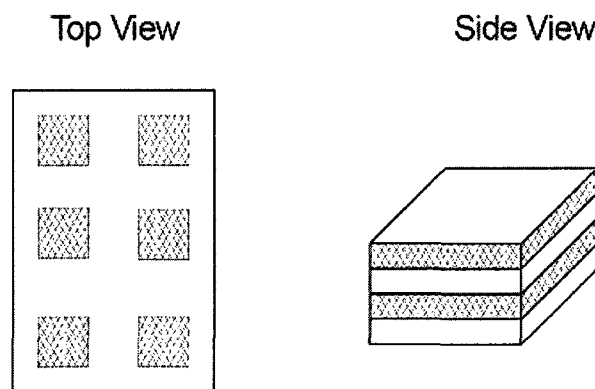


**Figure 5- 2:** Discretization of sheet

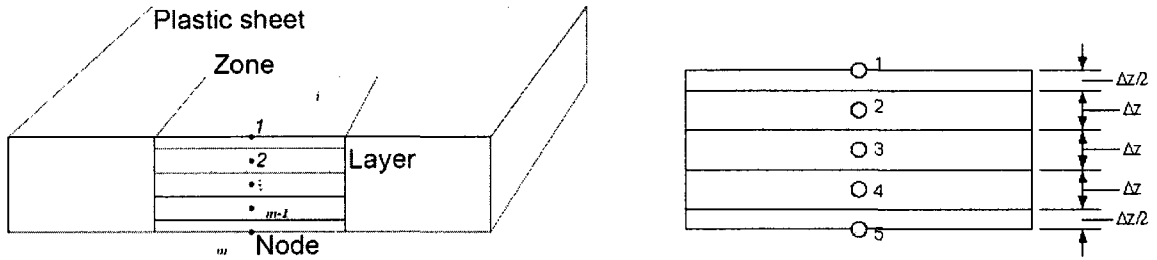


**Figure 5- 3: Sheet Nodes**

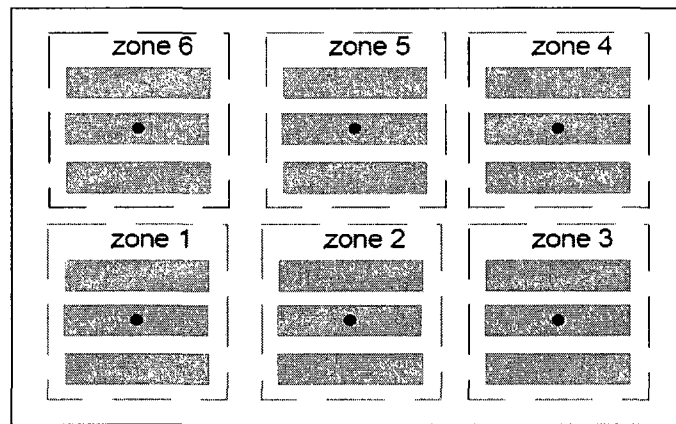


**Figure 5- 4: Oven Zones**

### 5.1.4 Assumptions

The following logical assumptions are made in order to simplify the procedure.

1. Heat transfer occurs only through the depth of sheet. Usually the sheets used for thermoforming have thickness much smaller than other two dimensions. When heat energy balance is set up for a volume element where the thickness is much smaller than the other two dimensions, then it can be assumed that the heat transfer occur only through the sheet thickness. In other words, it is assumed that the transfer of energy is occurring only through thickness of sheet while transfer

of energy through width and length of sheet is negligible. This assumption is valid since the temperature gradients across the sheet surface is relatively small as compared with the temperature gradient through the sheet thickness also considering the fact that thermoplastic materials are generally poor heat conductors, most of the energy will transfer across thickness of sheet. The three dimensional general conduction equation for the sheet with the above assumption reduce to the following form (Yousefi, 2002):

$$\rho C_p \frac{dT}{dt} = k \frac{d^2 T}{dz^2} + \dot{q}_{abs} \quad (5.6)$$

Where  $\rho$ ,  $C_p$ , and  $k$  are density, specific heat and thermal conductivity of the sheet respectively,  $T$  is the temperature,  $z$  is the coordinate of the sheet in the thickness direction, and  $t$  is the elapsed time in which heat transfer has occurred. The  $\dot{q}_{abs}$  accounts for the heat absorbed in the volume from a radiative heat source.

2. Sheet material is homogeneous and contains no impurities.
3. Absorptivity of the material is same throughout the sheet.
4. Sheet acts as a gray body to thermal radiations.
5. Temperature in horizontal layer is same throughout the layer at same depth. The validity of this assumption was proved experimentally by Kumar (2005). In his experiment, three thermocouples were inserted at different locations in the sheet but at same depth and the temperature was measured simultaneously. This experiment strongly supported this assumption.
6. The heat losses,  $q_{ref}$  and  $q_{los}$ , are small and can be neglected.

7. The convection coefficient remains constant throughout the heating process.
8. The oven air temperature remains constant throughout the heating process.
9. Thermal radiation causes the entire sheet temperature to increase from the very start and the temperature difference across the sheet remains very small. This assumption is supported by the experiments performed at IMI, Montreal by Kumar (2005). In these experiments, small thermocouples are inserted at various depths in a 12mm thick HDPE sheet. The results showed that all thermocouples at different sheet depths used in this experiment indicated an increase in temperature at approximately the same time with approximately 10 °C of difference as shown in Figure 5.5 (Kumar, 2005).

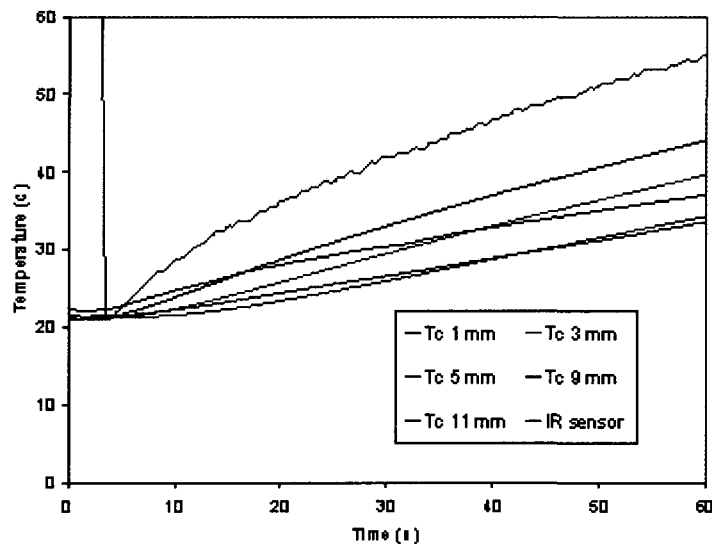


**Figure 5- 5:** Result for heating of HDPE sheet (Kumar, 2005).

### 5.1.5 Equations

The energy balance equation for the external layers can be written as:

**Top layer**

$$\rho C_p \frac{\partial T}{\partial t} = q_{radiation\_upper} + q_{convection\_upper} - q_{conduction\_upper} \quad (5.7)$$

**Bottom layer**

$$\rho C_p \frac{\partial T}{\partial t} = q_{radiation\_bottom} + q_{convection\_bottom} - q_{conduction\_bottom} \quad (5.8)$$

**Interior layers**

$$\rho C_p \frac{\partial T}{\partial t} = \dot{q}_{conduction\_from\_top\_layers} - \dot{q}_{conduction\_to\_next\_layer} + \dot{E}_{generated} \quad (5.9)$$

## 5.2 Basic Steady State Model

This model is based on assumption that the heat transfer through sheet is occurring under steady state conditions and there is no heat absorption in the sheet. With these assumptions the analytical model for the sheet shown in Figure 5.3 can be written as:

**Top layer**

$$\frac{dT_{i1}}{dt} = \frac{1}{\rho V_i C_p} \left[ q_{rad_i} + q_{conv_i} - \frac{kA}{\Delta z} (T_{i1} - T_{i2}) \right] \quad (5.10)$$

Where

$V = \frac{l^2 \Delta z}{2}$  is the volume of the top layer for the  $i$ th zone.

The term  $\frac{kA}{\Delta z} (T_{i1} - T_{i2})$  represents the conduction heat transfer from node 1 to 2 in zone  $i$

and  $i$  represent the  $i$ th zone in  $x$ - $y$  plane.

$$\dot{q}_{rad_i} = A_i \sigma \varepsilon_{eff} \sum_{j=1}^6 F_{ij} (T_{h_j}^4 - T_{m_i}^4)$$

$$\dot{q}_{conv_i} = A_i h_i (T_{\infty_i} - T_{i1})$$

$T$  is the average sheet surface temperature;  $j$  represents the corresponding heat bank of the furnace.

### Interior layers

$$\frac{dT_{im}}{dt} = \frac{1}{\rho V_{im} C_p} \left[ \frac{kA_i}{\Delta z} (T_{i(m-1)} - T_{im}) - \frac{kA_i}{\Delta z} (T_{im} - T_{i(m+1)}) \right] \quad (5.11)$$

Where  $V_{im} = l^2_{im} \Delta z$  and  $i$  represent sheet zone and  $m$  represent the layer number.

### Bottom layer

$$\frac{dT_{is}}{dt} = \frac{1}{\rho V_{is} C_p} \left[ q_{rad_i} + q_{conv_i} - \frac{kA_i}{\Delta z_5} (T_{is} - T_{i4}) \right] \quad (5.12)$$

Where  $V_{i5} = \frac{l_{i5}^2 \Delta z}{2}$  is the volume of bottom layer of *ith* zone. This model was developed by Moore (2002) in order to develop an *in-cycle control model* for thermoforming reheat process by using  $H_\infty$  control theory. The control strategy adopted by Moore is the direct control of the sheet surface temperature and indirect control of sheet center line temperature. The sheet surface temperature is measured directly by IR sensors while the indirect sheet center temperature control is made possible through soft sensor developed by Benqiang (2003) which estimates the sheet internal temperature. According to Benqiang, generally, the heating and cooling phase for a given element temperature can be represented accurately for the simulation and the experimental results by the following equation:

$$T_{t,d} = \exp \left[ \frac{a_1}{(a_3 + z)t} + a_2 \right] \quad (5.13)$$

Where T is the temperature, t is the time and z is the depth of sheet and the three coefficients  $a_1$ ,  $a_2$ ,  $a_3$  represent state variables for the system that can be found by tuning the model for any particular situation.

According to in-cycle control strategy, the sheet surface temperature measured by the IR sensor and the heater elements temperature measured by thermocouples were transferred to the “soft sensor” installed on a computer connected with thermoforming machine. The soft sensor estimates the sheet center line temperature and based on this estimate sends signals to adjust the heater elements’ temperature accordingly for that particular sheet.

Experimental results for Moore’s model showed that the slow cooling dynamics of the ceramic heating elements pose a major problem for the  $H_\infty$  design. Without any time domain predictive abilities, the  $H_\infty$  controller is susceptible to significant overshoot as a result of the nonlinear heater dynamics and is not suitable. It was concluded that the performance of any in-cycle control design should depend upon the reheat cycle time. Shorter cycle time applications will have to rely more on adaptive cycle-to-cycle control and soft sensor prediction since in in-cycle control performance is limited in such cases.

### 5.3 Absorptivity Based Steady State Model

An important factor that was ignored in Moore’s model is the absorptivity of the plastic sheet. Inside a radiation thermoforming oven, the heat energy is radiated by heating elements towards the plastic sheet in which about 95% of energy is absorbed by the sheet (for a typical plastic) and the rest is reflected. Of that 95%, some is “retained” by the sheet itself, and the rest is transmitted through the sheet (Ajersch, 2004) which means that Transmissivity cannot be taken as zero and must be included in the model. Transmissivity of any material can be estimated by Beer Lambert’s law which is:

$$\begin{aligned} \ln(\tau_\lambda) &= -\alpha_\lambda z \\ \tau_\lambda &= e^{-\alpha_\lambda z} \end{aligned} \tag{5.14}$$

Where

$\tau$  = transmissivity,

$\alpha_\lambda$  = absorptivity of the material in  $m^{-1}$ ,

$\lambda$  = wave length and

$z$  = thickness of material.

It can be inferred from the above equation that the transmissivity of a material depends on two main parameters: the spectral absorption coefficient of the material and the material thickness. Moreover, both the transmissivity and absorptivity depend on wavelength of the radiation. If  $\alpha_\lambda$  is assumed to be the average absorptivity of the material across its spectrum then by discretizing the continuous transmissivity function the amount of energy dissipated in each layer can be easily found.

Consider the sheet in Figure 5.3. When the net radiative heat flux of intensity  $q_{rad}$  strikes the sheet surface, a portion of  $q_{rad}$  is absorbed in the first layer and rest is transmitted through the layer. Let the absorbed fraction of  $q_{rad}$  in the depth of the sheet is  $\beta(z)$ , then the total absorbed energy in thickness of the sheet, say  $\Delta z$ , will be equal to the integral sum of all energies absorbed over that thickness  $\Delta z$ .

In case of the sheet model in Figure 5.3, the thickness of the sheet for external layers is  $\Delta z / 2$ . The total energy  $\beta(\Delta z/2)$  for external layers become:

$$\beta(\Delta z/2) = \int_0^{\Delta z/2} A_\lambda e^{-A_\lambda z} dz = \left[ 1 - e^{(-A_\lambda \Delta z/2)} \right] = \beta_1 \quad (5.15)$$

And total energy for internal layers is

$$\beta(\Delta z) = \int_0^{\Delta z} A_\lambda e^{-A_\lambda z} dz = \left[ 1 - e^{(-A_\lambda \Delta z)} \right] = \beta_2 \quad (5.16)$$

If  $Q$  is defined as the incident radiant energy on the sheet surface on zone  $i$ , then the absorbed energy  $Q_{a1}$  in layer 1 will be:

$$Q_{a1} = \beta_1 Q$$

The radiant energy transmitted through layer 1,  $Q_{t1}$ , is simply the non-absorbed fraction:

$$Q_{t1} = (1 - \beta_1) Q$$

The absorbed energy,  $Q_{a2}$ , in layer 2 is:

$$Q_{a2} = \beta_2 Q_{t1} = \beta_2 (1 - \beta_1) Q$$

And the transmitted part,  $Q_{t2}$ , through layer 2 is:

$$Q_{t2} = (1 - \beta_2) Q_{t1} = (1 - \beta_2)(1 - \beta_1) Q$$

For any layer  $m$ , the equations for the absorbed and transmitted energy can be written as:

$$Q_{am} = \beta_2 (1 - \beta_2)^{m-2} (1 - \beta_1) Q \quad (5.17)$$

$$Q_{tm} = (1 - \beta_2)^{m-2} (1 - \beta_1) Q \quad (5.18)$$

Then, for the bottom most layer (say layer  $m$ ), the equations become:

$$Q_{am} = \beta_1 (1 - \beta_2)^{m-2} (1 - \beta_1) Q \quad (5.19)$$

$$Q_{tm} = (1 - \beta_2)^{m-1} (1 - \beta_1)^2 Q \quad (5.20)$$

The last equation estimates the radiant energy transmitted across entire thickness of the plastic sheet. Thus energy absorbed in the plastic sheet is the difference between the energy entering the plastic sheet and the energy transmitted:

$$Q_{abs} = Q - Q_{tm} = \left\{ 1 - (1 - \beta_2)^{m-1} (1 - \beta_1)^2 \right\} Q \quad (5.21)$$

Figure 5.6 shows schematically the above mathematical procedure.

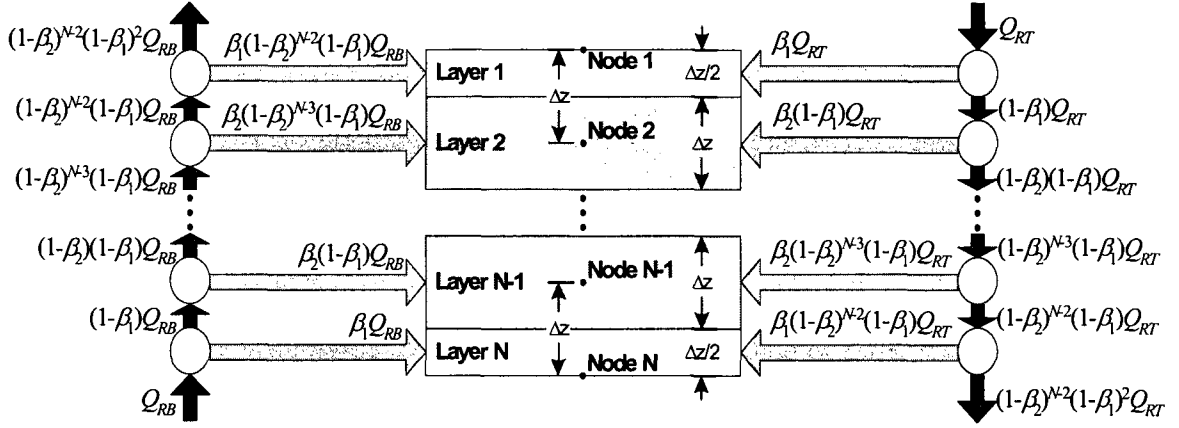


**Figure 5-6:** Schematic presentation of the absorption terms in sheet model (Gauthier, 2005)

For the top layer of sheet, the energy balance for any zone  $i$  with the absorption term is:

$$\frac{dT_{i1}}{dt} = \frac{2}{\rho C_p \Delta z} \left\{ (Q_{T_{i1}} + Q_{B_{i1}}) + h(T_{\infty} - T_{i1}) + \frac{k}{\Delta z} (T_{i2} - T_{i1}) \right\} \quad (5.22)$$

and for bottom layer only 1 needs to be replaced by number of layer.

The general energy balance equation for internal layer with absorption being included is:

$$\frac{dT_{im}}{dt} = \frac{1}{\rho C_p \Delta z} \left\{ \frac{k}{\Delta z} [T_{i1} - 2T_{i2} + T_{i3}] + [Q_{T_{im}} + Q_{B_{im}}] \right\} \quad (5.23)$$

Now it is needed to evaluate the incident energy hitting the  $i$ th zone. The top node of the  $i$ th zone receives:

$$Q_{RT_i} = \sigma \epsilon_{eff} \sum_{i=1}^{M_T} F_{T_{ij}} (T_{S_{T_j}}^4 - T_{i1}^4) \quad (5.24)$$

And the bottom one receives:

$$Q_{RB_i} = \sigma \varepsilon_{eff} \sum_{i=1}^{M_B} F_{B_{ij}} (T_{S_{B_j}}^4 - T_{is}^4) \quad (5.25)$$

Where,  $M_T$  and  $M_B$  represent the number of heating element zones on the top and bottom banks of the oven, respectively.  $T_{S_{B_j}}$  and  $T_{S_{T_j}}$  are the surface temperatures of bottom and top heating zone respectively and  $j$  represents the number of heating zone. The absorption term of the radiant energy coming from the top of the sheet is:

$$\begin{aligned} Q_{T_{i1}} &= \beta_1 Q_{RT_i} \\ Q_{T_{im}} &= \beta_2 (1 - \beta_2)^{m-2} (1 - \beta_1) Q_{RT_i}, m \in \{2, 3, 4, 5\} \end{aligned} \quad (5.26)$$

Similarly, the absorption term of the radiant energy coming from the bottom of the sheet is:

$$\begin{aligned} Q_{B_{i1}} &= \beta_1 Q_{RB_i} \\ Q_{B_{im}} &= \beta_2 (1 - \beta_2)^{m-2} (1 - \beta_1) Q_{RB_i}, m \in \{2, 3, 4, 5\} \end{aligned} \quad (5.27)$$

After writing Equations 5.22 to 5.27 in state space form, the above system of equations is simulated in Simulink and the results are found to be satisfactory when compared with the experimental results (Ajersch, 2004).

## 5.4 Sheet Color Based Model

In all of the above models, it was assumed that the sheet is transparent or semi-transparent and a portion of heat is absorbed in the sheet by absorption of thermal radiations following Beer Lambert's law. In fact a large number of sheets thermoformed

in industry are colored and allow no or very small amount of absorption of radiation. In all such cases the major mode of heat transfer inside the sheet is conduction which is relatively “slow” mode of heat transfer as compared to absorption of radiation in terms of time and needs a different setting of process parameters especially oven temperatures. In order to investigate this fact, two extreme cases are compared:

- 1) White sheet with only radiation heat transfer inside the sheet
- 2) Colored sheet with only conduction heat transfer inside the sheet

#### 5.4.1 Heating Model for White Sheet

The model for this case is based on assumption that the sheet is 100% transparent and radiation is the only mode of heat transfer inside the sheet and the sheet accumulates heat only through absorption. The sheet model can be written as:

##### Exterior layers

$$\frac{dT_{im}}{dt} = \frac{2}{\rho C_p dz_i} \{ (Q_{T_{im}} + Q_{B_{im}}) + h(T_{\infty_1} - T_{im}) \}, m \in \{1,5\} \quad (5.33)$$

##### Interior layers

$$\frac{dT_{im}}{dt} = \frac{1}{\rho C_p dz_i} \{ Q_{T_{im}} + Q_{B_{im}} \}, m \in \{2,3,4\} \quad (5.34)$$

#### 5.4.2 Heating Model for Colored Sheet

The model for this case is based on assumption that the sheet is 100% opaque and radiation is absorbed only at the surface of the sheet and conduction is the only mode of heat transfer inside the sheet. The sheet model can be written as:

### Top layer

$$\frac{dT_{i1}}{dt} = \frac{2}{\rho C_p dz_i} \left\{ (Q_{T_{i1}} + Q_{B_{i1}}) + h(T_{\infty_1} - T_{i1}) + \frac{kdT_{i2,i1}}{dz_i} \right\} \quad (5.35)$$

### Interior layers

$$\frac{dT_{im}}{dt} = \frac{1}{\rho V_i C_p} \left[ \frac{kA_i dT_{i(m-1),im}}{dz_i} - \frac{kA_i dT_{im,i(m+1)}}{dz_i} \right], m \in \{2,3,4\} \quad (5.36)$$

### Bottom layer

$$\frac{dT_{i5}}{dt} = \frac{2}{\rho C_p dz_i} \left\{ (Q_{T_{i5}} + Q_{B_{i5}}) + h(T_{\infty_5} - T_{i5}) + \frac{kdT_{i5,i4}}{dz_i} \right\} \quad (5.37)$$

Note that this model is same as the Moore's Model. Both models for colored and transparent sheet are simulated in Matlab and the results are discussed in the next chapter.

## 5.5 Sheet Heating Model with Variable Material Properties

The physical properties of material are considered thus far constant but in fact it changes with temperature. The three most important parameters that are representative of the physical properties of material are heat capacity,  $C_p$ , conductivity,  $k$ , density,  $\sigma$  and thermal diffusivity,  $\alpha$ .

### 5.5.1 Heat Capacity

Heat capacity at constant pressure,  $C_p$  is defined as the amount of energy required to raise the temperature of 1g of any substance by 1°C.

$$C_p = \frac{\text{enthalpy}}{\text{temperature}} = \left( \frac{\partial H}{\partial T} \right)_p \quad [\text{J/g } ^\circ\text{C}]$$

Energy is absorbed during melting and released when crystallization occurs for crystalline and semi-crystalline polymers. Enthalpy for these materials usually shows dramatic changes in the vicinity of the melting temperature and shows discontinuities which results in a rapid increase in heat capacity when the temperature is passing through the melting point and then decreased afterward. The heat capacity of amorphous polymer changes continuously with increasing temperature and above the glass temperature the enthalpy lines become quite linear and heat capacity remain only slightly dependent on temperature.

The overall effect of  $C_p$  on thermoforming reheat phase is studied by Yousefi et al. (2002) during the sensitivity analysis for key parameters of thermoforming process and found a normalized sensitivity coefficient decreasing from 0.28 to 0.1 with the process cycle time. The decrease is due to the fact that the value of  $C_p$  is very sensitive to the polymer density which changes with temperature (Santos, 2005).

A series of experiments have been performed at the IMI, Montreal in order to study the effect of temperature on  $C_p$  (Zhang, 2004) for both crystalline and amorphous plastic materials in both forced and natural convection systems during thermoforming reheat phase. Some experimental results are presented in Figures 5.7 to 5.9. Equations 5.38 and 5.39 are used to calculate the values of  $C_p$  for different conditions as described in Figures 5.7 to 5.9.

$$\overline{Nu}_x = \frac{h_x L}{K} = 0.453 Re_x^{1/2} Pr^{1/3} \quad (5.38)$$

$$C_p = \frac{2K \overline{Nu}_x (T_w - T_\infty) \Delta t}{\rho L x \Delta T} \quad (5.39)$$

On the basis of experiments, a software is developed at IMI that can predict the value of  $C_p$  quite accurately for any given process parameters for plastic materials (Zhang, 2004). Instead of the constant value of  $C_p$ , this software can be used to calculate the value of  $C_p$  as a function of temperature in the simulation of the process as shown in Figure 5.10.

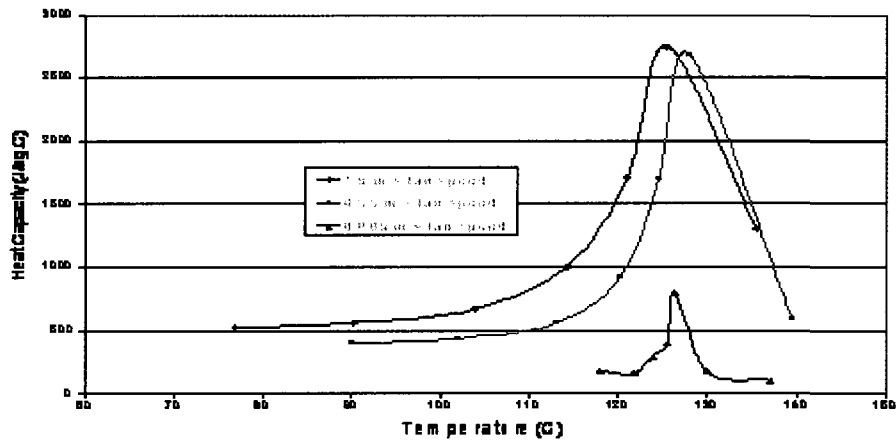


**Figure 5- 7:** Experimental heat capacity curves determined by different cooling rates obtained by varying fan speed and unadjusted Reynolds number (for bottom heating at 280°C) (Zhang, 2004).

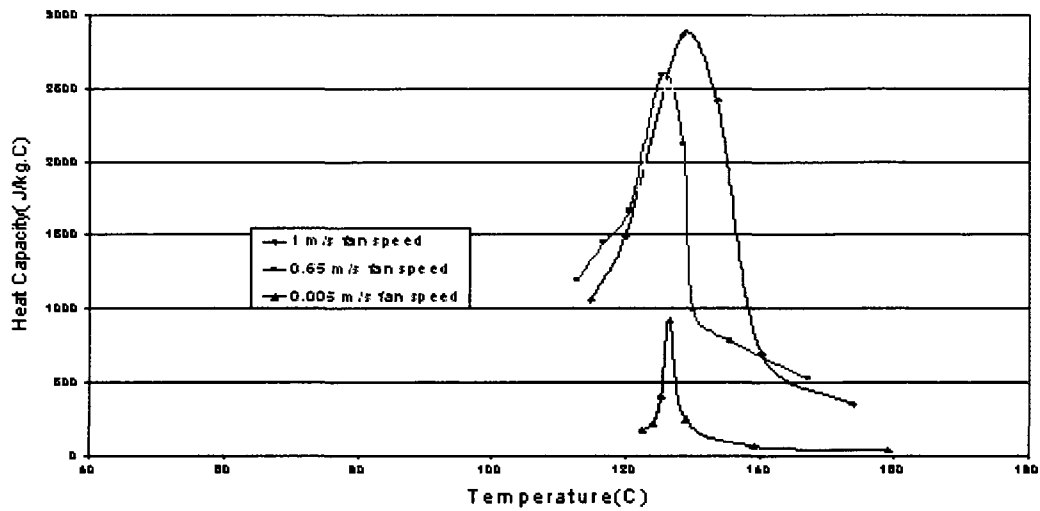


**Figure 5- 8:** Experimental heat capacity curves determined by different cooling rates obtained by varying fan speed and unadjusted Reynolds number (for bottom heating at 320°C) (Zhang, 2004).

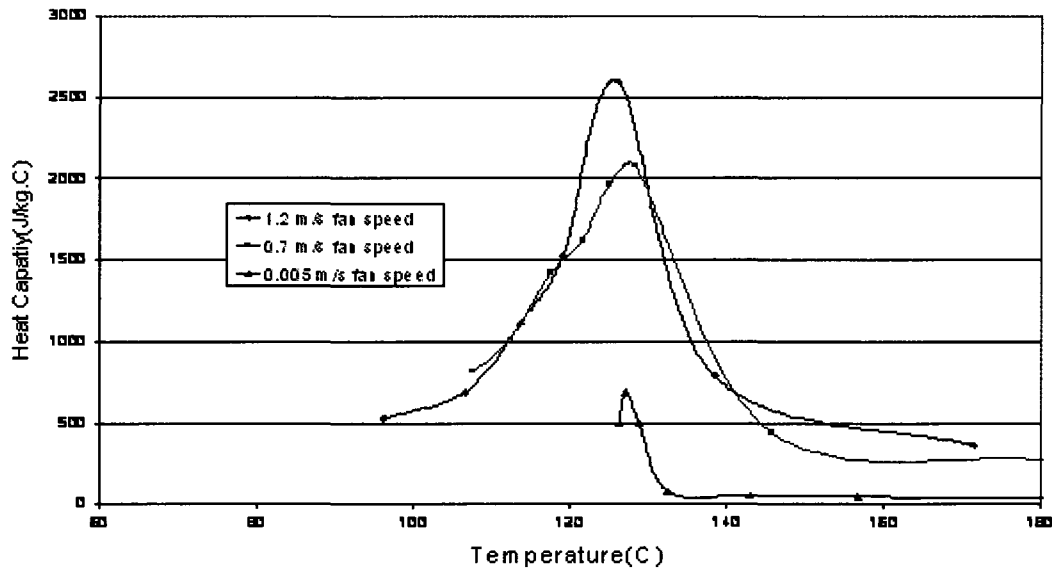


**Figure 5- 9:** Experimental heat capacity curves determined by different cooling rates obtained by varying fan speed and unadjusted Reynolds number (for bottom heating at 420°C) (Zhang, 2004).

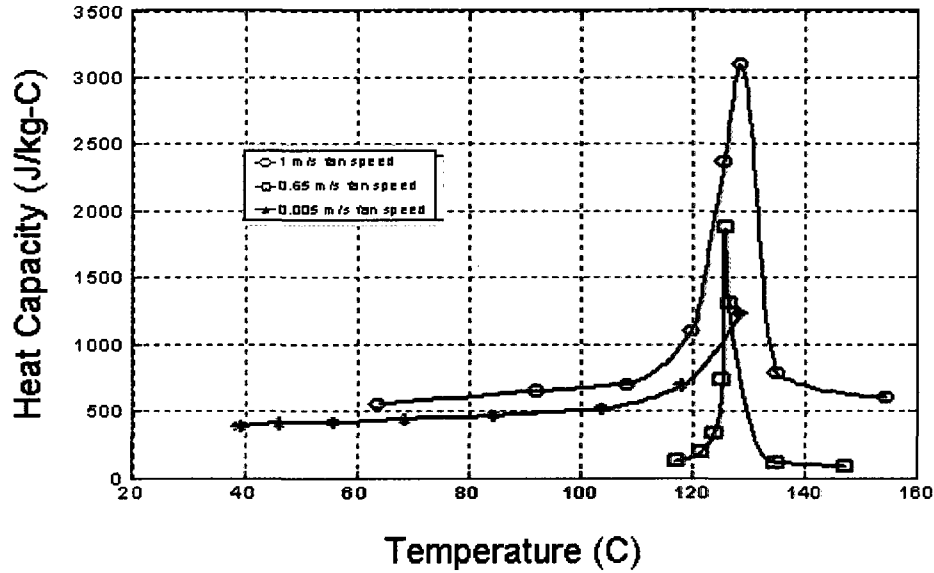


**Figure 5- 10:** Experimental heat capacity curves by using Matlab program for the top heating at 280°C with regard to three levels of fan (Zhang, 2004).

Another relation in Equation 4.40 is proposed by Woo et al. (1995) that is also useful to estimate heat capacity for HDPE as a function of temperature for HDPE.

$$C_p = 2.25 \left[ 1 + 5.5 \exp \left( - a (T - 135) \right)^2 \right] \quad (5.40)$$

where ,

$$a = 0.005 \text{ for } (T \leq 135 \text{ } ^\circ\text{C})$$

$$a = 0.05 \text{ for } (T > 135 \text{ } ^\circ\text{C})$$

The values of  $C_p$  (J/g- °C) from both the above methods are found close to each other for all practical purposes. In this work, Zhang’s software is used to calculate the temperature dependent value of  $C_p$  during simulation.

### 5.5.2 Density

The density of polymers changes considerably with temperature and changes differently below and above melting point (Woo et al., 1995). The following correlations are found for HDPE by Woo et al. (1995)

$$\frac{1}{\rho} = 1.05 \exp(0.00136 T) \quad (T \leq 135 \text{ }^\circ\text{C}) \quad (5.41a)$$

$$\frac{1}{\rho} = 1.14 + 0.0009 T \quad (T > 135 \text{ }^\circ\text{C}) \quad (5.41b)$$

where T is the temperature in  $^\circ\text{C}$  and density ( $\rho$ ) is in  $\text{g/cm}^3$ .

The above relations are used to predict the density of HDPE sheet during simulation. The temperature T during simulation is the sheet layer temperature calculated at the previous instant of simulation for the same layer.

### 5.5.3 Thermal Conductivity

In polymers, morphology (crystallinity and orientation), formulation (additives, filler and impurities), humidity, temperature and pressure are the most important factors that affect the thermal conductivity. But this very discussion is limited to consider only the effect of temperature on thermal conductivity. The thermal conductivity in polymer is greatly affected by crystallinity limit in polymer and is therefore treated differently for crystalline or semi-crystalline materials and amorphous materials.

## Crystalline Materials

In crystalline and semi-crystalline materials the thermal conductivity is almost a linear function of temperature as shown in Figure 5.11 in the range of  $T_g$  which is usually the working temperature for thermoforming process (Santos, 2005). This linear behavior can be formulated as a straight line equation (Equation 5.42) as shown in Figure 5.12.

$$k = -0.0022 T + k_0 \quad (5.42)$$

where ,  $k_0 = 0.6126 \text{ W / mK}$

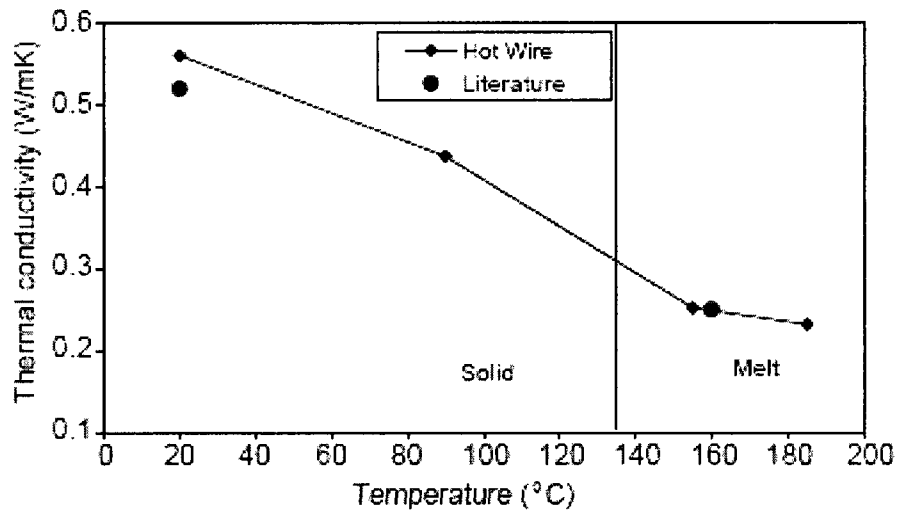


**Figure 5- 11:** HDPE thermal conductivity variation with temperature (Santos, 2005).

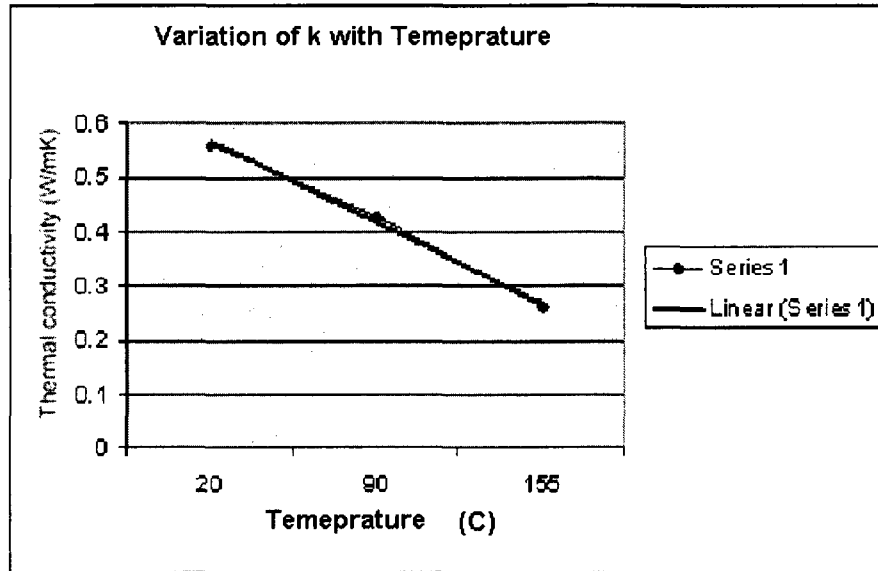


**Figure 5- 12:** HDPE fit for thermal conductivity

### Amorphous Materials

The thermal conductivity of amorphous materials can be predicted as a function of temperature if measured with respect to some reference temperature with the help of the following two equations suggested by Bicerano (1993).

$$k_T = k_{T_g} \left( \frac{T}{T_g} \right)^{0.22}, T \leq T_g \quad (5.43)$$

$$k_T = k_{T_g} \left[ 1.2 - 0.2 \left( \frac{T}{T_g} \right) \right], T > T_g \quad (5.44)$$

Where  $k_T$  is the thermal conductivity at any required temperature  $T$  in  $^{\circ}\text{C}$ ,  $k_{T_g}$  is the thermal conductivity at glass transition temperature. The relations in 5.43 and 5.44 are used to calculate the thermal conductivity of HDPE sheet during simulation. The

temperature  $T$  during simulation is the sheet layer temperature calculated at the previous instant of simulation for the same layer.

### 5.5.4 Thermal Diffusivity

Another more comprehensive parameter that accounts for physical properties of sheet material is thermal diffusivity. The variation in thermal diffusivity with temperature is shown in Figure 5.13. The variation in thermal diffusivity with temperature can be modeled with straight line equation 5.45 as shown in Figure 5.14 for HDPE.

$$\alpha = -0.02T + \alpha_0 \quad (5.45)$$

where,  $\alpha_0 = 4.205 \times 10^{-7} \text{ m}^2 / \text{s}$

The relation in Equation 5.44 is used in simulation to calculate the temperature dependent thermal diffusivity of HDPE sheet during simulation. The temperature  $T$  during simulation is the sheet layer temperature calculated at the previous instant of simulation for the same layer.

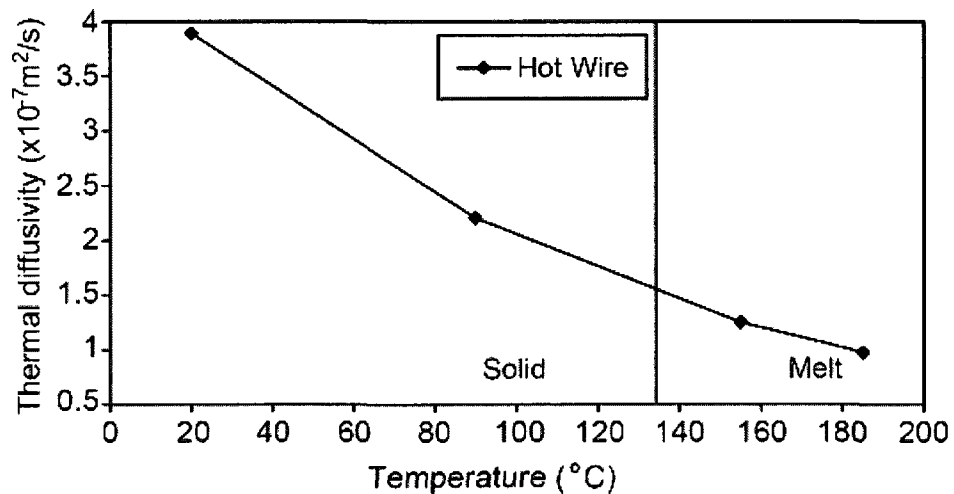


**Figure 5- 13:** Variation in Thermal Diffusivity with temperature for HDPE (Santos, 2005).

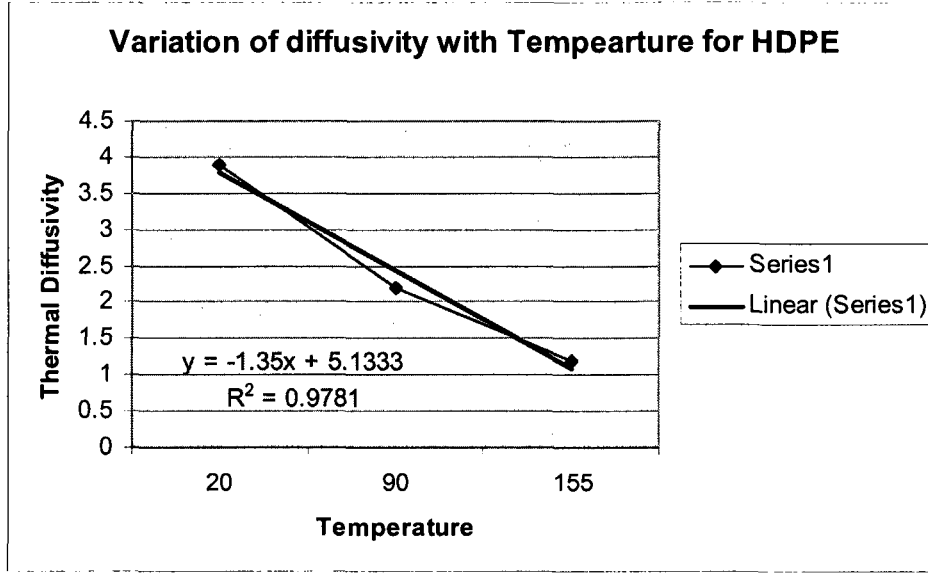


**Figure 5-14:** Fit for variation in thermal diffusivity with temperature.

The model in equation (4.7) for variable material properties can be written as:

### Surface layers

$$\frac{dT_{im}}{dt} = \frac{2}{\rho_m C_{p_m} dz_i} \left[ (Q_{T_{im}} + Q_{B_{im}}) + h(T_{\infty_m} - T_{im}) + k_m \frac{dT_{i(m,m-1)}}{dz_i} \right] \quad (5.46)$$

for  $m \in 1, 5$ .

### Interior layers

$$\frac{dT_{im}}{dt} = \frac{1}{\rho_m C_{p_m} dz_i} \left[ k_m \frac{dT_{i(m-1,m)}}{dz_i} - k_m \frac{dT_{i(m,m+1)}}{dz_i} + (Q_{T_{im}} + Q_{B_{im}}) \right] \quad (5.47)$$

for  $m \in 2, 3, 4$ , where

$$C_{p_m} = 2.25 \left[ 1 + 5.5 \exp(-a(T_m - 135))^2 \right]$$

$$a = 0.005 \quad \text{for} \quad (T_m \leq 135^\circ C)$$

$$a = 0.05 \quad \text{for} \quad (T_m > 135^\circ C)$$

$$k_m = -0.0022T_m + k_0$$

$$\text{where} \quad k_0 = 0.6126 \text{ W / m - K}$$

$$\frac{1}{\rho_m} = 1.05 \exp(0.00136T_m) \quad \text{for} \quad (T_m \leq 135^\circ C)$$

$$\frac{1}{\rho_m} = 1.14 + 0.0009T_m \quad \text{for} \quad (T_m > 135^\circ C)$$

## 5.6 Numerical Modeling

The sheet model becomes highly non linear when considered with the variable material properties and cannot be solved exactly. Therefore numerical techniques are needed to solve the model. There is large number of numerical techniques available in literature that can be used to solve this problem. After a careful survey of different techniques, a finite difference method called “Simple Explicit Method” is selected. This selection is made for two reasons:

- 1) Ease and simplicity of the method to apply to this particular situation.
- 2) Error level;  $O(\Delta t, \Delta x^2)$  i-e this technique has zero error for systems with first level of time derivative and second level of space derivative.

The only disadvantage of this model is that it poses limitation on time interval that is

$$\Delta t \leq \frac{(\Delta z)^2}{2\alpha}$$

In order to apply simple explicit method for the sheet model, control volume approach is used:

$$\underbrace{\left( \text{Rate of energy transfer through boundaries of System} \right)}_i + \underbrace{\left( \text{Rate of energy generation} \right)}_{ii} = \underbrace{\left( \text{Rate of increase of internal energy} \right)}_{iii}$$

Using the above equation, two possibilities arise for the sheet heating model in question:

1. When the sheet surface temperature is known from the IR sensors.
2. When the surface temperature is not known but the boundary conditions are known.

### 5.6.1 Model When Sheet Surface Temperature is known

In this case the sheet surface (top and bottom layer) temperatures are known through IR sensors and only the interior layers temperature is required. The model can be written as:

Internal layers temperature

$$\rho_i C_{p_i} \frac{T_m^{\theta+1} - T_m^\theta}{\Delta t} = \frac{1}{\Delta z} \left[ k_i \frac{T_{m+1}^\theta - T_m^\theta}{\Delta z} + k_i \frac{T_m^\theta - T_{m-1}^\theta}{\Delta z} \right] + \dot{q}_{abs}$$

Rearranging the above equation:

$$T_m^{\theta+1} = \frac{\Delta t}{\rho_i C_{p_i} \Delta z_i} \left[ k_i \frac{T_{m+1}^\theta - T_m^\theta}{\Delta z_i} + k_i \frac{T_m^\theta - T_{m-1}^\theta}{\Delta z_i} \right] + \frac{\Delta t}{\rho_i C_{p_i}} \dot{q}_{abs} + T_m^\theta$$

and solution for  $T_m^{\theta+1}$  is:

$$T_m^{\theta+1} = \frac{k_i \Delta t}{\rho_i C_{p_i} \Delta z_i^2} [T_{m+1}^\theta + T_{m-1}^\theta] + \left[ 1 - 2 \frac{k_i \Delta t}{\rho_i C_{p_i} \Delta z_i^2} \right] T_m^\theta + \frac{\Delta t}{\rho_i C_{p_i} \Delta z_i} \dot{q}_{abs}$$

The equation for sheet model can be written as

$$T_m^{\theta+1} = \frac{\alpha_{im} \Delta t}{\Delta z_i^2} [T_{m+1}^\theta + T_{m-1}^\theta] + \left[ 1 - 2 \frac{\alpha_{im} \Delta t}{\Delta z_i^2} \right] T_m^\theta + \frac{\alpha_{im} \Delta t}{k_{im} \Delta z_i} \dot{q}_{abs} \quad (5.48)$$

Where

$$k_{im} = -0.0022 T_{im} + 0.6126 \text{ W / mK} \quad (5.49a)$$

$$\alpha_{im} = -0.02 T_{im} + 4.205 \times 10^{-7} \text{ m}^2 / \text{s} \quad (5.49b)$$

$\theta$  = simulation step

In simulation,  $\theta$  is the time interval at which temperature values are recorded during experiments.

## 5.6.2 Model When Sheet Surface Temperature is Not Known

In the case where sheet surface temperature cannot be measured through IR sensors, the model can be written as follows:

### Exterior layers

$$\underbrace{\left( Ah(T_{air} - T_m^\theta) + Ak_i \frac{T_{m+1}^\theta - T_m^\theta}{\Delta z} \right)}_I + \underbrace{\left( A \frac{\Delta z}{2} \dot{q}_{abs} \right)}_{II} = \underbrace{\left( A \frac{\Delta z}{2} \rho_i C_{p_i} \frac{T_m^{\theta+1} - T_m^\theta}{\Delta t} \right)}_{III}$$

The solution for  $T_m^{\theta+1}$  is:

$$T_m^{\theta+1} = \left[ 1 - 2 \frac{\alpha_{im} \Delta t}{\Delta z_i^2} \left( 1 + \frac{h \Delta z_i}{k_{im}} \right) \right] T_m^\theta + 2 \frac{\alpha_{im} \Delta t}{\Delta z_i^2} T_{m+1}^\theta + 2 \frac{\alpha_{im} \Delta t}{\Delta z_i^2} \frac{h \Delta z_i T_{air}}{k_{im}} + \frac{\alpha_{im} \Delta t}{k_{im}} \left( \dot{q}_{rad} \right) \quad (5.50)$$

Where

$$T_m^{\theta+1} = \left[ 1 - 2s \left( 1 + \frac{h \Delta z_i}{k_{im}} \right) \right] T_m^\theta + 2s T_{m+1}^\theta + 2s \frac{h \Delta z_i T_{air}}{k_{im}} + \frac{\alpha_{im} \Delta t}{k_{im}} \left( \dot{q}_{rad} \right)$$

$$s = \frac{\alpha_{im} \Delta t}{\Delta z_i^2}$$

### Interior layers

$$T_m^{\theta+1} = \frac{\alpha_{im} \Delta t}{\Delta z_i^2} [T_{m+1}^\theta + T_{m-1}^\theta] + \left[ 1 - 2 \frac{\alpha_{im} \Delta t}{\Delta z_i^2} \right] T_m^\theta + \frac{\alpha_{im} \Delta t}{k_{im} \Delta z_i} \dot{q}_{abs} \quad (5.51)$$

The values of  $k_{im}$  and  $\alpha_{im}$  remain same as given by Equation 5.49.

The above model is simulated in Matlab, compared with experimental results and the findings are discussed in the next chapter. In some of simulations, instead of thermal diffusivity, the value of Cp, density and k are used.

## 5.7 Sheet Heating Model with Exact Solution to Conduction Equation

In previously discussed models it was assumed that the mode of heat transfer is steady state in the case of conduction. But in fact the temperature gradient remain non linear throughout the sheet especially in the first half of the sheet heating cycle. This means that the heat transfer to the sheet is transient in nature rather than steady state and needs to be

calculated with transient heat equation. The general heat transfer equation with transient heat conduction has exact solution as represented by Equation 4.7 in Chapter 4.

The transient conduction Equation 4.7 with convection as the boundary condition is used for the sheet model to estimate the temperature of the internal layers of the sheet. The radiation term is added to the conduction term following the superposition law. The two conditions that need to be satisfied to use Equation 4.7 are discussed in the following lines.

1. Equation 4.7 works well for the conditions where there is not large difference between the temperature of surface and interior of body during heating or cooling of body. In this case due to radiation absorption the sheet internal temperature increases rapidly and the difference remains small as shown in figure 5.5 reported by Kumar (2005).
2. The second condition, that is an extension of the first, is that

$$\frac{h(V/A)}{k} < 0.1$$

where V is the volume and A is the area of the body. In this case the volume to area ratio for sheet will result in depth of sheet i-e  $\Delta z$ . If h and k are known for some particular condition, the  $\Delta z$  can be found for that very condition. In other words, this will be the maximum depth of body across which Equation 4.7 is able to yield satisfactory results.

To estimate the value of sheet thickness that satisfy the above conditions, values of h and k are needed. The values of k for HDPE sheet are shown in Figure 5.12 and it can be seen

that it varies with temperature from 0.62 to 0.25 W/m-K. The coefficient of convection heat transfer  $h$  is more difficult to determine as it has different values on upper and lower side of sheet in oven (Yousefi, 2002). It is found that the value of  $h$  varies from 2 to 3.5 W/m<sup>2</sup> K for lower side and from 6.5 to 7.5 W/m<sup>2</sup>K for upper side (Yousefi, 2002) for natural convection conditions as shown in Figure 5.17. Selecting the average value of  $k = 0.405$  W/m-K and average value of  $h = 4.2$  W/m<sup>2</sup> K and inserting these values in the inequality  $\frac{h(V/A)}{k} < 0.1$  will result in  $\Delta z = 9.7\text{mm}$  i.e., Equation 4.7 can be used to estimate temperature with a reasonable accuracy to a 10mm depth in a HDPE sheet and fortunately a large number of sheets used for thermoforming are well within this thickness range.

In applying Equation 4.7 to our sheet heating model, the fact that sheet is heated from both sides should be considered. When the sheet is heated from both sides, heat flows in the sheet from top and bottom towards the middle of the sheet and there is a plane somewhere inside the sheet, depending on upper and lower oven temperatures, across which there will be no transfer of heat. If it is assumed that the upper and lower oven temperatures are same, then this plane should be in the middle of the sheet i-e at the depth of 6mm for a 12mm thick sheet. Thus in case of both side of heating, sheet is considered as two semi infinite bodies placed together such that they have a perfect contact at the plane of contact which is also the neutral plane as shown in Figure 5.15.

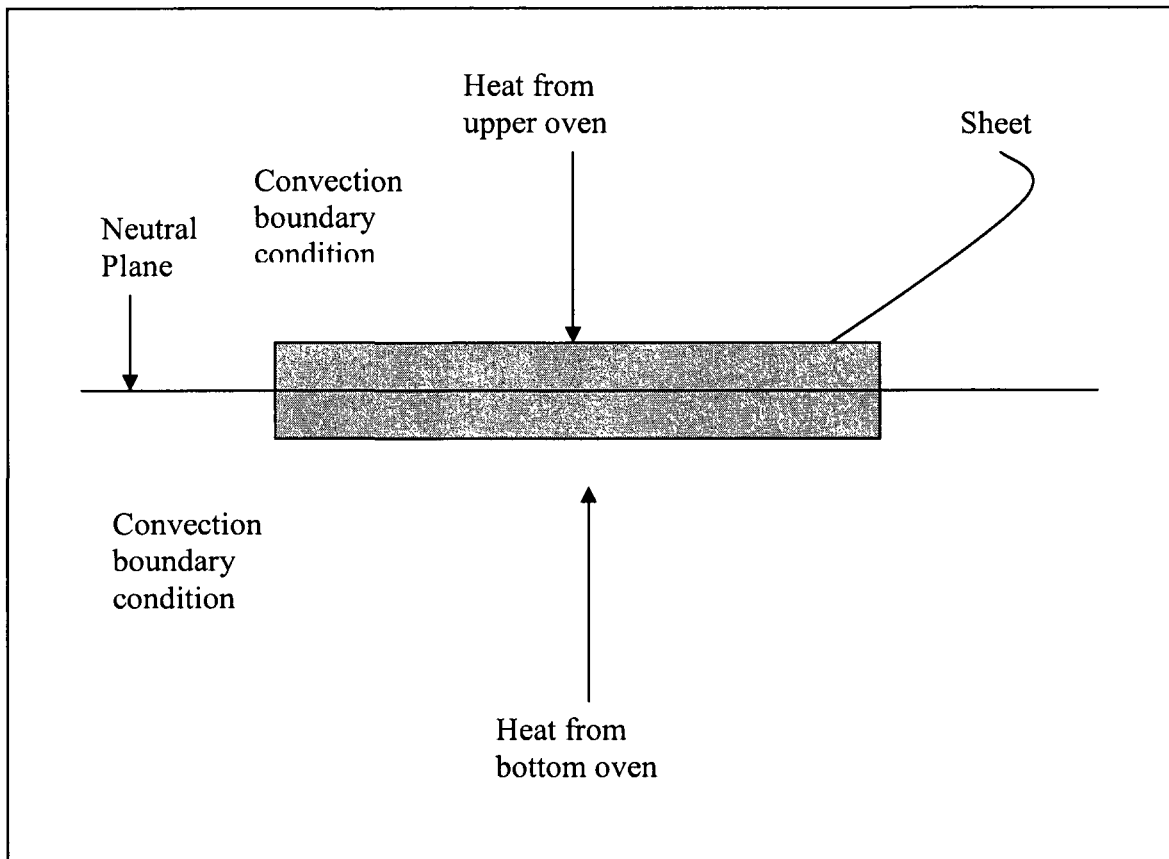


**Figure 5-15:** Sheet model for transient heating with neutral plane at the center

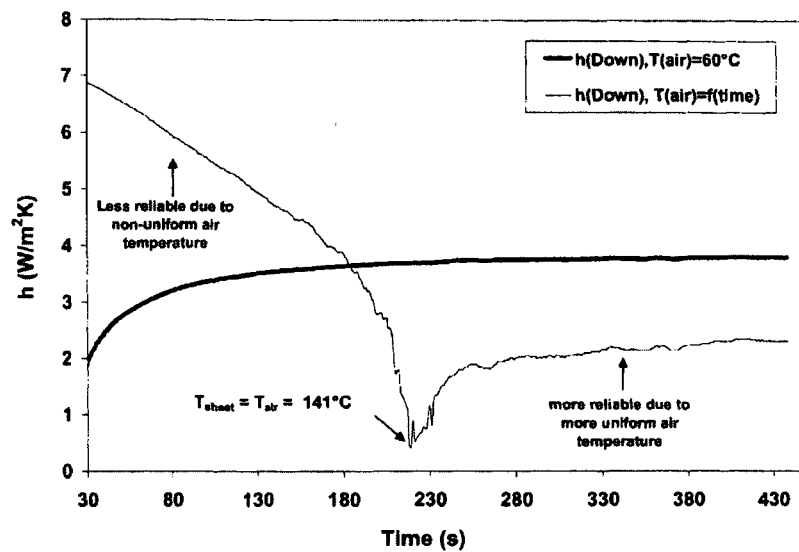


**Figure 5-16:** Transient heat transfer coefficient for the lower side of the sheet for transient and constant air temperature (Yousefi, 2002).

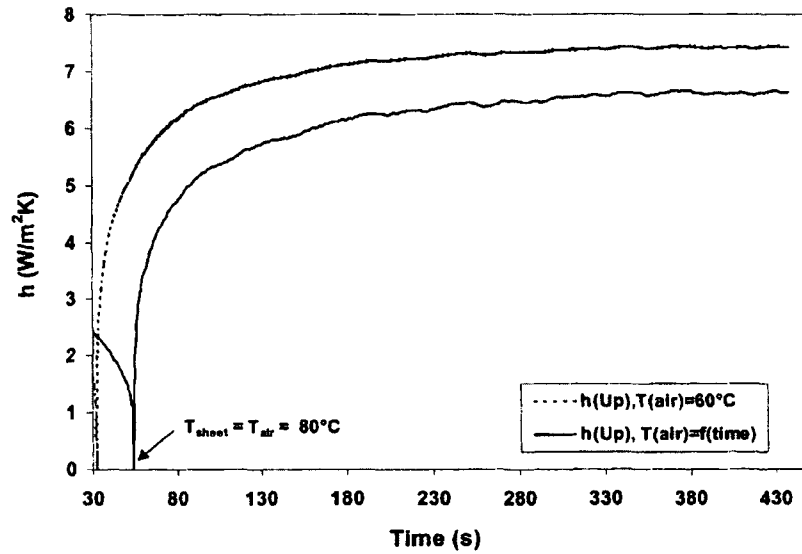


**Figure 5-17:** Transient heat transfer coefficient for the upper side of the sheet for transient and constant air temperature (Yousefi, 2002).

The boundary condition for sheet inside oven is convection heating. The initial and boundary condition for sheet can be written as:

$$T(z,0) = T_i$$

$$hA(T_\infty - T)_{z=0} = -kA \left. \frac{\partial T}{\partial x} \right|_{z=0}$$

The solution to equation 5.6 with the above initial and boundary is given as follows by

Holman (1997)

$$\frac{T(z,t) - T_i}{T_{air} - T_i} = 1 - \operatorname{erf} \frac{\Delta z}{2\sqrt{\alpha t}} - \left[ \exp\left(\frac{h\Delta z}{k} + \frac{h^2 \alpha t}{k^2}\right) \right] \times \left[ 1 - \operatorname{erf}\left(\frac{\Delta z}{2\sqrt{\alpha t}} + \frac{h\sqrt{\alpha t}}{k}\right) \right] + \frac{\alpha t}{k} (Q_{T_m} + Q_{B_m}) \quad (5.52)$$

Where  $T_i$  is the initial temperature of the sheet and the absorption term is added to the equation by assuming law of superposition. The above model is simulated in Matlab and

simulation results are compared with the experimental results and discussed in the next chapter.

## 5.8 Convection Heat Coefficient and Its Effect on Thermoforming

The convection heat coefficient is an important factor that influences convection heat transfer to the sheet surface. It depends on the air moment inside the thermoforming oven. In order to calculate the effect of air velocity, experiments are performed by blowing an auxiliary fan across the oven with different fan speeds. The air velocity is calculated by using anemometer. Based on these experiments, Zhang (2004) has derived the following relation for convection heat transfer coefficient

$$\bar{h} = 2 \frac{K}{L} \overline{Nu}_x \quad (5.53)$$

Where

$$\overline{Nu}_x = \frac{h_x L}{K} = 0.453 \text{Re}_x^{1/2} \text{Pr}^{1/3}$$

$$\bar{h} = 2h_x$$

$$\text{Re}_x = \frac{u_\infty L}{\nu}$$

$u_\infty$  is the air velocity,  $\nu$  is the kinematic viscosity of air,  $L$  is the sheet length,  $\text{Re}_x$  is the Reynolds' number,  $\overline{Nu}_x$  is the average Nusselt number,  $\text{Pr}$  is Prandtl number,  $h_x$  is the heat transfer coefficient which varies with distance  $x$ ,  $K$  is the thermal conductivity of the air.

Unfortunately the simulation results for the values of  $h$  calculated with Equation 5.53 are deviated largely from the experimental results. It is believed that the large number of

variables in Equation 5.53 and the experimental errors associated with each variable resulted in high probability of erroneous value of convection heat transfer coefficient. An empirical relation 5.54 is widely used to calculate the convection heat transfer coefficient.

$$h = 10.45 - v + 10\sqrt{v} \quad (5.54)$$

where  $v$  is the air velocity in m/s.

This relation incorporates the effect of air velocity in calculating convection heat transfer coefficient and mainly used to estimate the “chill factor” (Tao Xiaoming, 2001). Equation 5.54 is selected to eliminate use of many variables and hence decrease the possibility of calculation and experimental errors. Simulation results agree with experimental results when simulated with the values of convection heat coefficient for different air velocities calculated with Equation 5.54 and the results are presented in Chapter 6.

To investigate the effect of convection coefficient on thermoforming reheat process, an auxiliary fan is blown at different speeds across the sheet during heating process. The fan air speed is measured with anemometer. The sheet model is simulated for different values of convection coefficient ranging from  $5 \text{ W/m}^2 \text{ K}$  to  $40\text{W/m}^2 \text{ K}$  and the results are presented and discussed in Chapter 6.

## **Chapter 6 Experimental Setup and Results**

This chapter is dedicated to describing the experimental setup, results and analyzing the models against experimental results. The experiments were performed to find the plastic sheet temperatures at different depths across the sheet thickness by inserting thermocouples while the sheet is heated to some desired temperature. The models developed in this work are simulated by using Matlab coding and are then compared with the experimental results for validation. As mentioned earlier that these results are necessary to verify accuracy of the developed models to help to establish a real time controller for thermoforming process.

All the experimental trials were conducted on standard industrial thermoforming machines located at the IMI Boucher Ville lab. The “White Sheet” experiments were performed in October 2002 by Girard et al. (Benqiang, 2003). While the “Black Sheet” experiments were performed by Girard and author. All the procedures and equipments used are same except for the plastic sheets. The experimental measurements were performed on AAA machine model MBE-2438M. The top and bottom sheet surface temperatures were measured at the middle of each zone using mounted infrared sensors of type RayMID 10-4. The sheet internal temperatures at different depths and oven air temperatures of the AAA machine were measured using J and K-type thermocouples. The ambient air velocity was also measured using anemometer.

A brief description of the equipments used in IMI for the experiments is presented in the following lines.

## 6.1 IMI Thermoforming Machine

The large scale and well equipped laboratory at the Industrial Material Institute (IMI), National Research Council Canada (NRC), located in Boucherville Montreal, Quebec, contains commercial shuttle-type thermoforming machines, manufactured by AAA Plastic Equipment Inc. in Fort Worth, Texas. The model number of the AAA machine is MBE – 2438 M. The oven of MBE-2438M has an upper and a lower heater bank of ceramic elements that are divided into 6 x 3 zones in order to control the sheet heating profile. The heaters are 650W ceramic elements.

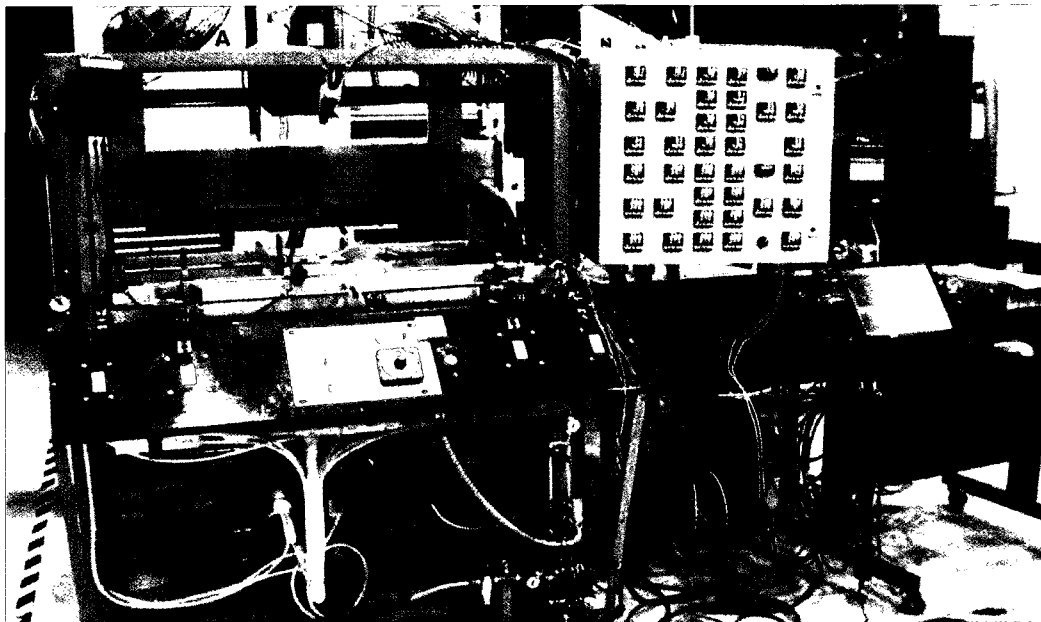


**Figure 6- 1:** AAA thermoforming machine at IMI (Benqiang, 2003)



**Figure 6- 2:** Ceramic heater elements of AAA machine (Benqiang, 2003).

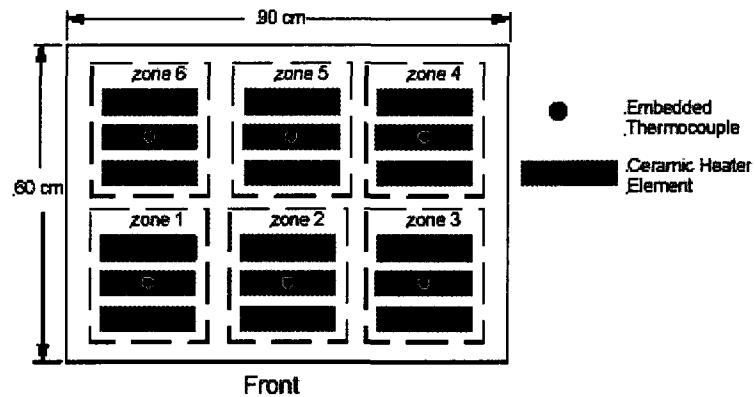


**Figure 6- 3:** Oven layout for AAA model MBE-2438 M thermoforming machine (Benqiang, 2003)

For precise temperature control, Proportional-integral-derivative (PID) controllers are used for MBE-2438 M type of thermoforming machine at IMI. The controller derivatively applies the temperature input signals to an integrator that can adjust power input ratio when the actual temperature approaches the set point.

## **6.2 Thermocouples and Infrared Sensors**

Since the experiments were performed to measure the temperature profile across the sheet thickness during heating phase of thermoforming process, the role and hence the selection of temperature sensors become very important. Due to ability to withstand high temperatures, accuracy of about 1 °C, quick response time and low cost; J and K-type thermocouples were selected to measure temperature profile inside sheet and air temperature inside the oven respectively. In order to avoid any errors that may arise by radiation from furnace heating elements, the thermocouples used to measure air temperature inside furnace were placed inside short aluminum tube open from both ends to allow air movement around the sensor. All the thermocouples used are supplied by OMEGA Engineering Inc. The sheet top and bottom surface temperatures were found using non-contact infrared sensors RayMID 10-4 IR provided by Raytek Canada. Further details about equipments can be found in reference (Benqiang, 2003)

## **6.3 Experiments**

Experiments were performed to find the temperature profile across the sheet thickness. The thermoforming machine, thermocouples and other equipment used along with procedures adopted were the same. Due to similarity of the experimental procedures and data collected, it is more convenient to present the information/data under two titles: 1) White Sheet Experiment and 2) Colored Sheet Experiment.

### **6.3.1 White Sheet Experiments**

*Material used for the experiments:* The sheets are made of high-density polyethylene (HDPE BA-50) that is used commonly in the thermoforming industry. The material

properties are summarized in Table 6.1.

**Table 6-1:** Material properties of HDPE BA-50

Length (mm)	305
Width (mm)	305
Thickness (mm)	12
Density (kg/m <sup>3</sup> )	950
Thermal conductivity (W/M/°C)	0.62
Specific heat at 180 (kJ/kg K)	2.7

*Experimental setup:* In order to measure the temperature profile across the sheet thickness, five thermocouples were inserted at depths of 1mm, 3mm, 6mm, 9mm and 11mm from the top of the sheet respectively. The temperature settings of the oven heater were 280 °C, 320 °C, 380 °C and 420 °C. To ensure reliability of data, the sheet was heated in two ways: 1) using the top heaters only, 2) using the bottom heaters only.

Five holes were drilled into the sheet to accommodate five thermocouples at depths of 1mm, 3mm, 6mm, 9mm and 11mm from the top of the sheet respectively.

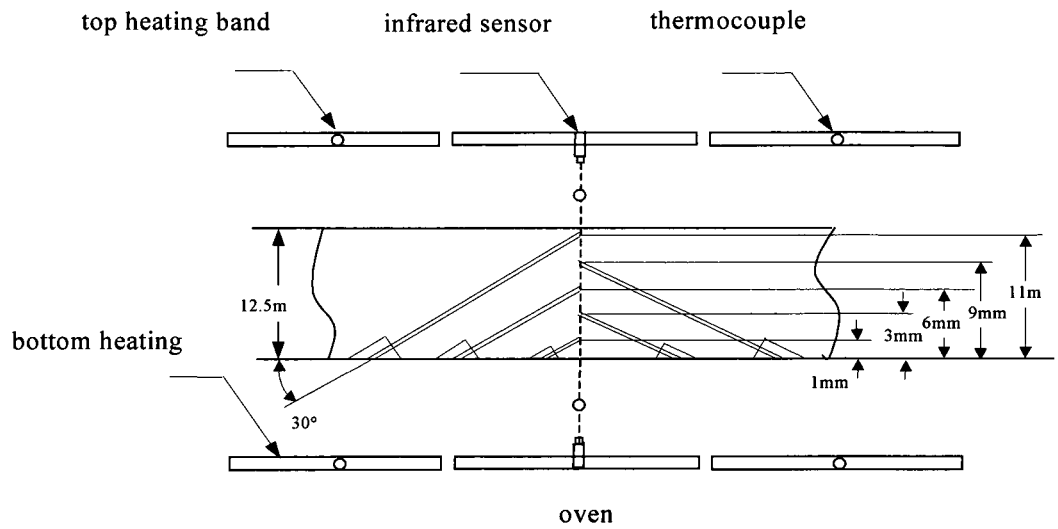


**Figure 6-4:** Experimental setup of a HDPE BA 50 sheet (Benqiang, 2003)

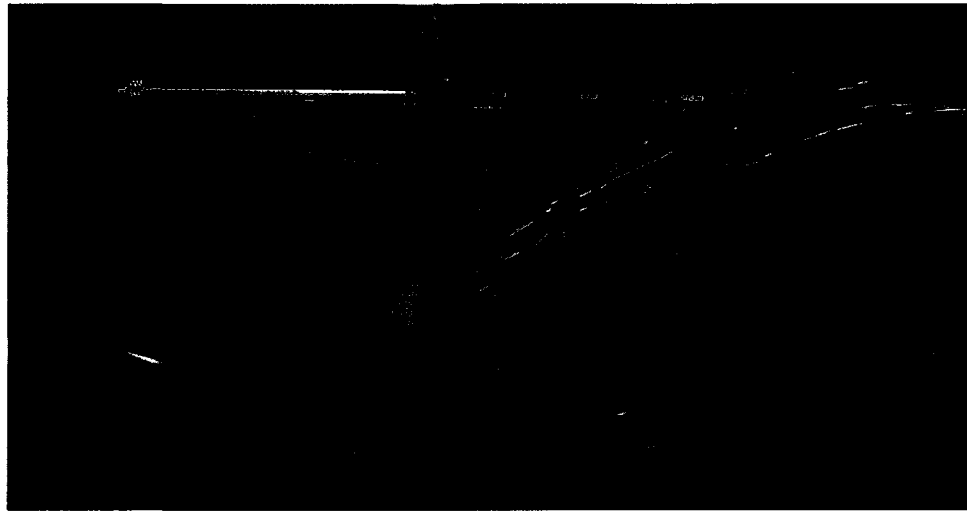


**Figure 6-5:** Sheet after heating implanted with five thermocouples (Benqiang, 2003)

The holes were drilled at an angle of  $30^\circ$  but with different drilling depths  $L$  in order to minimize heat losses near the temperature sensing tip of thermocouples. As shown in Figure 6.6, if  $L$  is the length of hole to be drilled at angle of  $30^\circ$  and  $h$  is the required depth from the top of the sheet, then the required depth of drill can be calculated as  $L = h/\sin 30^\circ$ .

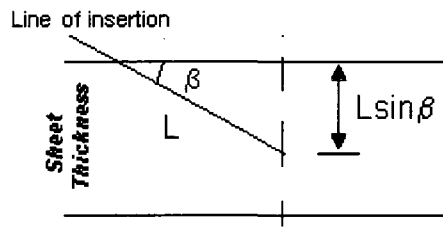


**Figure 6-6:** Length and depth of hole for thermocouple insertion (Benqiang, 2003)

In industry, the sheet is heated in an oven that is open from both ends and therefore the air velocity around the oven is an important factor. To examine the effect of different air velocities on the sheet heating process, an auxiliary fan is used to blow air into the oven at various speeds. A total of 19 experimental trials were performed.

The oven air temperature during sheet heating in thermoforming process is an important factor responsible for convection heat transfer. Oven air temperature is measured using K-type thermocouples, midway between the heaters and the HDPE sheet with the thermocouples inserted into a cylinder to avoid radiation heat disturbance that may affect the actual reading. The temperatures of both upper and lower surfaces of sheet were measured at the specified middle spots using mounted infrared sensors of type RayMID 10-4. An Agilent 34970A Data Acquisition Unit was used to log and record the temperature measurements. Each channel was logged every 0.5 second and the data was transferred to a laptop for post processing using the HP Benchlink Data Logger Software. Table 6.2 shows 19 experimental trials which were performed during October 2002 by Girard and Hou (Benqiang, 2003).

**Table 6-2:** Experimental design for October 2002 (Benqiang, 2003)

No. of test	Heater temp. setting (°C)	Fan	Top Anemometer (ft/min)	Heating time (min)	Cooling time (min)	Scan interval (s)	Remarks
<b>Top heater on</b>							
1	280	0	3	92	18	0.5	
2	280	1	200	80	13	0.5	
3	280	2	250	64	18	0.5	
4	380	0	20	42	13	0.5	
5	380	1	190	42	13	0.5	
6	380	2	300	43	13	0.5	
7	420	0	20	30	13	0.5	
8	420	1	140	26	13	0.5	
9	420	2	220	26	13	0.5	
<b>Bottom heater on</b>							
10	280	0	10	73	13	0.5	
11	280	1	110	77	13	0.5	
12	280	2	280	77	13	0.5	
13	320	0	20	45	13	0.5	
14	320	1	150	45	13	0.5	
15	320	2	200	46	13	0.5	
16	420	0	5	20	13	0.5	
17	420	1	170	20	13	0.5	
18	420	2	200	16	13	0.5	
19	420	0	10	20	13	0.5	

### 6.3.2 Black Sheet Experiment

*Material used for the experiments:* The material used is high-density polyethylene sheets that are used commonly in the thermoforming industry.

**Table 6-3:** Material properties of HDPE for Black Sheet

Length (mm)	470
Width (mm)	355
Thickness (mm)	20
Density (kg/m <sup>3</sup> )	950
Specific heat at 180 (kJ/kg K)	2.7

*Experimental setup:* In this experiment, two sheets were clamped together as shown in figure 6.7 in order to maximize the sheet thickness. To measure the temperature profile across the sheet thickness, six thermocouples were inserted at depths of 2mm, 5mm, 8mm, 12mm, 15mm and 18mm from the top of the sheet respectively. The sheet was first heated at oven temperature of 100 °C and then 120 °C. The sheet was heated from both top and bottom sides simultaneously. To ensure reliability of data, the experiment was repeated twice for each temperature. Rest of equipment and procedures remained the same as explained in white sheet experiment.

The data acquisition station Agilent 34970A was set at 10 Hz (about 3 readings per second) for the first 4 minutes of sheet heating process. The data acquisition frequency was then reset to 3 Hz (approximately 1 reading per second) for the next 26 minutes in order to accommodate longer heating period. This resetting took about two minutes while the sheet remained in the oven for this time and no data was recorded for these two minutes. After 32 minutes the sheet was removed from the oven and was cooled by fan to 20 °C and again the above procedure was repeated for 100 °C and then for 120 °C.

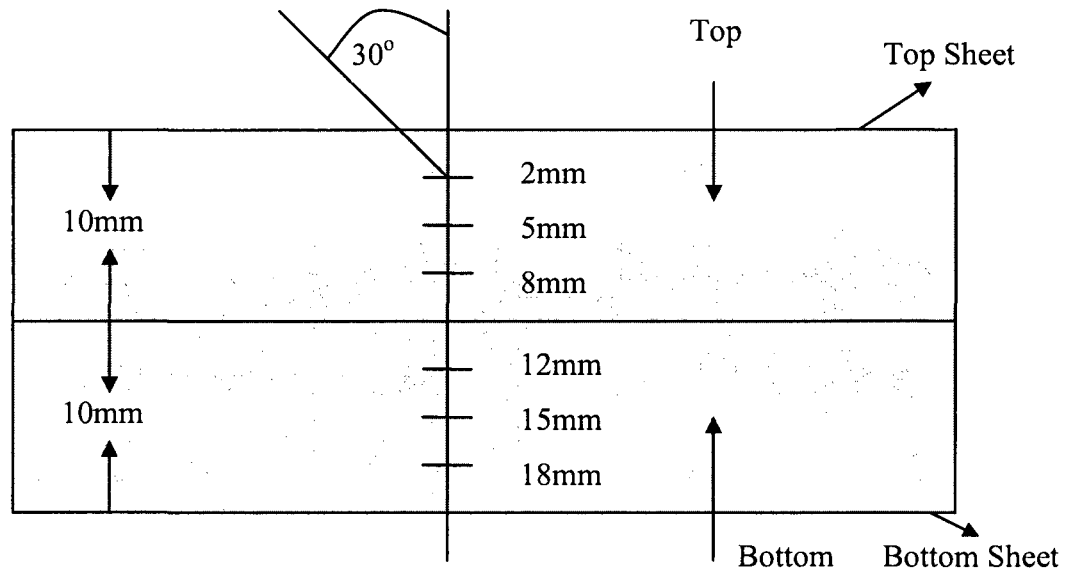


**Figure 6-7: Colored Sheet experimental setup.**

## 6.4 Oven Air Temperature

The temperature of air inside oven is also an important factor in determining the heat transfer to the sheet. The air temperature is measured by K-type thermocouple midway between the sheet and the heating banks of the oven. As mentioned before, the sensor of the thermocouple was placed inside an open tube in order to avoid radiation effects. It is worth mentioning that the air temperature on lower side of sheet is more than on the upper side during heating due to hot air drift phenomenon. Also, as the temperature is measured midway, it does not reflect the actual temperature of the air film next to the sheet surface that is causing heat transfer.

The air temperature varies throughout during sheet heating process but the variation is not more than 10 to 15 °C for a particular oven heating temperature. The oven air

temperature is considered constant in simulation and is calculated by taking an average over the recorded experimental values as shown in Table 6.4.

**Table 6-4: Experimental oven air temperatures for white sheet (Benqiang, 2003)**

No. of test	Heater temp. setting (°C)	Fan	Top Anemo meter (ft/min)	Maximum Oven Air Temperature (°C)	Minimum Oven Air Temperature (°C)	Average Oven Air Temperature (°C)	Remarks
<b>Top heater on</b>							
1	280	0	3	89.7	82	85.6	
2	280	1	200	82.7	77.7	80.8	
3	280	2	250	90.3	81.8	85.3	
4	380	0	20	124	115	121	
5	380	1	190	123	115	120	
6	380	2	300	125	114	122	
7	420	0	20	139	131	136	
8	420	1	140	140	130	135	
9	420	2	220	139	131	136	
<b>Bottom heater on</b>							
10	280	0	10	102	91.2	99	
11	280	1	110	99	92.3	96.6	
12	280	2	280	98.6	90.3	95.2	
13	320	0	20	113	96.8	109	
14	320	1	150	113	104	109	
15	320	2	200	113	100	110	
16	420	0	5	141	129	136	
17	420	1	170	146	108	133	
18	420	2	200	141	134	139	
19	420	0	10	145	129	143	

## 6.5 Results and Discussion

The proposed models presented thus far are simulated in Matlab and the simulation results are compared with the experimental results to establish the validity of models. All the models are simulated at the same conditions as was recorded during experiments.

### **6.5.1 Variable Material Properties Model**

The comparison of variable material properties model simulation results, constant properties model simulation results and experimental results are presented in Figure 6.8 through Figure 6.11. The following conclusions are obvious:

1. The comparison of the variable properties model against the constant properties model revealed a significant effect of temperature dependent properties on model predictability. The model predictability is found to be better with variable properties model as shown in Figures 6.8 and 6.9 for individual depth of different oven temperatures. More figures are given in appendix C.
2. When the model is compared against experimental data, it is found that the model fits well for lower furnace temperatures i-e for 280°C and 320°C but shows deviation as the oven temperature is increased to 380 °C and 420 °C as shown in Figures. The deviation at higher temperatures is largely due to the non linear factor of radiation heat transfer (fourth power of absolute temperature). The model predictability is well under 10 °C for most of oven temperatures but shows considerable deviation for 420 °C oven temperature as shown in Figures 6.10. More figures are presented in appendix C. This poses a challenge in implementing the model for real time controller and needs more investigation.
3. The average deviation of the variable properties model in comparison to constant properties model for 3mm, 6mm, and 9mm depths at different sheet temperatures are shown in figure 6.11. More can be found in appendix C. The deviation at different sheet depths increases from 5 °C to 35 °C as the oven temperature

increases from 280 °C to 420 °C. This variation is significant as the forming window for HDPE is only 20 °C and an error of 10 °C can result in burning the sheet surface and hence in a rejected part. This situation can give rise to a complete failure of the model when implemented for real time controller. This situation is expected to worsen and generate more waste in materials which have a forming window in range of a few degrees centigrade. As a rough rule of thumb, a 10 °C rise in sheet temperature for any depth leads to one degree of temperature deficiency between the two models. Therefore use of a variable material properties model is strongly recommended.

4. It is also observed that the proposed variable properties model fits better for bottom heating than the top heating for same oven temperatures. This can be attributed to the fact that during bottom heating, due to hot air drift, the oven air temperature is higher and more uniform near the sheet bottom surface and results in more uniform convection heating of sheet lower surface.

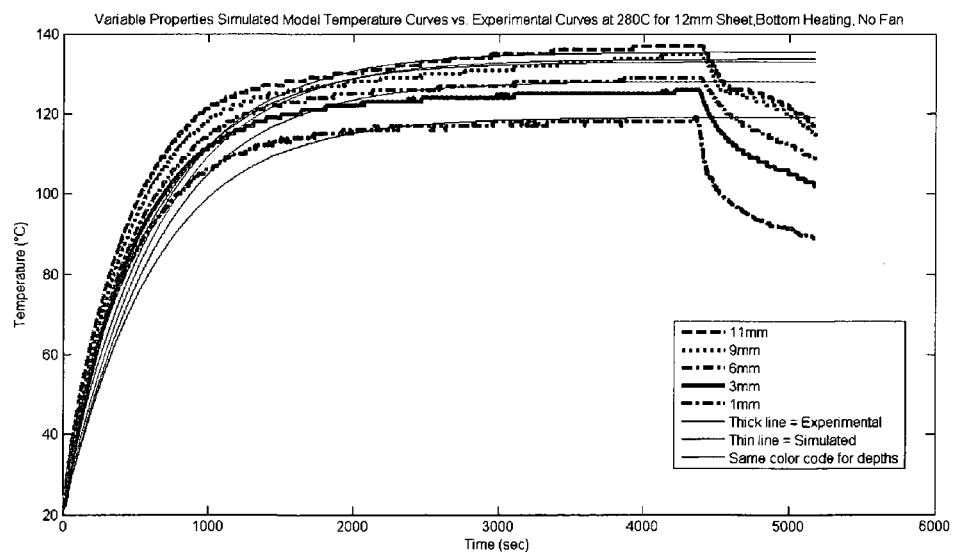


**Figure 6-8:** Comparison of simulation model results against experimental result.

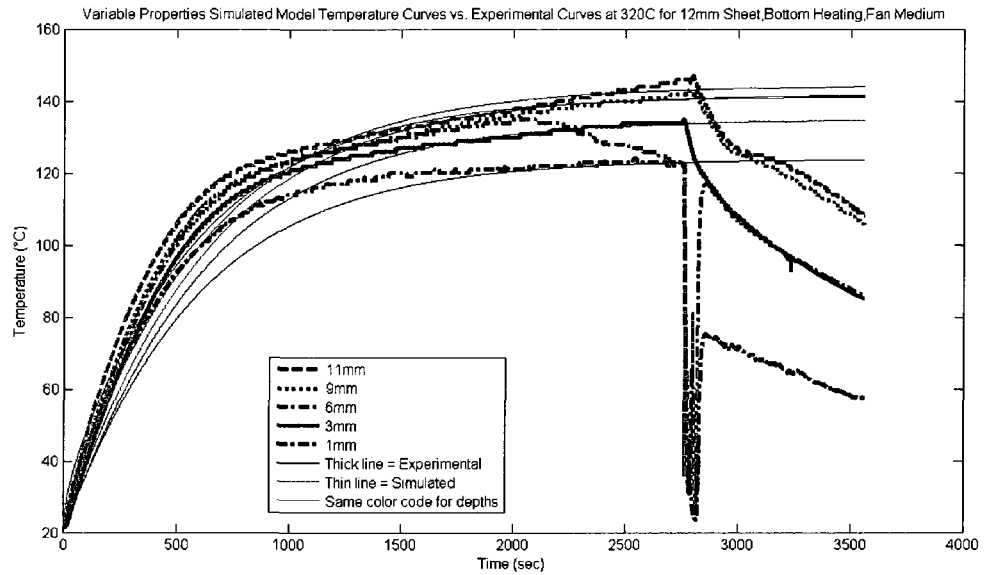


**Figure 6-9:** Comparison of simulation model temperature against experimental result.

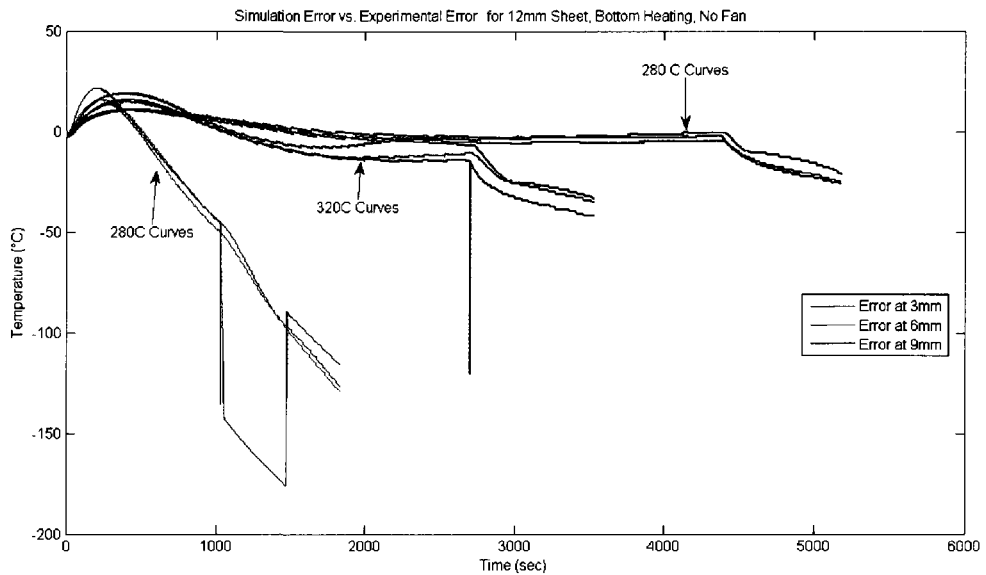


**Figure 6-10:** Comparison of simulation model and experimental results at different oven temperatures.

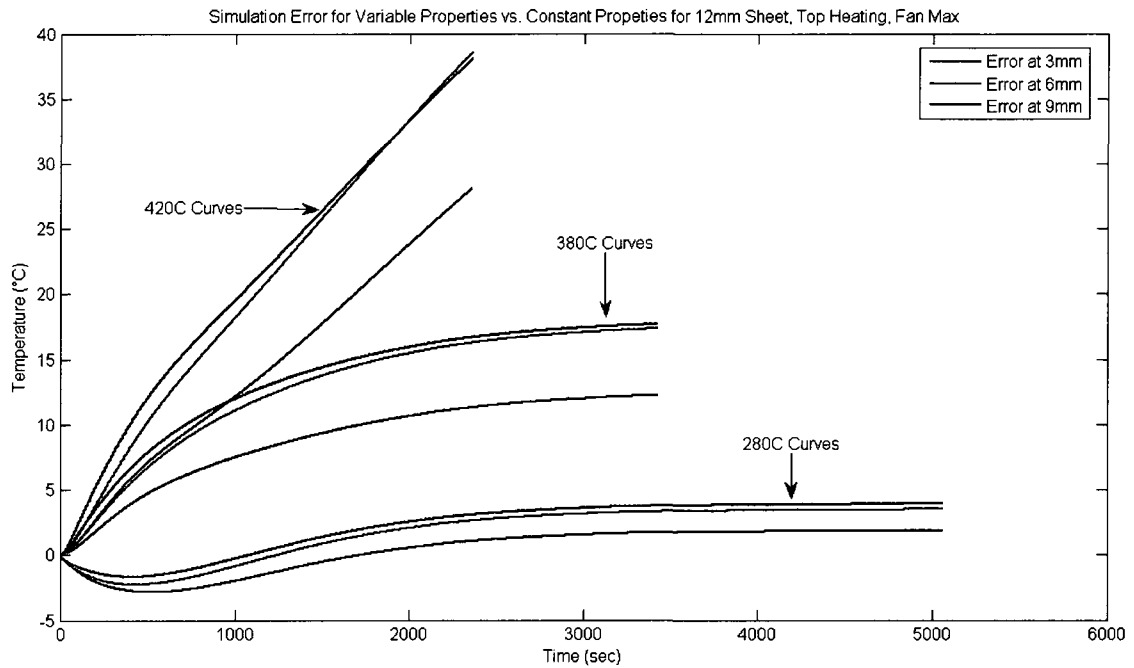


**Figure 6-11:** Difference of variable properties model and constant properties model at different oven temperatures.

### 6.5.2 Sheet Heating Model with Exact Solution to the Heating Equation

The model with exact solution to heat equation presented in equation 5.52 is simulated in Matlab and compared with the experimental results. The conclusions are summarized in the following lines:

1. The model with exact solution to the heat equation shows a slower response at the start of heating phase but start predicting very high sheet temperature values as compared to experimental value (in excess of 50 °C) after sheet temperature exceeds 80 °C as shown in Figure 6.12. More figures are given in appendix C. This behavior of the exact model can be explained on the basis of convection heat transfer inside oven. This model is unable to incorporate the fact that when the sheet temperature rises than oven air temperature, the convection started cooling

the sheet rather than heating and the curves become flat. This model assumes that the boundary condition is always such that the heat is flowing into the sheet.

2. Another drawback of exact model is that due to mathematical methods constraints, the heat equation cannot be solved simultaneously for variable material properties of the sheet and variable boundary condition. Even there is no exact solution available to the heat equation when all the considered properties of sheet material are taken as function of temperature simultaneously. It is therefore recommended to avoid using the exact model with convection as boundary conditions.

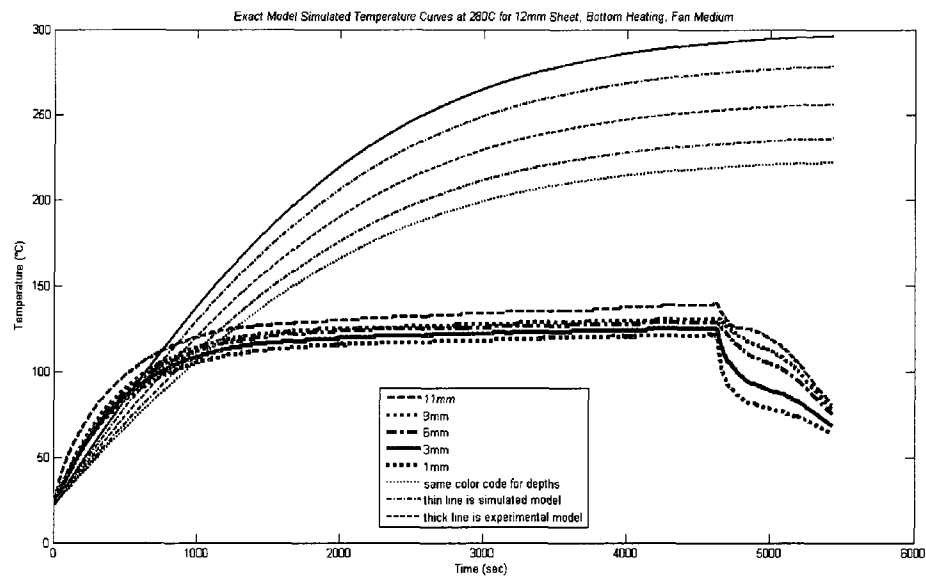


**Figure 6-12:** Exact model simulation vs. experimental data.

### 6.5.3 Sheet Color Based Model

In all the previously described models and experiments, white or semi transparent sheet is used. In order to investigate the effect of sheet color on proposed model, experiments are performed with a black color sheet. The results are summarized in the following lines:

1. It can be inferred from results that the radiation factor is less dominant inside sheet in black sheet than white sheet. In Figures 6.13 and 6.14, it can be seen that the experimental curves are better represented by radiation model near the sheet surface where as the experimental curves are more closely represented by conduction model toward the depth of the sheet. This clearly establishes that the radiation heating is less dominant factor in colored sheet heating than “white Sheet or Transparent Sheet”. Further results are given in appendix C.
2. The temperature difference for the same depth from top and bottom surfaces is shown in Figures 6.15 and 6.16. The temperature difference at different depths increases considerably from 5 °C to 20 °C with the increase in oven temperature from 100 °C to 120 °C. This also establishes the fact that heat propagation inside the sheet is dominated by conduction heat transfer which is a “slower” heating process as compared to radiation. Thus black sheet would need more time than the same white sheet to bring the sheet into forming window for shaping. Further results are presented in appendix C.
3. Another important fact that can be established from Figures 6.15 and 6.16 is that the temperature difference between top side heating and bottom side heating due

to hot air drift should be considered more seriously in black sheet. At higher oven temperatures this difference can cause significant difference in sheet temperatures between sheet surfaces and hence leads to overheating of bottom surface of sheet. It is therefore advised to consider different top and bottom oven bank temperatures for black sheet. Further results are presented in appendix C.

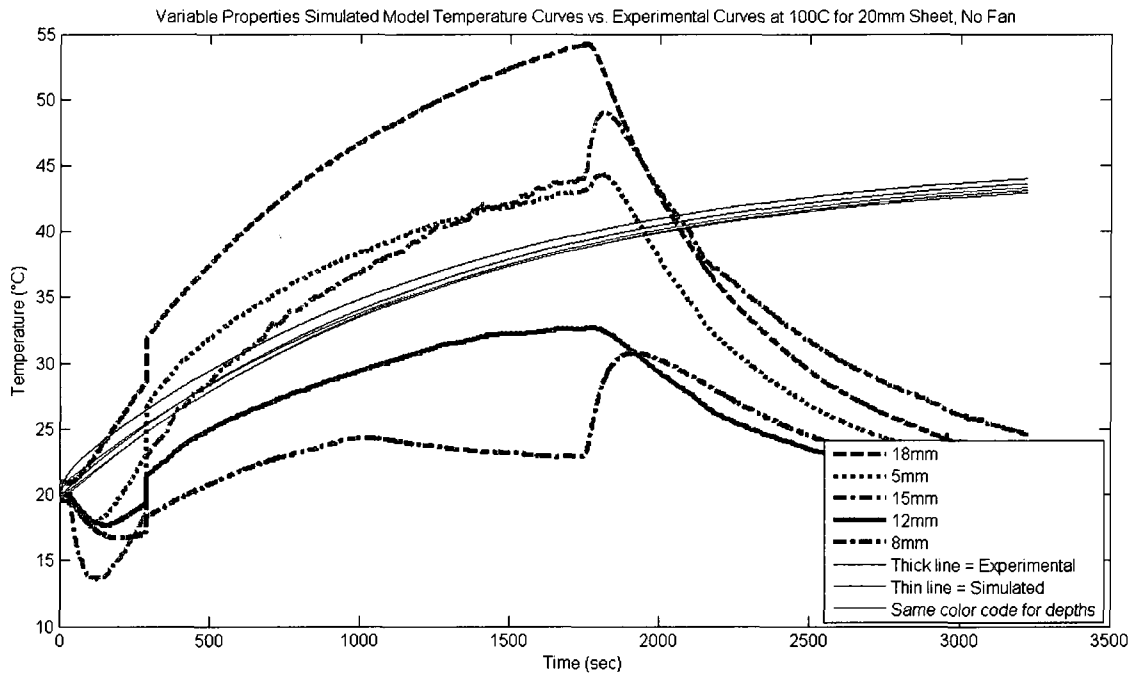


**Figure 6-13:** Colored Sheet combined models simulation vs. experimental data.

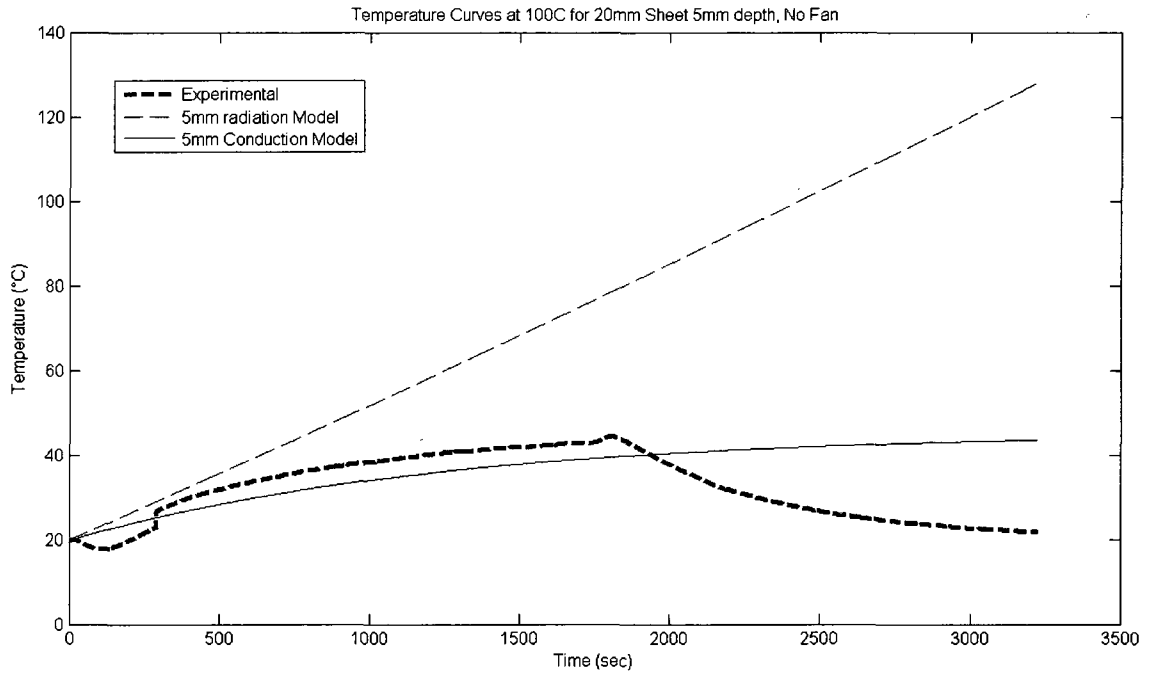


**Figure 6-14:** Colored Sheet models simulation vs. experimental data.

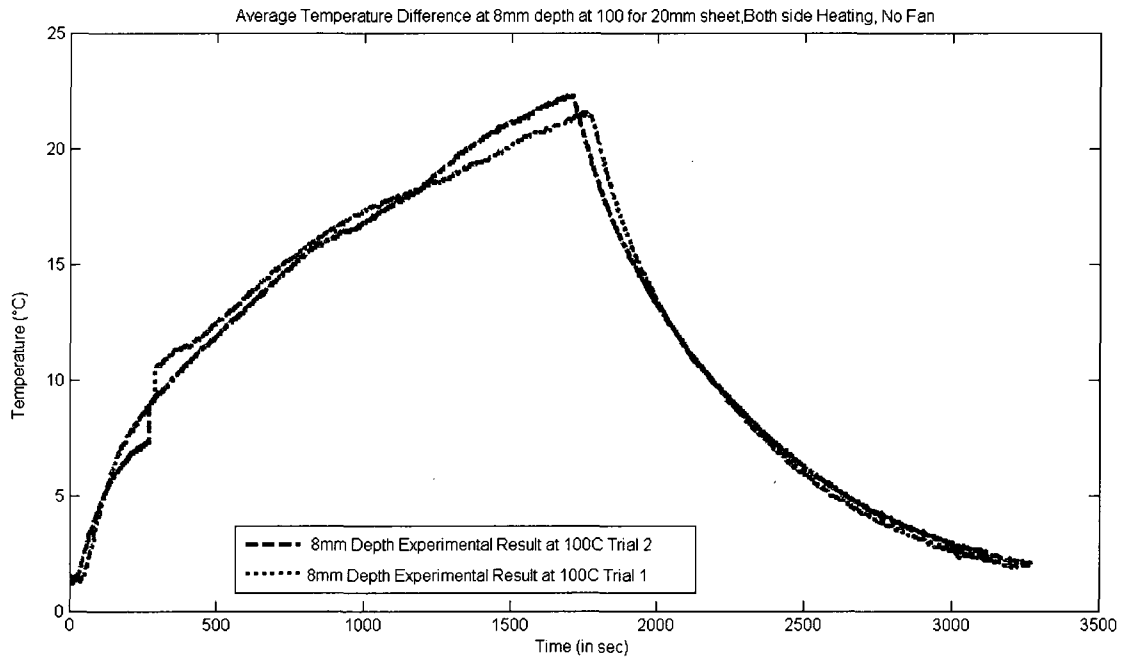


**Figure 6-15:** Average Temperature Difference at 8mm.

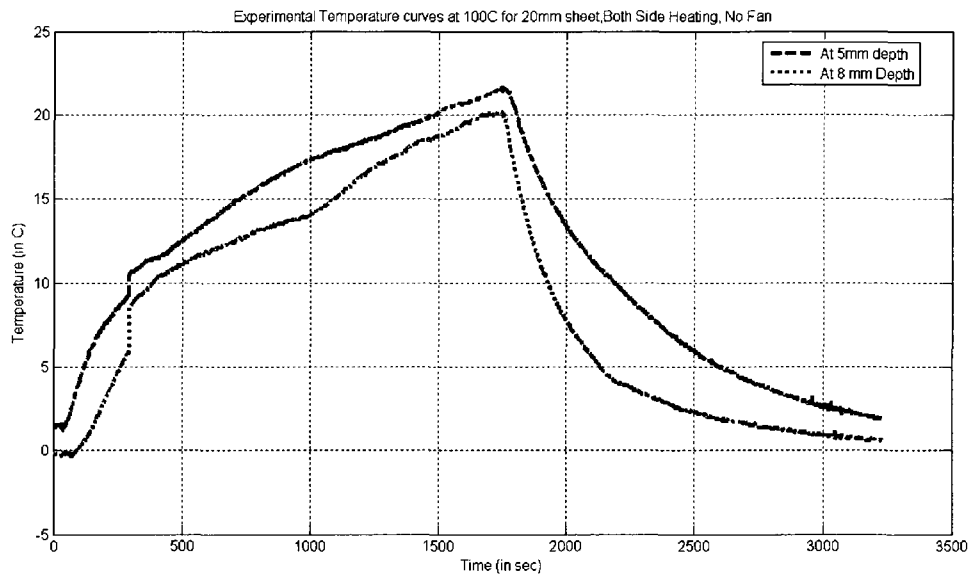


**Figure 6-16:** Temperature difference for 100 °C oven temperature.

#### 6.5.4 Effect of Convection Heating Coefficient on Sheet Reheat Phase

The effect of convection heat transfer is also investigated due to its significant effect on the model. Industrial Thermoforming ovens are open from both ends and therefore are susceptible to any air convection around the oven. The analysis is performed on the variable properties simulation model and the results are presented in Figures 6.17 and 6.18 and summarized in the following lines:

1. When the values of convection coefficient  $h$  are varied from  $5\text{W/m}^2\text{--K}$  to  $40\text{W/m}^2\text{--K}$ , temperature variation for any one particular depth across the sheet thickness is shown in Figure 6.17. Further results are presented in appendix C. The steady state average temperature variation is about  $80\text{ }^\circ\text{C}$  for any particular

depth and oven temperature. It is also observed that the temperature variation increases with the increase of oven temperature.

2. The effect of the convection coefficient at steady state at a time instant of 900th second of sheet heating process is summarized for different oven temperatures in Figure 6.18. Further results are presented in appendix C. It is evident that linear increase in the value of convection coefficient results in exponential decrease in sheet temperature for any particular depth and oven temperature and hence decreases heating efficiency of the process. The values of  $h$  can vary from 10 to 25  $\text{W/m}^2 \text{K}$  in any industrial setup and the effects are more prominent in this range as can be seen from Figure 6.17. Sheet heat losses also increase for higher oven temperatures. Thermoforming reheat phase is an energy intensive process and in order to attain better heating efficiency, high air speed in the vicinity of oven should be avoided.

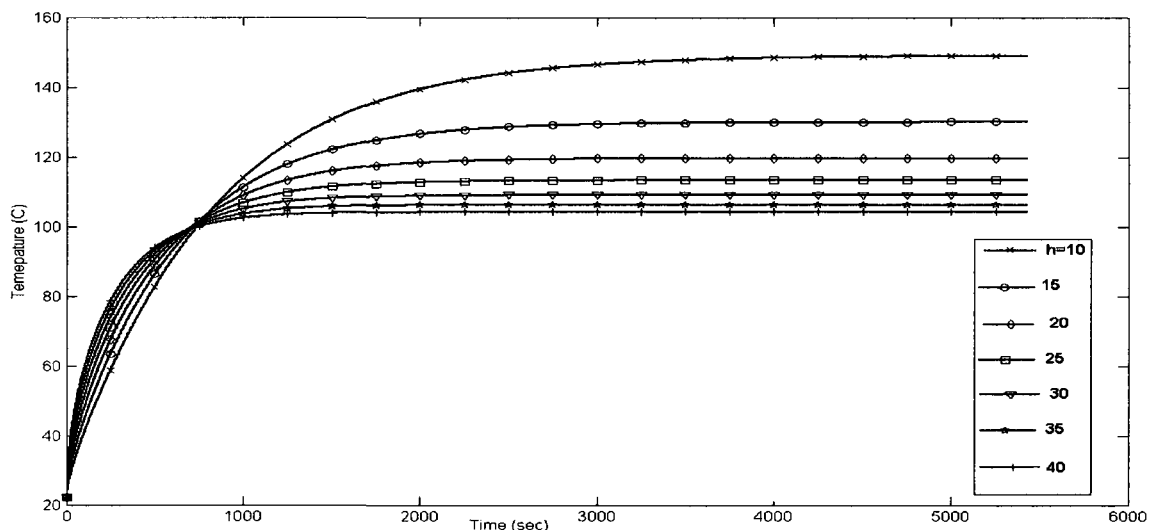


**Figure 6-17:** Variation in sheet temperature with change in convection heat coefficient at 280 °C oven temperature for 12mm HDPE sheet, heating from both sides.

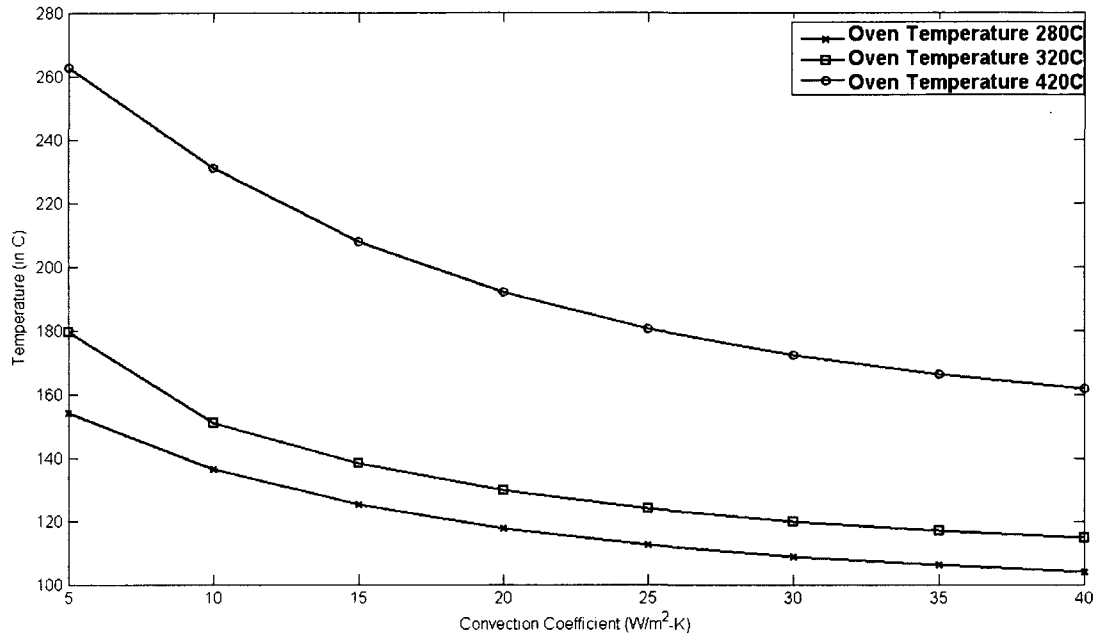


**Figure 6-18:** Change in sheet temperature with change in convection coefficient values at the steady state time instant of the 900<sup>th</sup> second of simulation for 12mm HDPE sheet, bottom heating.

## **Chapter 7 Conclusion**

This thesis is the extension of the work carried out at IMI to understand and develop a model based control system for the thermoforming process. The main focus is to improve the existing mathematical model for the thermoforming sheet reheat phase and to understand the effect of temperature on sheet material properties. Another important aspect studied is the effect of sheet color on current model predictability and effect of convection coefficient on sheet reheat phase. The existing models assume constant material properties and are developed and tested against experimental data on “white sheet” only. Large errors are reported in the simulation because the change in material properties with temperature is not considered. Also, models failed when used for dark colored sheets. This thesis is an effort to provide a better estimation of the process by incorporating temperature dependent material properties of the sheet and to investigate the effect of sheet color and convection coefficient on sheet reheat phase.

This thesis discusses in detail the importance, development methodologies and experimental details of the temperature dependent variable material properties model for thermoforming sheet reheat phase and effect of sheet color and convection coefficient on the process. Chapter 1 is dedicated to defining the problem and highlighting briefly previous works that are performed in this area. This sets the groundwork for the objectives of this work which are then presented briefly. In Chapter 2, the thermoforming process is described in detail to understand the process dynamics and related issues. Also, the industrial scope, related materials and future prospects of the thermoforming process is discussed briefly. Chapter 3 describes the heat transfer theory which is the basis for

understanding and developing the mathematical model of thermoforming process. Through previous works, it was learned that in order to improve production rate, product quality and to develop a better control system, one has to understand and improve the existing mathematical models for sheet heating phase of the thermoforming process. This requires detailed modeling of the heating process as well as characterization of various process parameters and material properties that are prone to change with temperature during heating of sheet. Chapter 4 discusses the proposed model and development procedures. Chapter 5 presents the details about experimental setup, machines, equipments and results. Results are comparison of proposed models simulated in Matlab against the experimental data that is collected at industrial standard thermoforming machines.

The objectives of the thesis can be summarized as follows:

- Model the energy transfer from the heating elements to the sheet.
- Model the temperature profile inside the sheet with temperature dependent material properties.
- Understand the effect of sheet color on the proposed model.
- Understand the effect of convection coefficient on sheet heating phase.

A set of 24 experiments were performed on industrial standard thermoforming machines in which HDPE plastic sheets of 12mm and 20mm thickness were heated at different oven temperatures and temperature data is collected by inserting thermocouples at different depths across the thickness of sheet in order to find a temperature profile. The proposed models are simulated in Matlab by generating temperature profiles at the same depths and assuming the same conditions as in the experiments and then compared to the

experimental results obtained in the Matlab environment. The difference between the experimental and simulated temperature profile is used as criteria for the validity of the proposed models.

Finally, the conclusion of this thesis is:

- The proposed temperature dependent variable material properties model performed better than the constant material properties model in predicting the heat profile inside sheet. The difference between two models ranges from 5C to 35C depending on oven temperatures. Due to this large difference, the proposed variable material properties model is recommended to use in future works for modeling of thermoforming processes for less than 400C oven temperatures.
- The sheet color has a “slowdown” effect on heating of the sheet as the radiation heating is less effective due to dark color of sheet. This leads to the fact that a dark colored sheet needs more time to be brought to forming temperature.
- The results for exact solution of heat equation show that the model lags behind the experimental results in the first part of heating phase and predicts much higher temperature ( $\Delta 50$  C) in the later part of heating phase. It is therefore not feasible to use for modeling.
- The convection coefficient has a pronounced effect on the thermoforming process and must be considered as an important factor in any future work for thermoforming process.
- Unfortunately due to the non linear nature of radiation heating, the proposed model shows a deviation in excess of 30C for oven temperatures higher than 400C

for different depths of sheet. This can cause failure of the model if used for higher oven temperatures.

## **7.1 Future Work**

The sheet reheating process in thermoforming is very complex due to non linear heat transfer and intricate material properties of plastic. The following opportunities can be identified on the basis of this work:

- One opportunity is to investigate and incorporate into the model the sheet sag during the heating process that affect the view factor which is an important factor in determining the radiation heat transfer to the sheet.
- The sheet color has a “slowdown” effect on the heating of the sheet and a new model is needed that can be used for colored sheets.
- The proposed model predicts higher temperatures as compared to experimental temperatures for oven temperatures higher than 400C. This also needs to be investigated in terms of radiation heat losses both from the sheet and oven.

## References

Ajersch, M. H.; “Modeling and real-time control of sheet reheat phase in thermoforming”, M.Eng thesis submitted to Department of Electrical and Computer Engineering, McGill University , Montreal, Canada August 2004.

Benqiang, H.; “A Soft Sensor System for the Estimation of Sheet Internal Temperature Distribution in Thermoforming”, M.Eng thesis submitted to Mechanical Engineering department, McGill University, Montreal , Canada, January 2003.

Bicerano, J. “Prediction of Polymer Properties” Marcel Dekker, Inc. New York, USA, 1993.

Brinken, F.; Potente, H.; “Some Considerations of Heat-Transfer Problems in Thermoforming”, Polymer Engineering and Science, No. 15, Vol. 20, October 1980.

Chang, Yau-Zen; Wen, Ting-Ting; Liu, Shih-Jung; “Derivation of Optimal Processing Parameters of Polypropylene Foam Thermoforming by an Artificial Neural Network”, Polymer Engineering Science, 45:375–384, 2005.

Gauthier, G.; Ajersch, M. A.; Haurani, A.; Boulet,B.; Girard,P.; DiRaddo,R.; “A New Absorption Based Model for Sheet Reheat in Thermoforming”; ANTEC. SPE, Boston, MA, May 2-4 2005.

Kumar, V.; “Estimation of Absorptivity and Heat Flux at the Reheat Phase of Thermoforming Process” M.Eng. thesis submitted to the Department of Mechanical Engineering, McGill University\_Montreal, Quebec, Canada, June 2005.

Kumar, V.; “Estimation of Absorptivity and Heat Flux at the Reheat Phase of Thermoforming Process” M.Eng. thesis submitted to the Department of Mechanical Engineering, McGill University\_Montreal, Quebec, Canada, June 2005.

Holman, J.P.; “Heat Transfer” McGraw Hill Inc., 8<sup>th</sup> Ed, 1997.

Moore, B.; "In-Cycle Control of the Thermoforming Reheat Process", M.Eng. Thesis, Department of Electrical and Computer Engineering, McGill University, 2002, Montreal, Quebec, Canada.

Monteix, S.; Schmidt, F.; Maoult, Y. Le; BenYedder, R. ; Diraddo, R. W.; Laroche, D.; "Experimental Study and Numerical Simulation of Preform or Sheet Exposed to Infrared Radiative Heating", Journal of Material Processing Technology, 119(2001)90-97.

Santos, W.N. dos, "Thermal properties of melt polymers by the hot wire technique", Polymer Testing 24 (2005) 932–941.

Tao Xiaoming "Smart fibers, fabrics and clothing" Textile Institute (Manchester, England), CRC Press, 2001, page 59.

Thomas, S. M.; "Time Minimization by Maximizing Heater Cycle Temperature Profile that Prevents Sheet over Temperature", 2005 SAE World Congress Detroit, Michigan April 11-14, 2005.

Throne, J.L.; "Heating Semi-transparent Polymers in Thermoforming", Thermoforming Quarterly, 7, 1996.

Walter, G.N.; "Calculation of Obstructed View Factors by Adaptive Integration", National Institute of Standards and Technology, Technology Administration, U.S. Department of Commerce, November 2002.

Woo, M.W.; Wong, P.; Tang, Y.; Triacca, V.; Gloore, P.E.; Hrymak, A.N.; and Hamielec, A.E.; "Melting Behaviour and Thermal Properties of High Density Polyethylene", Polymer Engineering and Science, No. 2, Vol. 35, January 1995.

Yousefi, A.; Bendada, A.; Diraddo, D.; "Improved Modeling for the Reheat Phase in Thermoforming through an Uncertainty Treatment of the Key Parameters", Polymer Engineering and Science, No. 5, Vol. 42, May 2002.

Zhang, Y.; "Generation of Component Libraries for the Thermoforming Process Using On-Line Characterization" M.Eng thesis submitted to Mechanical Engineering department, McGill University, Montreal , Canada, October 2004. Page 309-317.

## Appendix A: List of Symbols

$\alpha$  : Absorptivity.

$\rho$  : Density.

$\alpha$  : Diffusivity.

$\varepsilon$ : Emissivity.

$\rho$ : Reflectivity.

$\tau$  : Transmissivity.

$E_b$ : Energy emitted per unit area by the blackbody.

$T_\infty$  : Fluid temperature.

$C_p$ : Heat capacity.

$F$ : Radiation shape factor.

$I$ : Incident radiation.

$q_{in}$  : Internal energy generated within the body.

$k$ : Thermal Conductivity.

$h$ : Coefficient of convection heat transfer.

$T$ : Temperature.

$A$ : Area.

$Q_T$ : Heat energy from top heater.

$Q_B$ : Heat energy from bottom heater.

$\theta$  : Simulation step.

$z$  : Sheet thickness.

$\beta$  : Fraction of radiation energy absorbed by sheet.

## Appendix B: Matlab Codes for Simulation

```
function Thermal_light ()
% (c) Sohail Akbar Khan and Salman Saeed
% 12 January 2009
% This function simulates sheet reheat phase model of the plastic sheet temperatures.
% It also compares the model output to an input test vector, for tuning purposes.
% Inputs: - Experimental test name
%         - Bottom Heat flag, Top heat flag
%         - Input Heater Settings
%
% Outputs: - Nodal sheet temperature distributions
%          - Error fcn between model and test data
%          - Error fcn between model with constant and with variable
%          material properties

test_name = '280 Bottom No Fan.csv'; %input ('\n Please enter Test Name here: ');
H_bottom = 1; %input ('Heating from bottom (1 for Yes, 0 for No): ');
H_top = 0; %input ('Heating from top (1 for Yes, 0 for No): ');
Heater_temp = 280; %input ('Enter heater setpt temperatures (in C): ');
h = 0.5; %delta time
N = 12000; %number of points
t = (0:h:N*h); %time vector
Zt = 0.141; %distance in m from sheet to upper oven
Zb = 0.171; %distance in m from sheet to lower oven
Vft = AAA_view_factors_patrick(Zt); %view Factor top
Vfb = AAA_view_factors_patrick(Zb); %view Factor bottom
sbc = 5.669e-8; %boltzmann constant(W-m^2-k^4)
emis = 0.45;%0.85; %effective emissivity (dimensionless quantity)
l = 0.012/4; % delta thickness (meters)
```

```

Tambt = 40+273; %ambient air temperature top/air temp inside oven at midpoint
between sheet and oven top heating elements
Tambb = 100+273; %ambient air temperature bottom side
hh = 14; % Convection coefficient (w/m^2-K)
kk =(0.6128/l)*.9; % Conduction coefficient (W/m-K = m kg/s^3 K)
rho = 950; %density (kg/m^3)
Cp = 1800;%300; %heat capacity (J/kg-K=m^2/s^2-K)
rho1 = 950; %density (kg/m^3)
Cp1 = 1800;%300; %heat capacity (J/kg-K=m^2/s^2-K)
sx = 76.67e-3; %sheet zone width (m)
sy = 102.5e-3; %sheet zone height(m)
lo = 304.8e-3; %oven zone size (m)

sevt = sbc*emis*Vft*(lo^2/sx*sy); %finding upper and lower multiplying factors
sevb = sbc*emis*Vfb*(lo^2/sx*sy);
%ct = 1/(rho*Cp*1);
x=zeros(5*6,N+1); % it is added to run the program fast i-e now no dynamic memory
allocation
x(:,1) = (22+273)*ones(5*6,1); %initial sheet temps
x1=zeros(5*6,N+1); % it is added to run the program fast i-e now no dynamic memory
allocation
x1(:,1) = (22+273)*ones(5*6,1); %initial sheet temps
%H_top = 1; % If 0, heaters off # If 1, heaters work
%H_bottom = 0;
B_coef = 30; %absorption coefficient
Beer_1 = exp(-B_coef*1/2); %Beer-Lambert output for external layer (m)
Beer_2 = exp(-B_coef*1); %Beer-Lambert output for internal layer (m)
u =
([ones(6,1)*(Heater_temp+273)*H_top;ones(6,1)*(Heater_temp+273)*H_bottom]).^4;
%input vector

```

```

BB1 = []; BB2 = []; SEVt = [0;0;0;0;0;0]; SEVb = [0;0;0;0;0;0]; RAD1=[]; RAD5=[];
%initializations

for k=1:6;
    SEVt = SEVt + sevt(:,k);
    SEVb = SEVb + sevb(:,k);
    BB1 = [BB1; 2*sevt(k,:)*(1-Beer_1);
          sevt(k,:)*Beer_1*(1-Beer_2);...
          sevt(k,:)*Beer_1*Beer_2*(1-Beer_2);...
          sevt(k,:)*Beer_1*Beer_2^2*(1-Beer_2);...
          2*sevt(k,:)*Beer_1*Beer_2^3*(1-Beer_1)]; %coefficients for absorbed energy
top
    BB2 = [BB2;2*sevb(k,:)*Beer_1*Beer_2^3*(1-Beer_1);...
          sevb(k,:)*Beer_1*Beer_2^2*(1-Beer_2);...
          sevb(k,:)*Beer_1*Beer_2*(1-Beer_2);...
          sevb(k,:)*Beer_1*(1-Beer_2);
          2*sevb(k,:)*(1-Beer_1)]; %coefficients for absorbed energy bottom
    RAD1 = [RAD1 ;2*(1-Beer_1);...
            Beer_1*(1-Beer_2); ...
            Beer_1*Beer_2*(1-Beer_2); ...
            Beer_1*Beer_2^2*(1-Beer_2); ...
            2*Beer_1*Beer_2^3*(1-Beer_1)]; %coefficients for transmitted energy top
    RAD5 = [RAD5 ;2*Beer_1*Beer_2^3*(1-Beer_1);...
            Beer_1*Beer_2^2*(1-Beer_2);...
            Beer_1*Beer_2*(1-Beer_2);...
            Beer_1*(1-Beer_2);...
            2*(1-Beer_1)]; %coefficients for transmitted energy bottom
end
BB = [BB1 BB2]; % coefficients for absorbed energy
for k = 1:N
    if mod(k,100)==0 fprintf('*'); end

```

```

if mod(k,1000)==0 fprintf('|'); end
if mod(k,4000)==0 fprintf('\n'); end
%rho = diag(1./(1000*Rho_poly_HDPE(x(:,k))));
%Cp = diag(1./Cv_poly_HDPE(x(:,k)));
xt=(x(1,k)-273);
if xt<135
rho = (1/(1.05*exp(0.00136*xt)))*1000;
else
rho = (1/(1.14+0.0009*xt))*1000;
end
if xt<136
Cp=2.25*(1+5.5*exp((-0.005*(xt-135))^2))*100;
end
if xt>135

Cp=2.25*(1+5.5*exp((-0.05*(xt-135))^2))*100;
end

% if xt<150
% Cp=90;
%end
% if xt<135
%Cp=112;
%end
% if xt<126
% Cp=1300;
% end
% if xt<125
% Cp=1880;
% end
%if xt<124

```

```

% Cp=728;
%end
%if xt<123;
% Cp=337;
%end
%if xt<121
% Cp=185;
%end
%if xt<111
% Cp=123;
%end

ct = 1/(l*Cp*rho);
B = ct*h*BB;
ct1 = 1/(l*Cp1*rho1);
B1 = ct1*h*BB;
SS1 = []; SS5 = [];
for k1 = 1:6
    for k2 = 1:5
        SS1 = [SS1 SEVt(k1)*x(1+(k1-1)*5,k)^4*H_top];
%Sheet initial Temperature for all 6 zones at Top

        SS5 = [SS5 SEVb(k1)*x(k1*5,k)^4*H_bottom]; %Sheet initial Temperature for
all 6 zones at Bottom
    end
end
Sh = ct*h*(diag(SS1)*RAD1+diag(SS5)*RAD5); %radiant energy transmitted
through sheet
Qrad = (B*[u(1:6)*H_top;u(7:12)*H_bottom]-Sh)/l; % radiant energy absorbed by
the sheet

```

```

    %display (Qrad);
    dx = ct*h*deltaTemp_six_zones(x(:,k),Tambt, Tambb ,hh); %conduction and
convection energies
    x(:,k+1) = x(:,k) + dx + Qrad; %total energy distribution
    Sh1 = ct1*h*(diag(SS1)*RAD1+diag(SS5)*RAD5); %radiant energy transmitted
through sheet
    Qrad1 = (B1*[u(1:6)*H_top;u(7:12)*H_bottom]-Sh1)/l; % radiant energy absorbed
by the sheet
    dx1 = ct1*h*deltaTemp_six_zones1(x1(:,k),Tambt, Tambb ,hh ); %conduction and
convection energies for consatnt properties
    x1(:,k+1) = x1(:,k) + dx1 + Qrad1; %total energy distribution for consatnt properties
end

% Plotting Experimental results
data = load(test_name);
time = data(:,1);
T1 = data(:,2); %exp temperature at 1mm
T3 = data(:,4); %exp temperature at 3mm
T6=data(:,6); %exp temperature at 6mm
T9 = data(:,8); %exp temperature at 9mm
T11 = data(:,10); %exp temperature at 11mm

% plotting experimental curves

figure(3)
P3= plot(time, T1,'r',time, T3,'g',time, T6,'c',time, T9,'b',time, T11,'k');
set(P3(1),'LineWidth',2.5, 'LineStyle','--');
set(P3(2),'LineWidth',2.5,'LineStyle',':');
set(P3(3),'LineWidth',2.5,'LineStyle','-');
set(P3(4),'LineWidth',2.5,'LineStyle','-');
set(P3(5),'LineWidth',2.5,'LineStyle','-');

```

```

xlabel ('Time (in sec)')
ylabel ('Temperature (in C)')
title ('Experimental Temperature curves vs. Simulated Model curves at 280C for 12mm
sheet,Bottom Heating, No Fan')
grid ;
hold on;
total = max(time);
if total > N
    fprintf ('Simulation shorter than file length, please increase to at least %f seconds',
max(time));
else

    %concatenate simulation to data file length

    index = max(time)- mod(max(time),1);
    x7_sh = x(7,1:index*2)-273;
    x8_sh = x(8,1:index*2)-273;
    x11_sh = x(10,1:index*2)-273;
    T3_sh = T3(2:length(T3));
    T6_sh = T6(2:length(T6));
    T11_sh = T11(2:length(T11));
    x7_sh1 = x1(7,1:index*2)-273; % simulation for variable properties
    x8_sh1 = x1(8,1:index*2)-273;% simulation for variable properties
    x11_sh1 = x1(10,1:index*2)-273; % simulation for variable properties
    %calculating errors
    error_T3 = T3_sh - x7_sh'; % error for simulation vs experimental
    error_T6 = T6_sh - x8_sh';
    error_T9 = T11_sh - x11_sh'; % error for simulation vs experimental
    % error for simulation with variable Properties vs simulation with
    % Constant Properties

```

```

    error_T3_1 = x7_sh - x7_sh1; % error for simulation with variable Properties vs
simulation with Constant Properties
    error_T6_1 = x8_sh - x8_sh1;
    error_T9_1 = x11_sh - x11_sh1; % error for simulation with variable Properties vs
simulation with Constant Properties
end

% plotting errors at 3mm, 6mm and 9mm depths

figure (4)
P4 =plot (time(2:length(time)), error_T3,'b',time(2:length(time)),
error_T6,'c',time(2:length(time)), error_T9,'g');
grid;
set (P4(1), 'LineStyle', '--', 'Color', 'b');set(P4(2), 'Color', 'c'); set(P4(3), 'Color', 'g');
xlabel ('Time (sec)'); ylabel('Temperature (°C)'); title('Simulation Error vs. Experimental
Error at 280C for 12mm Sheet, Bottom Heating, No Fan');
legend ('Error at 3mm','Error at 6mm','Error at 9mm',0)

% calculating steady-state errors

ss_error3 = error_T3 (length (error_T3))/max (T3_sh)*100;
ss_error6 = error_T6 (length (error_T6))/max (T6_sh)*100;
ss_error9 = error_T9 (length (error_T9))/max (T11_sh)*100;
fprintf ('\n The percent error at steady-state for 3mm is %5.2f%% \n,Bottom No Fan',
ss_error3);
fprintf ('\n The percent error at steady-state for 6mm is %5.2f%% \n,Bottom No Fan',
ss_error6);
fprintf ('The percent error at steady-state for 9mm is %5.2f%% \n, Bottom No Fan',
ss_error9);
% plotting errors at 3mm and 9mm depths for Variable k simulation vs Constant
properties simulation

```

figure (6)

```
P6 =plot (time(2:length(time)), error_T3_1,'b',time(2:length(time)),  
error_T6_1,'c',time(2:length(time)), error_T9_1,'g');  
grid;
```

```
set (P6(1), 'LineStyle', '--', 'Color', 'b'); set(P6(2),'LineStyle', '-', 'Color', 'c');  
set(P6(3),'LineStyle', ':', 'Color', 'g');  
xlabel ('Time (sec)'); ylabel('Temperature (°C)'); title('Simulation Error for Variable  
Properties vs. Constant Propeties at 280C for 12mm Sheet, Bottom Heating, No Fan');  
legend ('Error at 3mm','Error at 6mm','Error at 9mm',0)  
% calculating steady-state errors
```

```
ss_error3 = error_T3 (length (error_T3))/max (T3_sh)*100;  
ss_error6 = error_T6 (length (error_T6))/max (T6_sh)*100;  
ss_error9 = error_T9 (length (error_T9))/max (T11_sh)*100;  
fprintf ('\n The percent error at steady-state for 3mm is %5.2f%% \n, Bottom Heating, No  
Fan', ss_error3);  
fprintf ('\n The percent error at steady-state for 6mm is %5.2f%% \n, Bottom Heating, No  
Fan', ss_error6);  
fprintf ('The percent error at steady-state for 9mm is %5.2f%% \n, Bottom Heating, No  
Fan', ss_error9);  
% plotting centre zone temperatures for variable properties model
```

figure (3)

```
P2(1)=plot (t(1:index*2),x(6:6,1:index*2)-273);  
set(P2(1),'LineWidth',.5, 'LineStyle','-', 'Color', 'k');  
xlabel ('Time (sec)'); ylabel('Temperature (°C)');  
title('Simulated Model Temperature Curves for varaible and constant properties at 280C  
for 12mm Sheet at 1mm depth,Bottom Heating, No Fan');  
hold on;
```

figure (3)

```
P2(2)=plot (t(1:index*2),x(7:7,1:index*2)-273);
```

```

set(P2(2),'LineWidth',.5, 'LineStyle','-', 'Color', 'b');
xlabel ('Time (sec)'); ylabel('Temperature (°C)');
title('Simulated Model Temperature Curves for constant properties at 280C for 12mm
Sheet at 3mm depth,Bottom Heating, No Fan');
hold on;
figure (3)
P2(3)=plot (t(1:index*2),x(8:8,1:index*2)-273);
set(P2(3),'LineWidth',.5, 'LineStyle','-', 'Color', 'c');
xlabel ('Time (sec)'); ylabel('Temperature (°C)');
title('Simulated Model Temperature Curves for constant properties at 280C for 12mm
Sheet 6mm depth,Bottom Heating, No Fan');
hold on;
figure (3)
P2(4)=plot (t(1:index*2),x(9:9,1:index*2)-273);
set(P2(4),'LineWidth',.5, 'LineStyle','-', 'Color', 'g');
xlabel ('Time (sec)'); ylabel('Temperature (°C)');
title('Simulated Model Temperature Curves for constant properties at 280C for 12mm
Sheet at 9mm depth,Bottom Heating, No Fan');
hold on;
figure (3)
P2(5)=plot (t(1:index*2),x(10:10,1:index*2)-273);
set(P2(5),'LineWidth',.5, 'LineStyle','-', 'Color', 'r');
xlabel ('Time (sec)'); ylabel('Temperature (°C)');
title('Variable Properties Simulated Model Temperature Curves vs. Experimental Curves
at 280C for 12mm Sheet,Bottom Heating, No Fan');
legend ('11mm','9mm','6mm','3mm','1mm','Thick line = Experimental','Thin line =
Simulated','Same color code for depths',0)
hold on;
grid
%Comparing simulation results of varaible properties and constant
%properties models

```

```

figure(7)
P7= plot(time, T11,'k');
set(P7(1),'LineWidth',2.5, 'LineStyle','--')
hold on;
figure (7)
P77(1)=plot (t(1:index*2),x1(6:6,1:index*2)-273);
set(P77(1),'LineWidth',.5, 'LineStyle','-', 'Color', 'k');
xlabel ('Time (sec)'); ylabel('Temperature (°C)');
title('Temperature Curves at 280C for 12mm Sheet 1mm depth,Bottom Heating, No
Fan');
hold on;
figure (7)
P5=plot (t(1:index*2),x(6:6,1:index*2)-273);
set(P5(1),'LineWidth',.5, 'LineStyle','-', 'Color', 'k');
legend ('Experimental','1mm ','1mm var',0);
figure(8)
P8= plot(time, T9,'b');
set(P8(1),'LineWidth',2.5, 'LineStyle','--','Color','b');
hold on;
figure (8)
P88(1)=plot (t(1:index*2),x1(7:7,1:index*2)-273);
set(P88(1),'LineWidth',.5, 'LineStyle','-', 'Color', 'b');
xlabel ('Time (sec)'); ylabel('Temperature (°C)');
title('Temperature Curves at 280C for 12mm Sheet 3mm depth,Bottom Heating, No
Fan');
hold on;
figure (8)
P5=plot (t(1:index*2),x(7:7,1:index*2)-273);
set(P5(1),'LineWidth',.5, 'LineStyle','-', 'Color', 'b');
legend ('Experimental','3mm','3mm var',0);
figure(9)

```

```

P11= plot(time, T6,'c');
set(P11(1),'LineWidth',2.5, 'LineStyle','--','color','c')
hold on;
figure (9)
P2(3)=plot (t(1:index*2),x1(8:8,1:index*2)-273);
set(P2(3),'LineWidth',.5, 'LineStyle','--', 'Color', 'c');
xlabel ('Time (sec)'); ylabel('Temperature (°C)');
title('Temperature Curves at 280C for 12mm Sheet 6mm depth,Bottom Heating, No
Fan');
hold on;
figure (9)
P5=plot (t(1:index*2),x(8:8,1:index*2)-273);
set(P5(1),'LineWidth',.5, 'LineStyle','-','Color', 'c');
legend ('Experimental','6mm','6mm var');
hold on;
figure(10)
P10= plot(time, T3,'g');
set(P10(1),'LineWidth',2.5, 'LineStyle','--','color','g');
hold on;
figure (10)
P1010(1)=plot (t(1:index*2),x1(9:9,1:index*2)-273);
set(P1010(1),'LineWidth',.5, 'LineStyle','--', 'Color', 'g');
xlabel ('Time (sec)'); ylabel('Temperature (°C)');
title('Temperature Curves at 280C for 12mm Sheet 9mm depth,Bottom Heating, No
Fan');
hold on;
figure (10)
P5=plot (t(1:index*2),x(9:9,1:index*2)-273);
set(P5(1),'LineWidth',.5, 'LineStyle','-','Color', 'g');
legend ('Experimental','9mm','9mm var',0);%,'6mm_k','6mm','Bottom Surface',0)
figure(11)

```

```

P11= plot(time, T1,'r');
set(P11(1),'LineWidth',2.5, 'LineStyle','--')
hold on;
figure (11)
P11(1)=plot (t(1:index*2),x1(10:10,1:index*2)-273);
set(P11(1),'LineWidth',.5, 'LineStyle','-', 'Color', 'r');
xlabel ('Time (sec)'); ylabel('Temperature (°C)');
title('Temperature Curves at 280C for 12mm Sheet 11mm depth,Bottom Heating, No
Fan');
hold on;
figure (11)
P5=plot (t(1:index*2),x(10:10,1:index*2)-273);
set(P5(1),'LineWidth',.5, 'LineStyle','-', 'Color', 'r');
legend ('Experimental','11mm','11mm var',0);
grid
function dx = deltaTemp_six_zones(x,Tambt,Tambb,h)
% Calculates conduction and convection temperature rises for variable
k=(-0.0022*(x-273)+0.6128)*300;
dx=zeros(size(x));
for i=1:5:26
    dx(i)= 2*(h*(Tambt-x(i)) + k(i)*(x(i+1)-x(i)));
    for j=1:3
        dx(i+j)=k(i+j)*( x(i+j+1)-2*x(i+j)+x(i+j-1) );
    end
    dx(i+4)= 2*(h*(Tambb-x(i+4)) + k(i+4)*(x(i+4-1)-x(i+4)));
end
function dx1 = deltaTemp_six_zones1(x,Tambt,Tambb,h)
% Calculates conduction and convection temperature rises for constant
% material properties k
l=0.012/4;
k=(0.6128/l)*.9;

```

```

dx1=zeros(size(x));
for i=1:5:26
    dx1(i)= 2*(h*(Tambt-x(i)) + k*(x(i+1)-x(i)));
    for j=1:3
        dx1(i+j)=k*( x(i+j+1)-2*x(i+j)+x(i+j-1));
    end
    dx1(i+4)= 2*(h*(Tambb-x(i+4)) + k*(x(i+4-1)-x(i+4)));%[replace] 4=numLayers-1
end

```

## Appendix C: Experimental Results

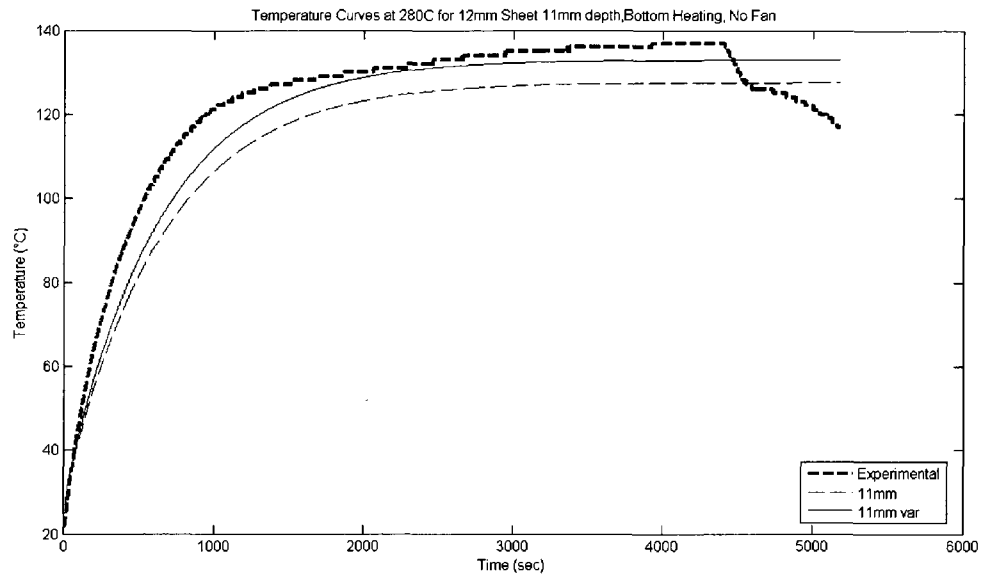


**Figure C-1:** Comparison of simulation model temperature against experimental result at 11mm depth.

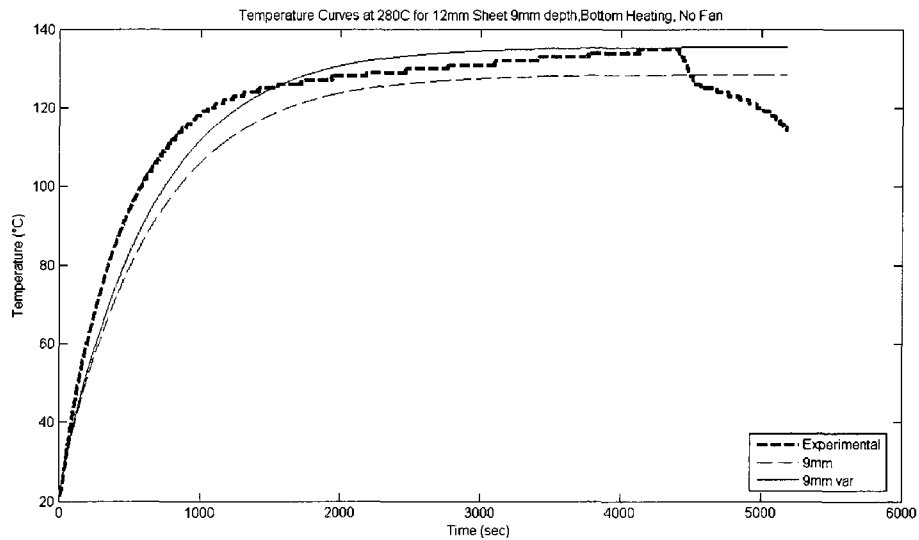


**Figure C-2:** Comparison of simulation model temperature against experimental result at 9mm depth.

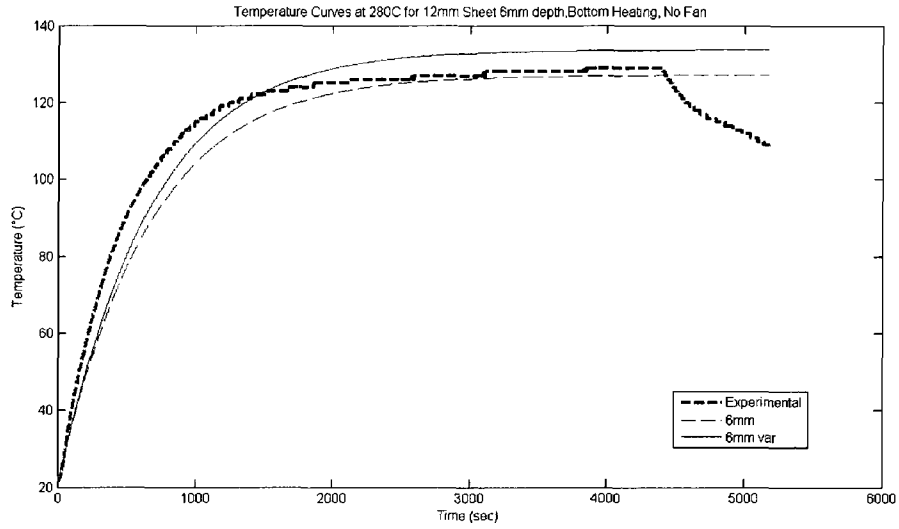


**Figure C-3:** Comparison of simulation model temperature against experimental result at 6mm depth.

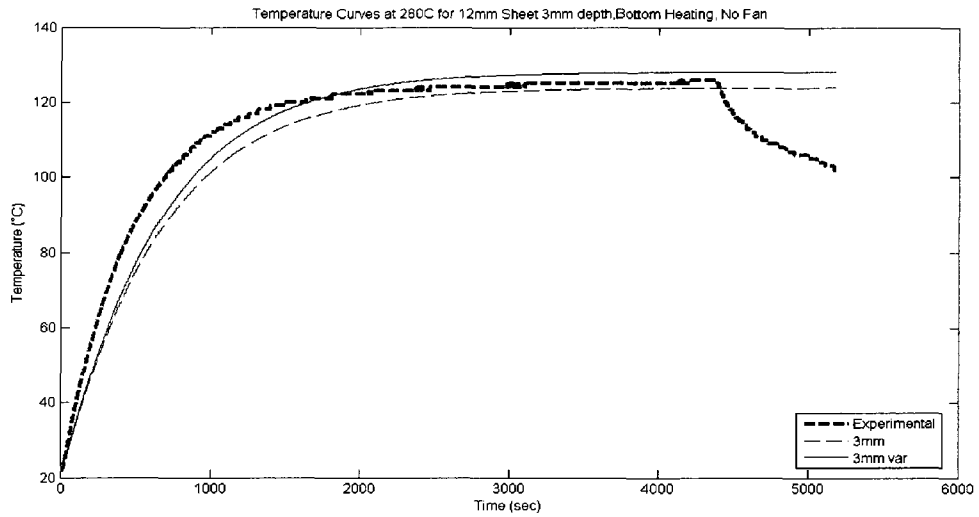


**Figure C-4:** Comparison of simulation model temperature against experimental result at 3mm depth.

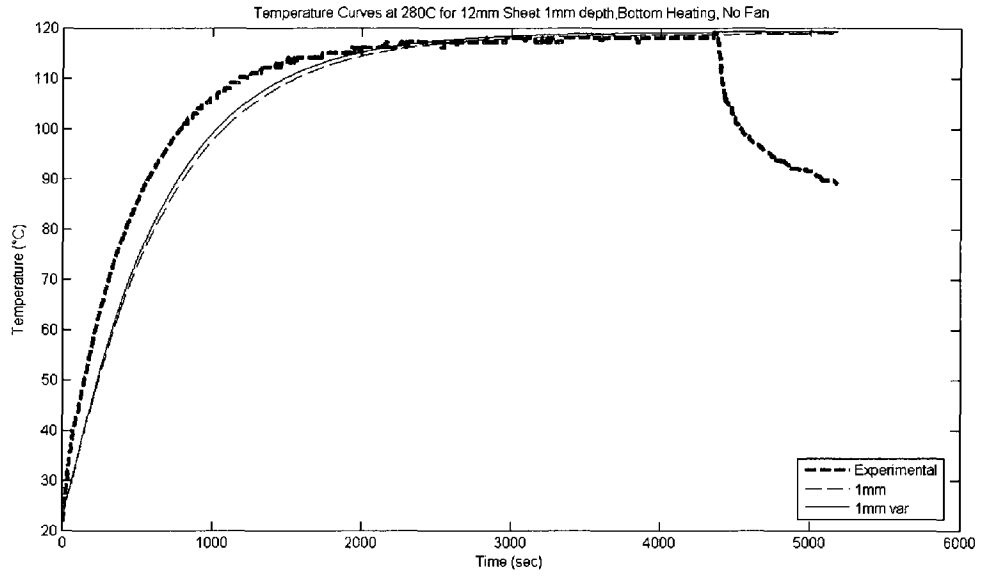


**Figure C-5:** Comparison of simulation model temperature against experimental result at 1mm depth.

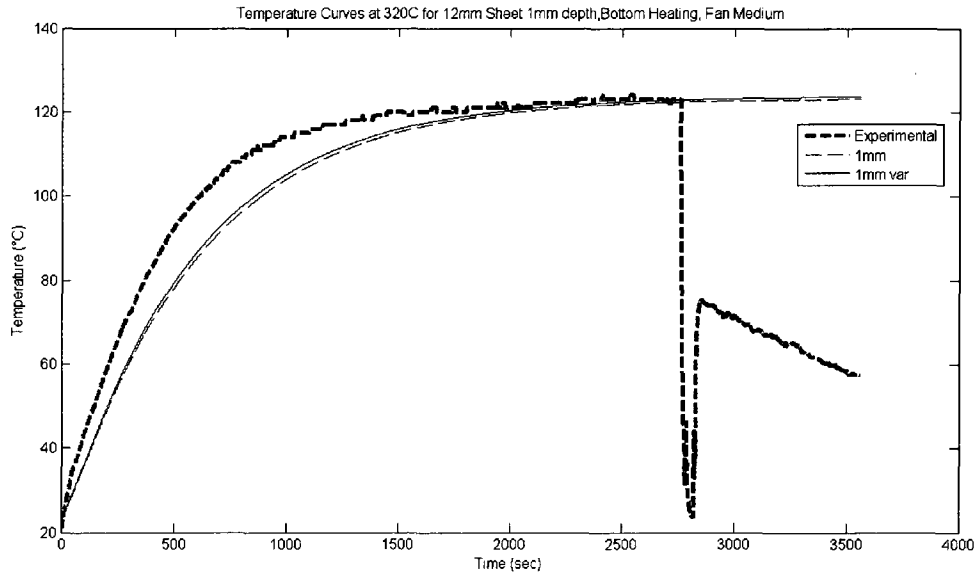


**Figure C-6:** Comparison of simulation model temperature against experimental result at 1mm depth

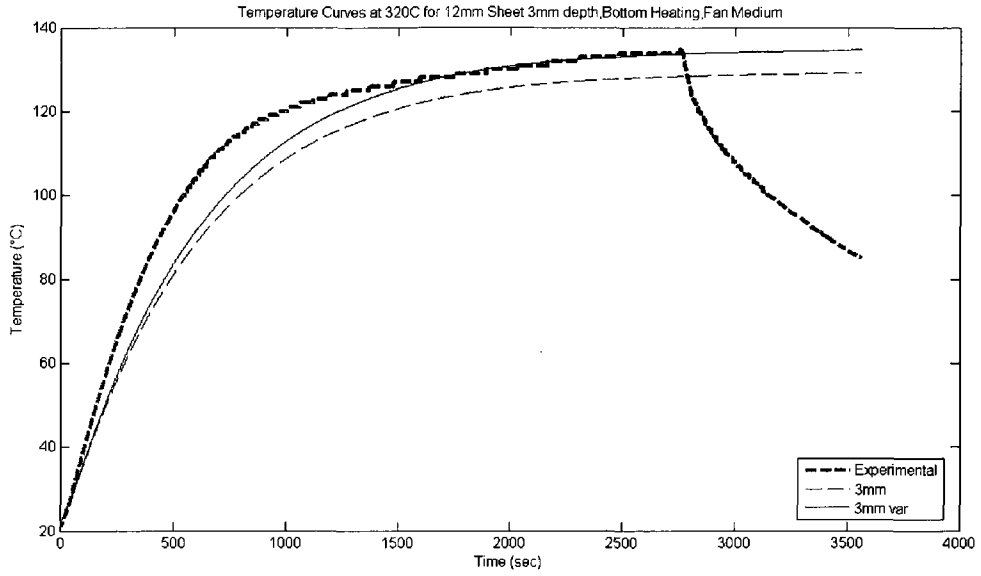


**Figure C-7:** Comparison of simulation model temperature against experimental result at 3mm depth.

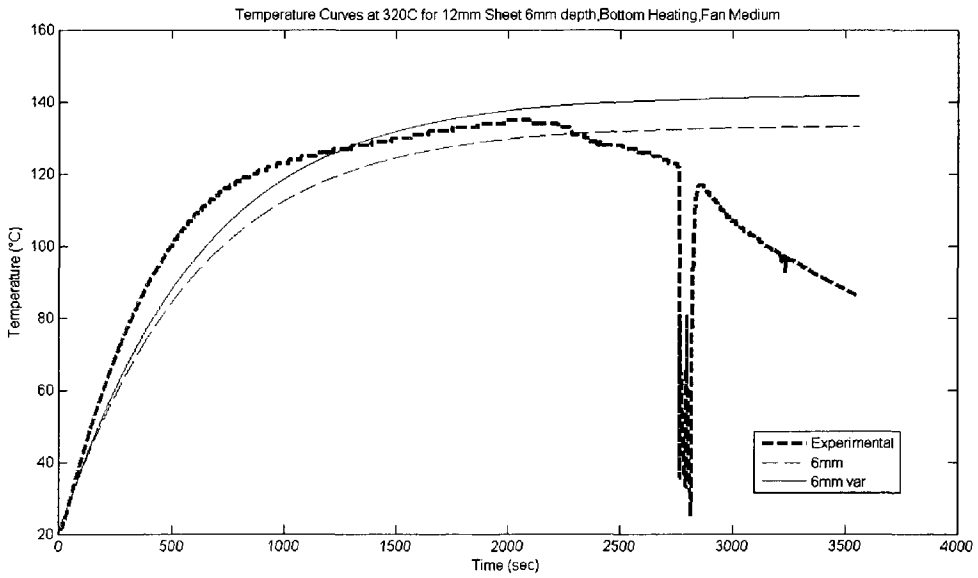


**Figure C-8:** Comparison of simulation model temperature against experimental result 6mm depth.

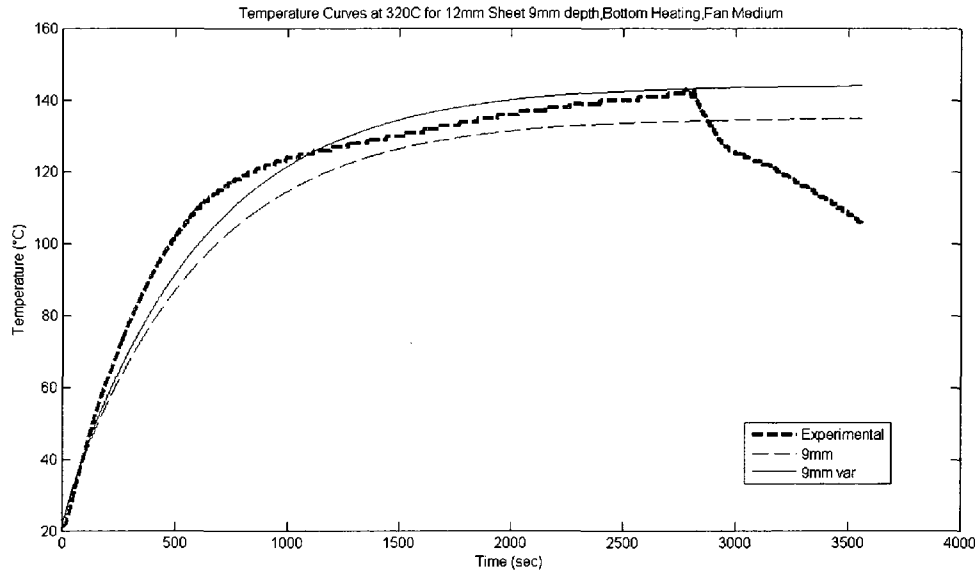


**Figure C-9:** Comparison of simulation model temperature against experimental result 9mm depth.

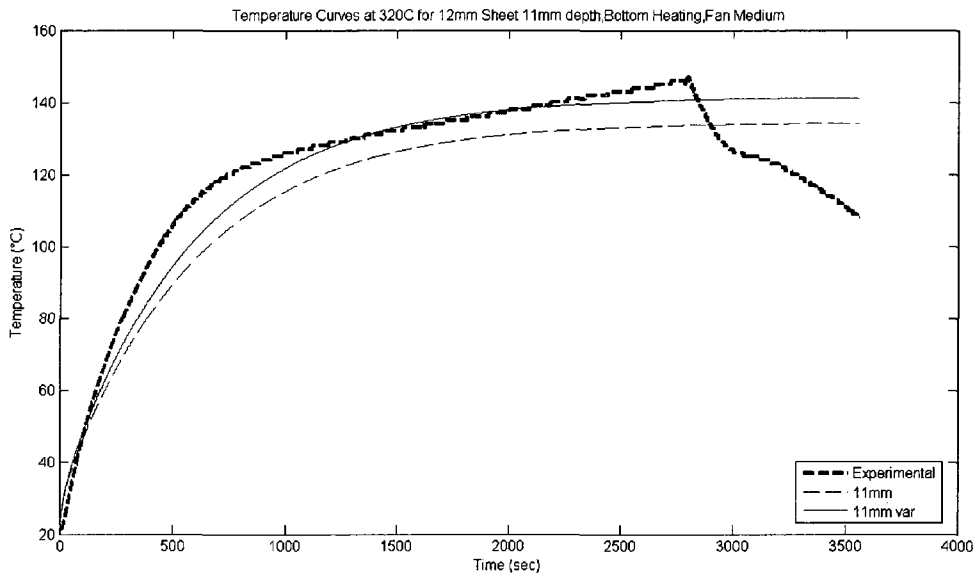


**Figure C-10:** Comparison of simulation model temperature against experimental result at 11mm depth.

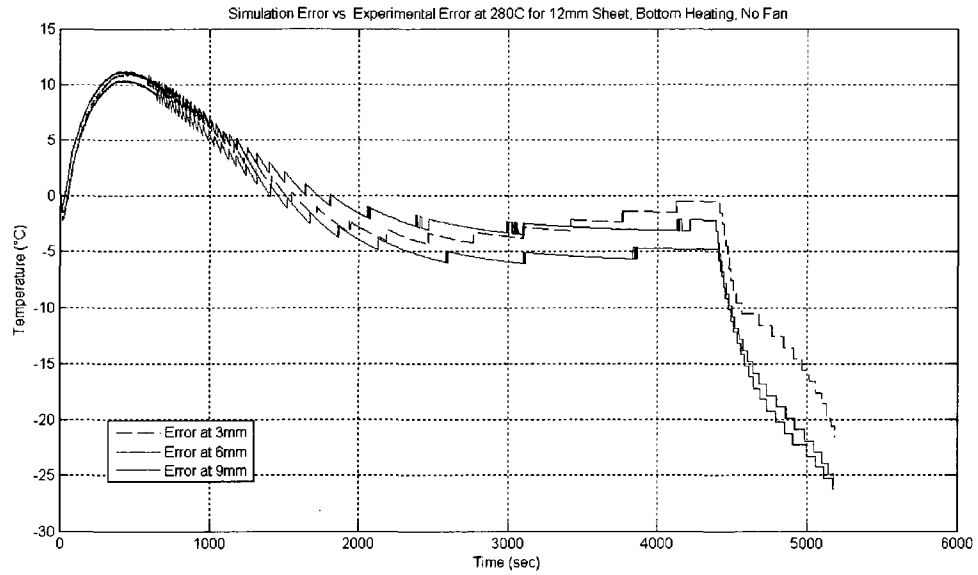


**Figure C-11:** Difference between variable properties model and experimental result.

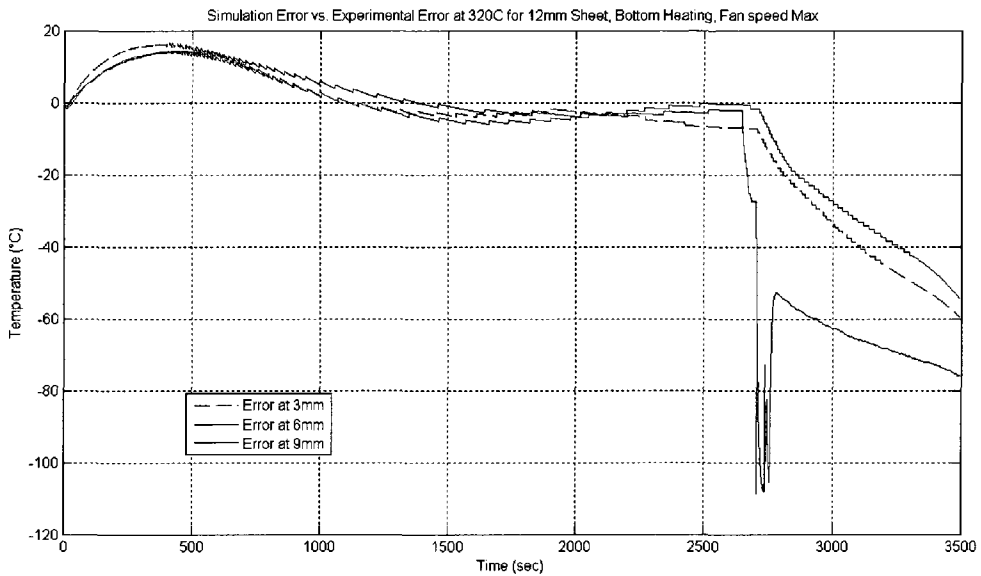


**Figure C-12:** Difference between variable properties model and experimental result.

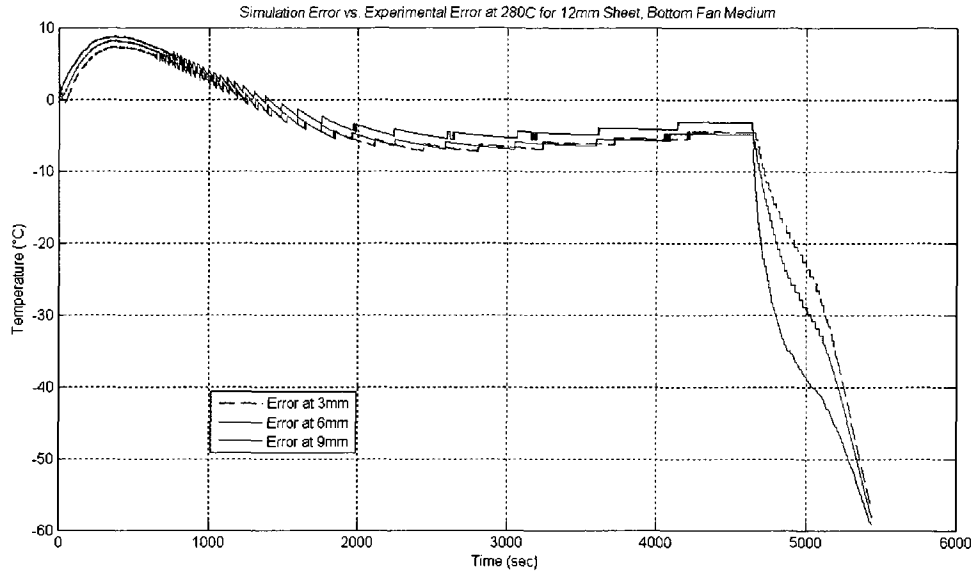


**Figure C-13:** Difference between variable properties model and experimental result.

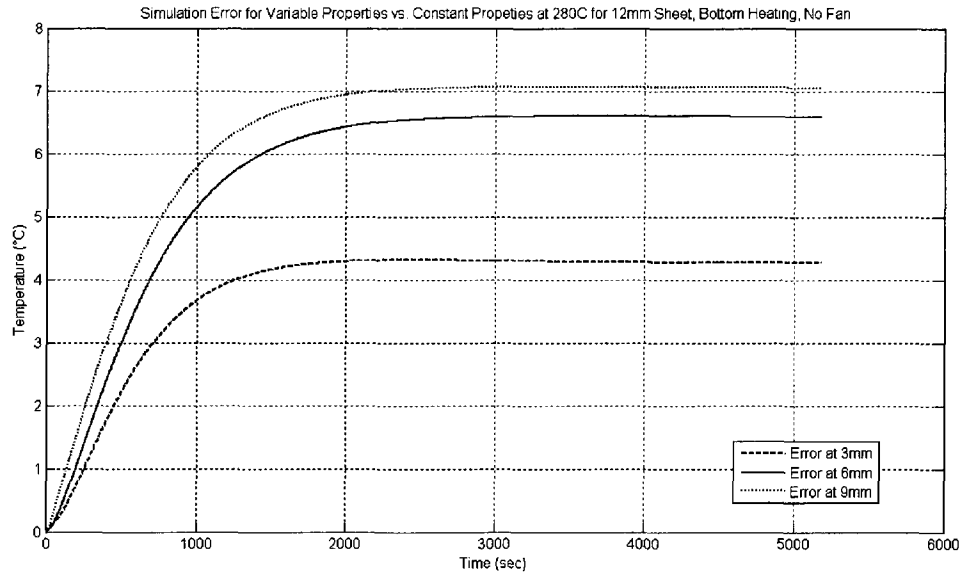


**Figure C-14:** Difference between variable properties model and constant properties model.

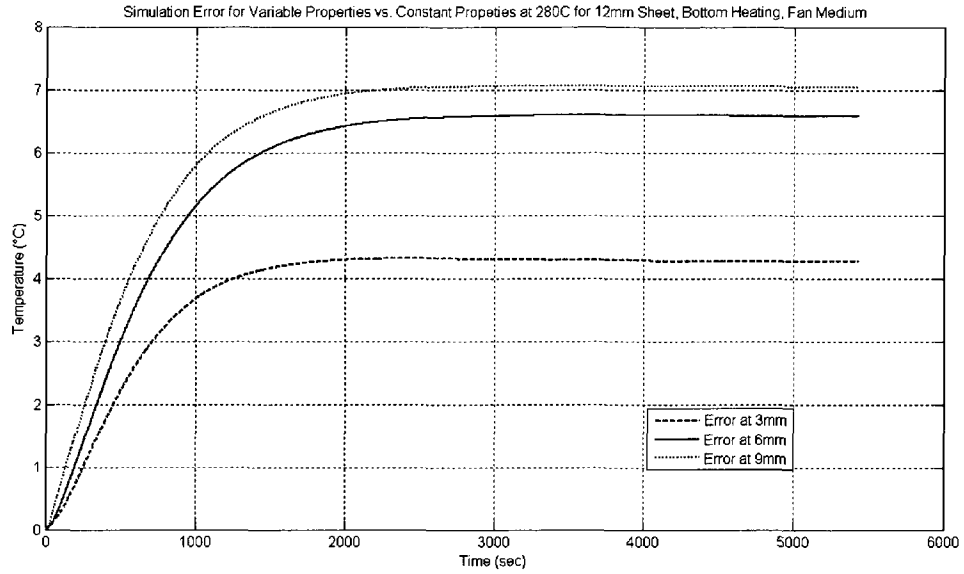


**Figure C-15:** Difference between variable properties model and constant properties model.

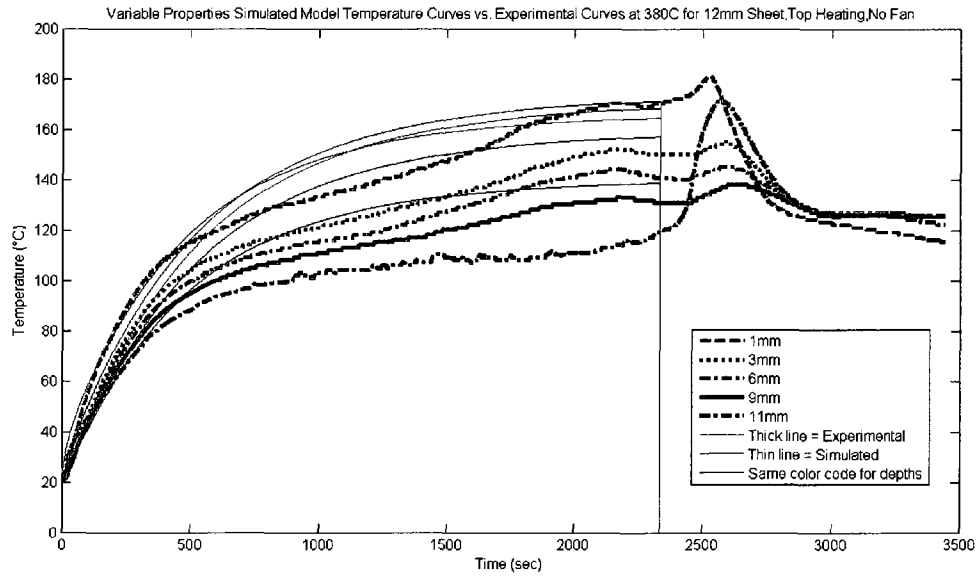


**Figure C-16:** Comparison of simulation model temperature against experimental result.

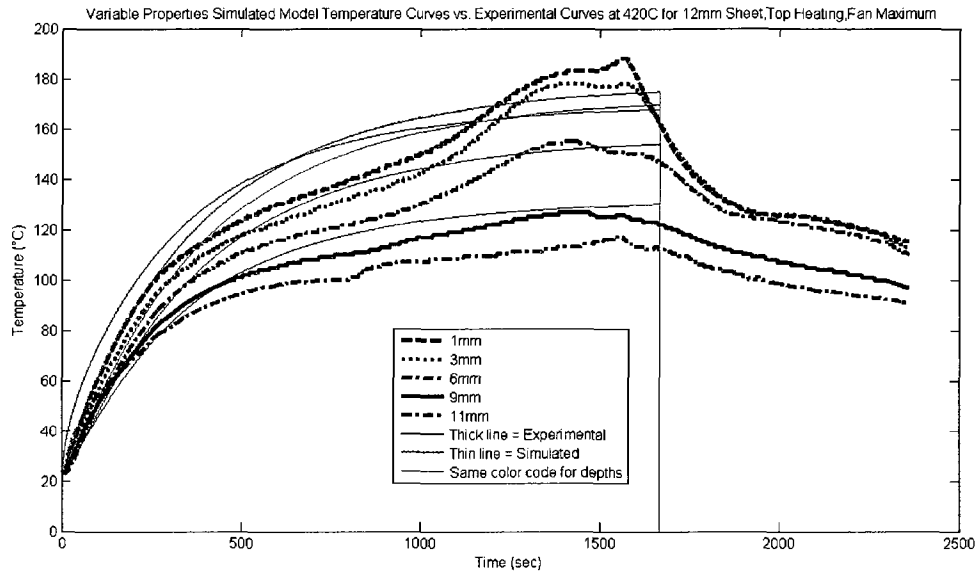


**Figure C-17:** Comparison of simulation model temperature against experimental result.

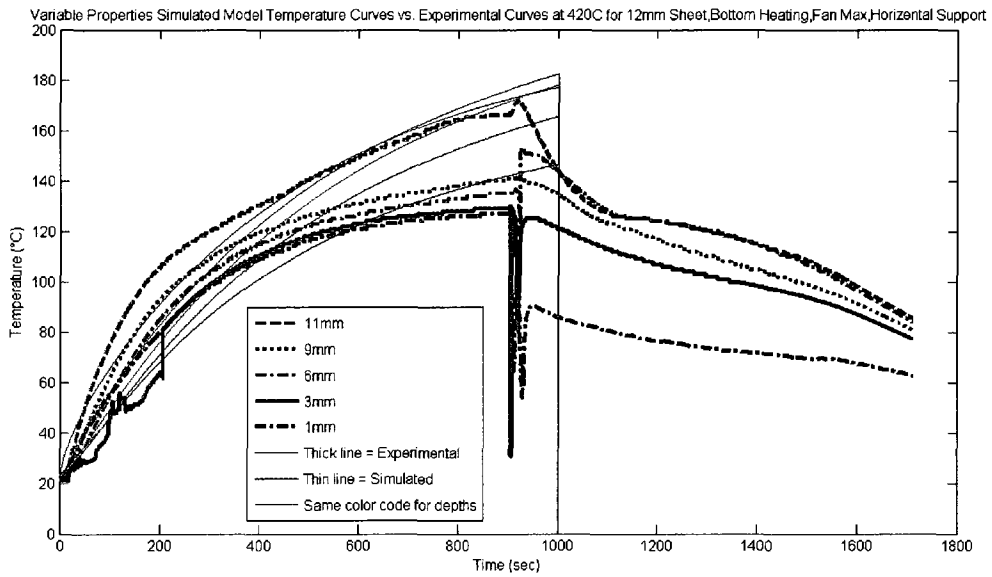


**Figure C-18:** Comparison of simulation model temperature against experimental result.

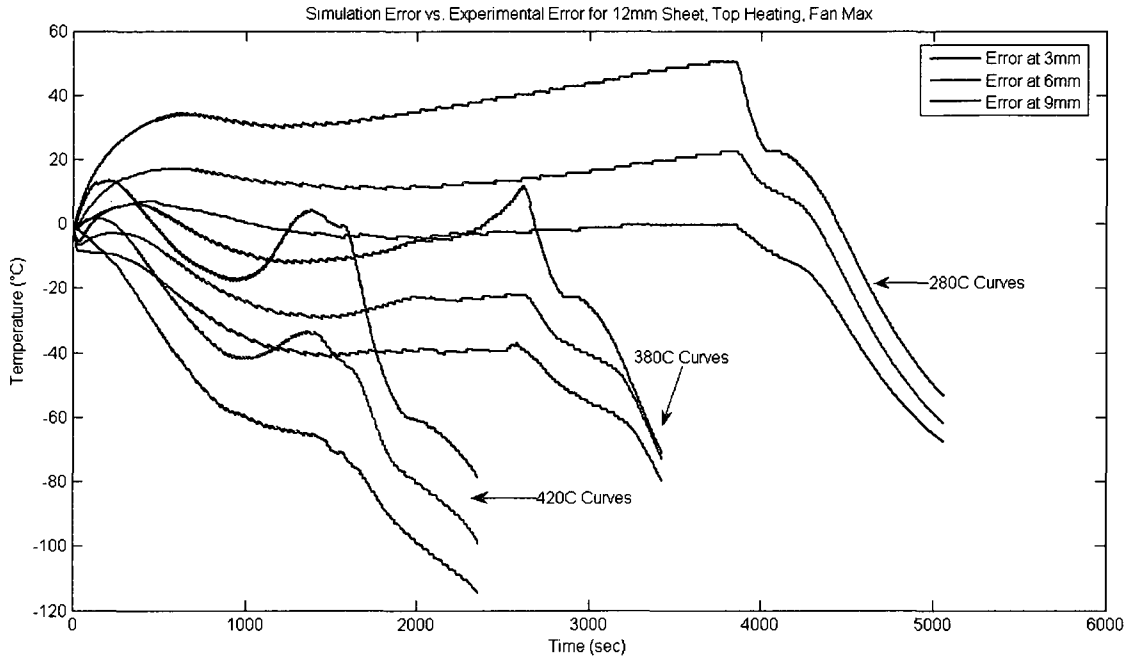


**Figure C-19:** Comparison of simulation model and experimental results at different oven temperatures.

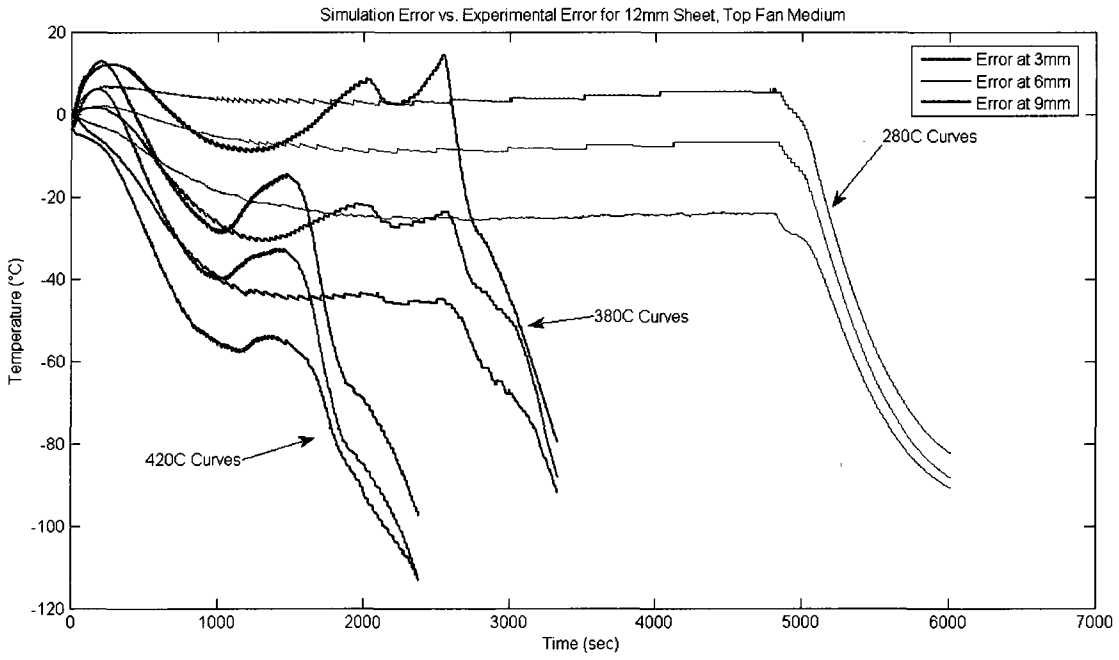


**Figure C- 20:** Comparison of simulation model and experimental results at different. oven temperatures.

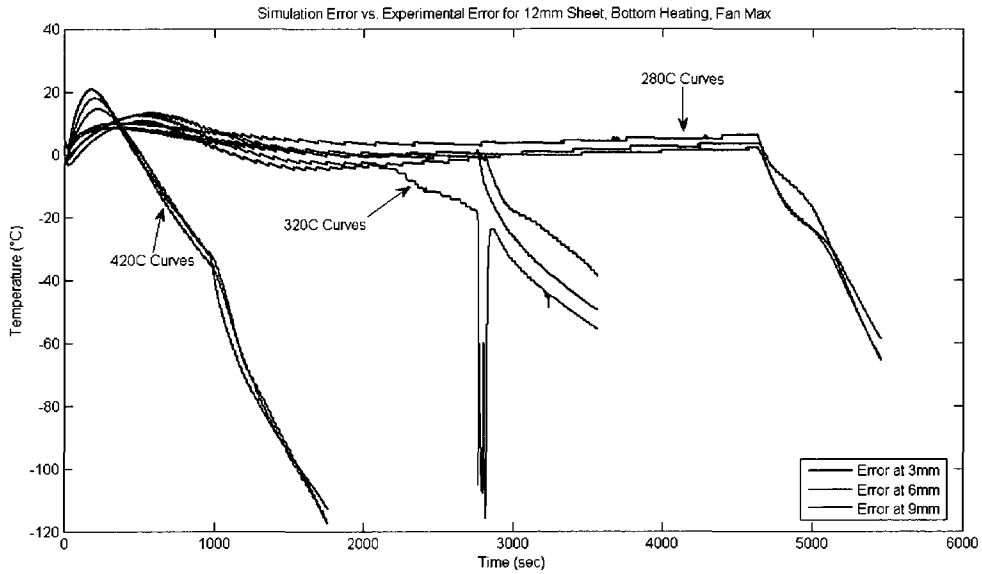


**Figure C-21:** Comparison of simulation model and experimental results at different oven temperatures.

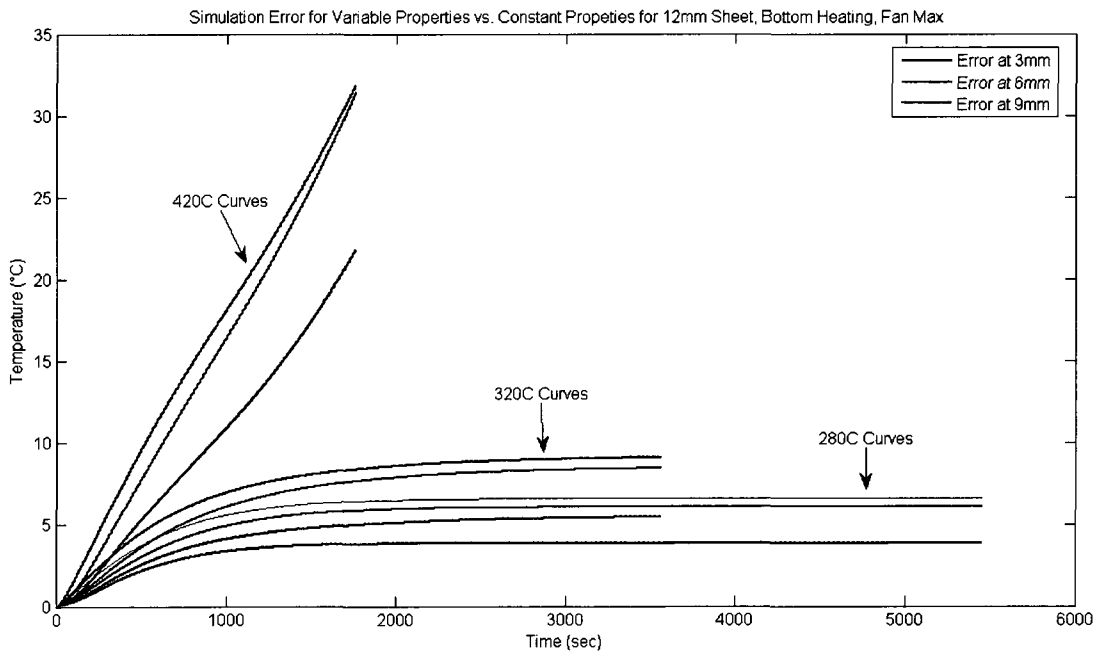


**Figure C-22:** Difference of variable properties model and constant properties model at different oven temperatures.

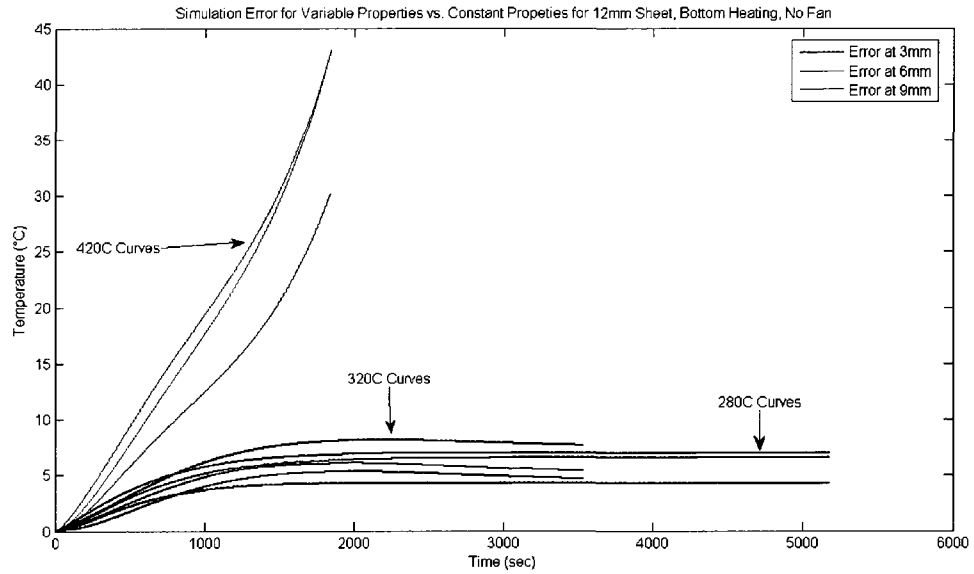


**Figure C-23:** Difference of variable properties model and constant properties model at different oven temperatures.

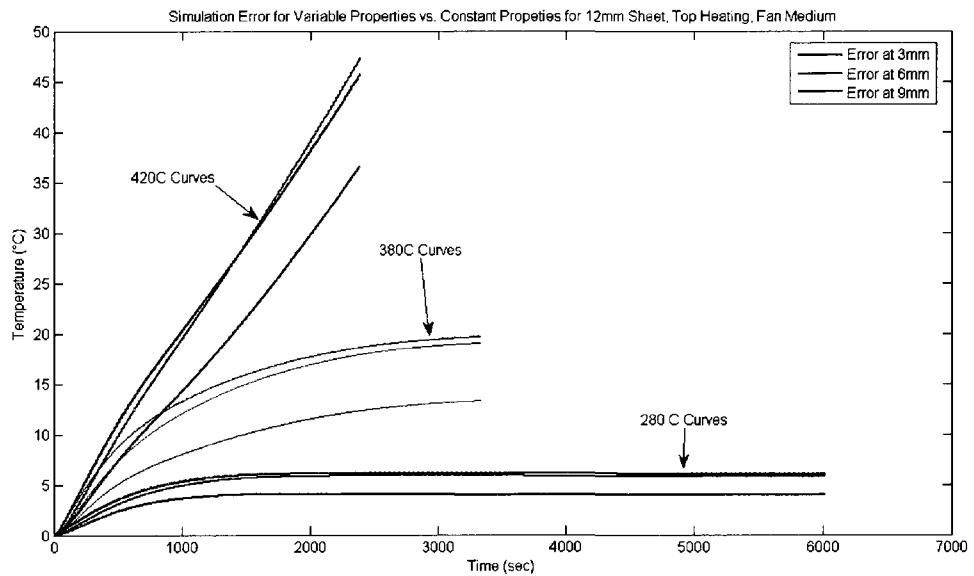


**Figure C-24:** Difference of variable properties model and constant properties model at different oven temperatures.

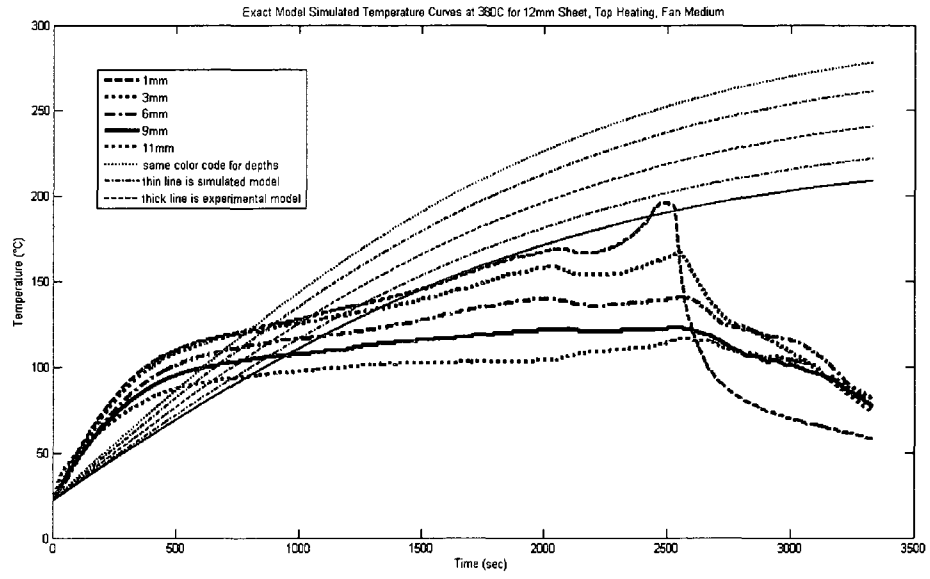


**Figure C-25:** Exact model simulation vs. experimental data.

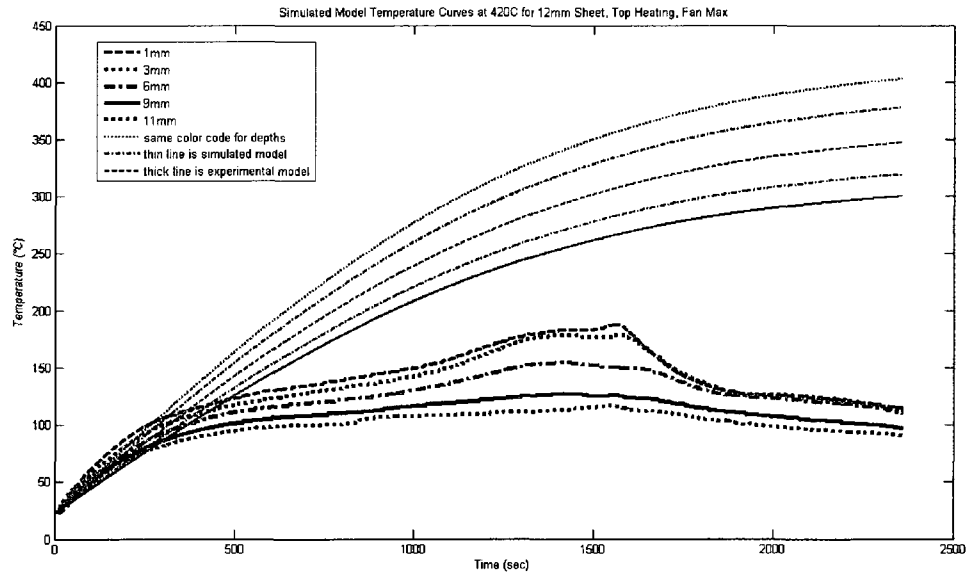


**Figure C- 26:** Exact model simulation vs. experimental data.

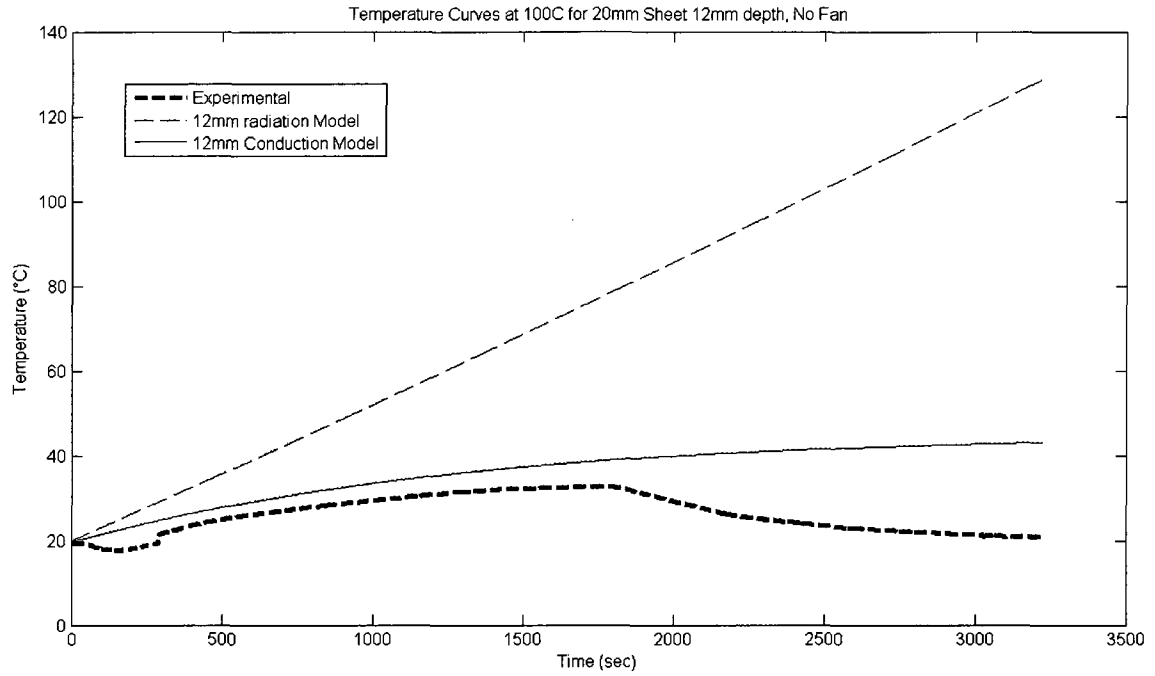


**Figure C-27:** Colored Sheet models simulation vs. experimental data.

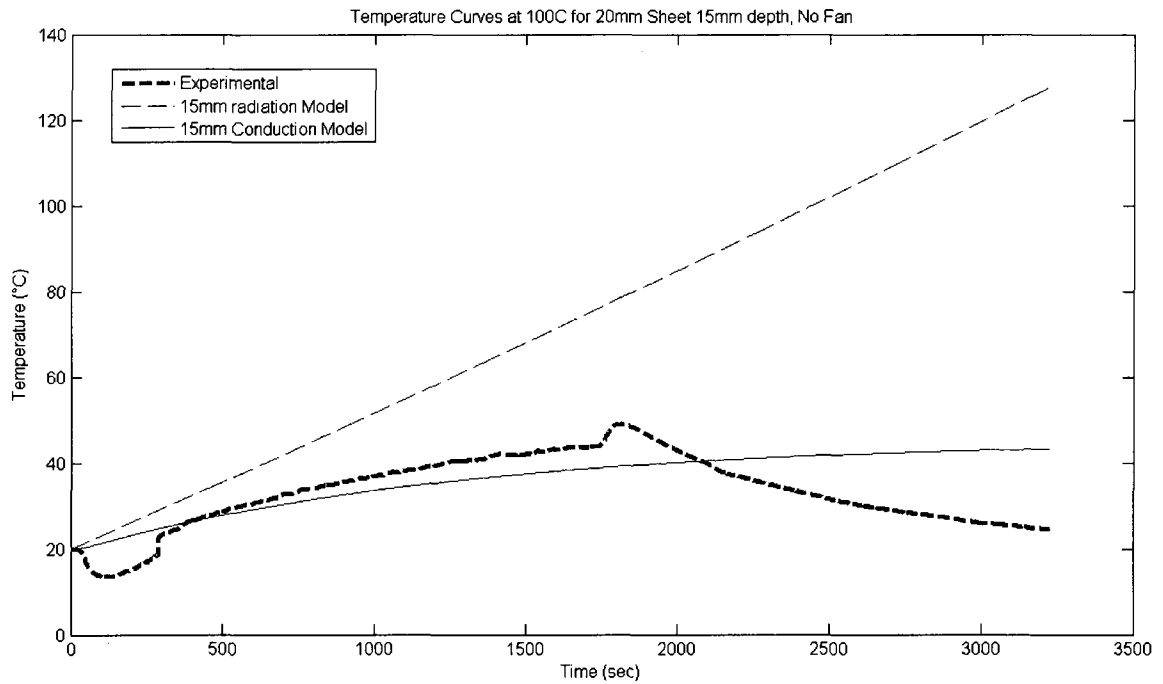


**Figure C-28:** Colored sheet models simulation vs. experimental data.

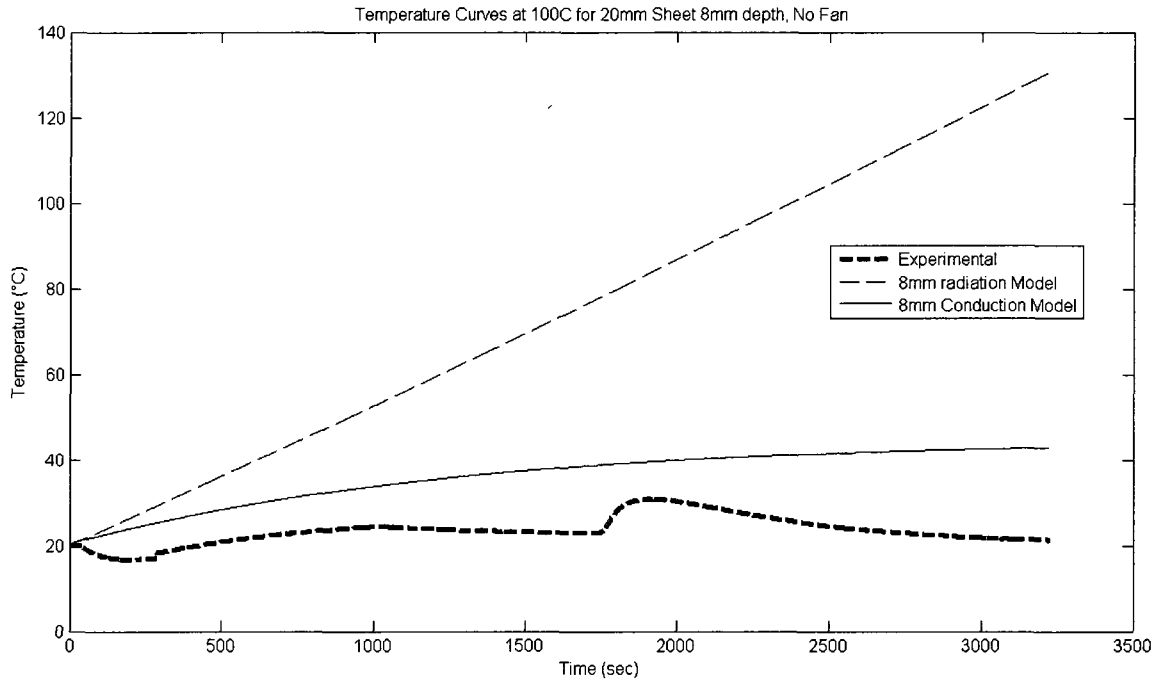


**Figure C-29:** Colored Sheet models simulation vs. experimental data.

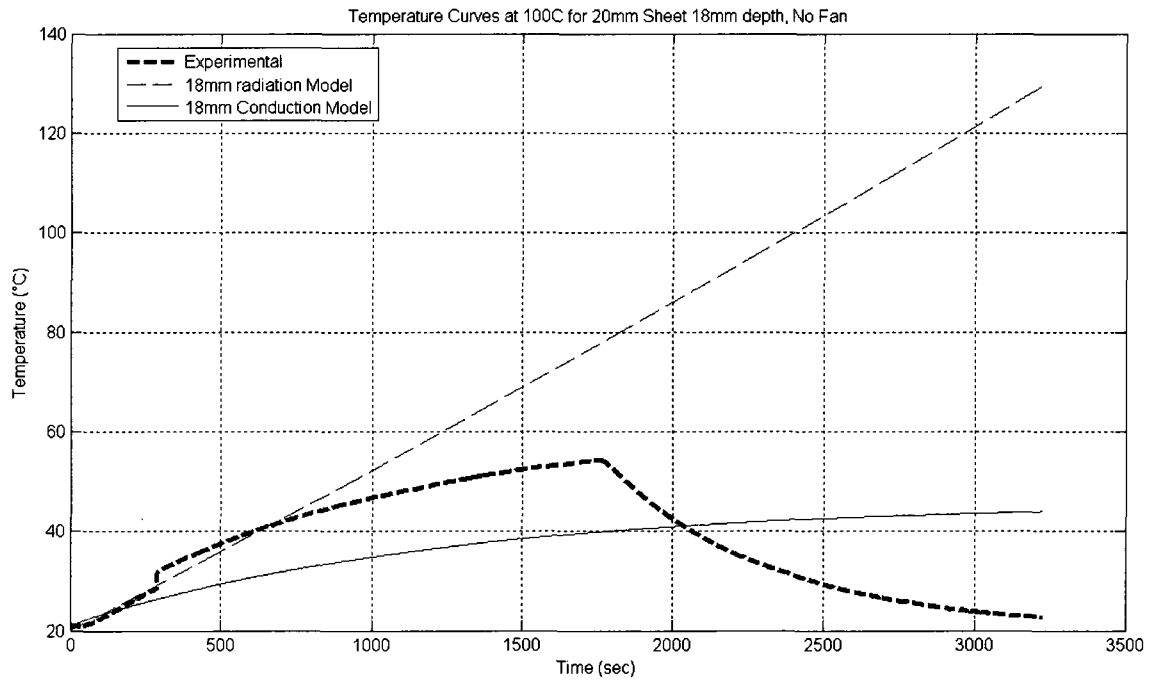


**Figure C-30:** Colored Sheet models simulation vs. experimental data.

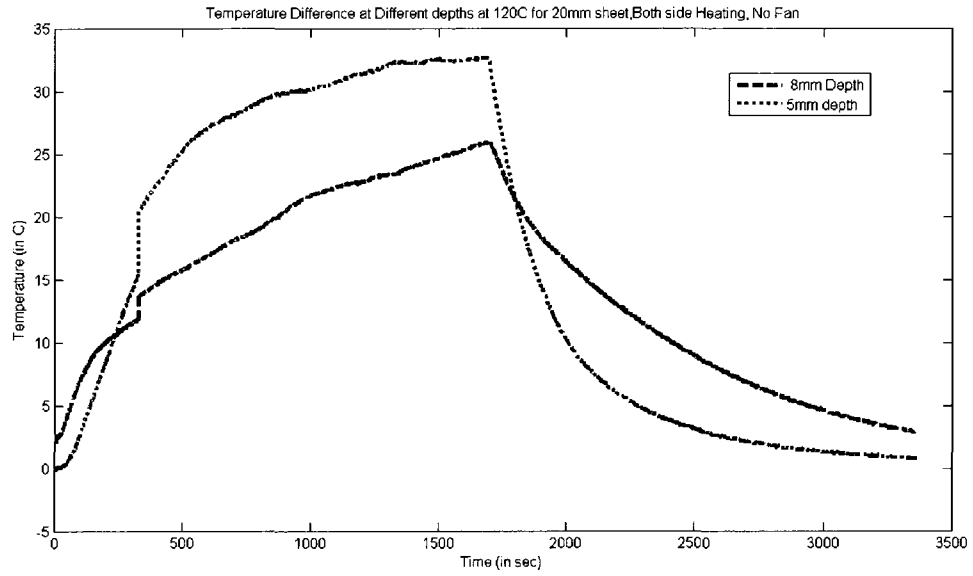


**Figure C- 31:** Temperature difference for 100 °C oven temperature.

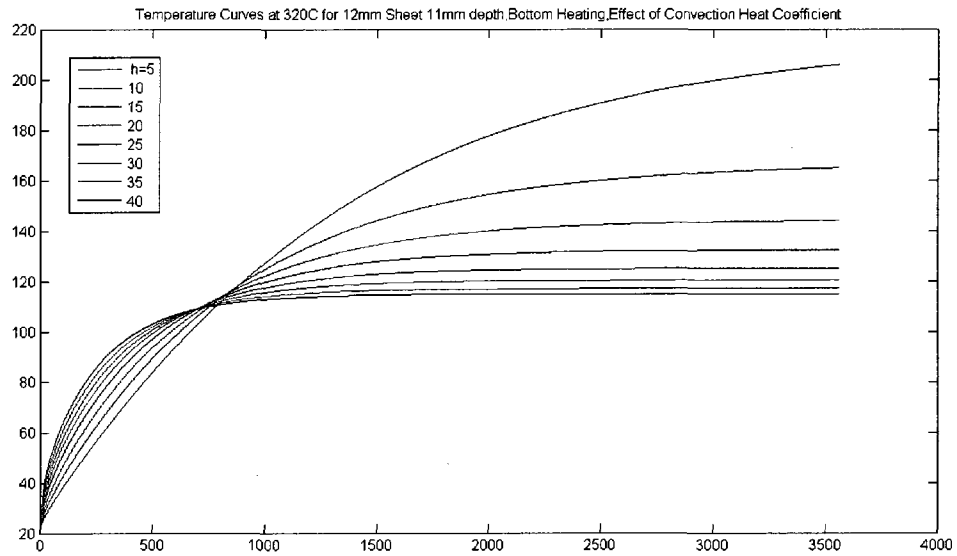


**Figure C-32:** Variation in sheet temperature for different values of convection coefficient

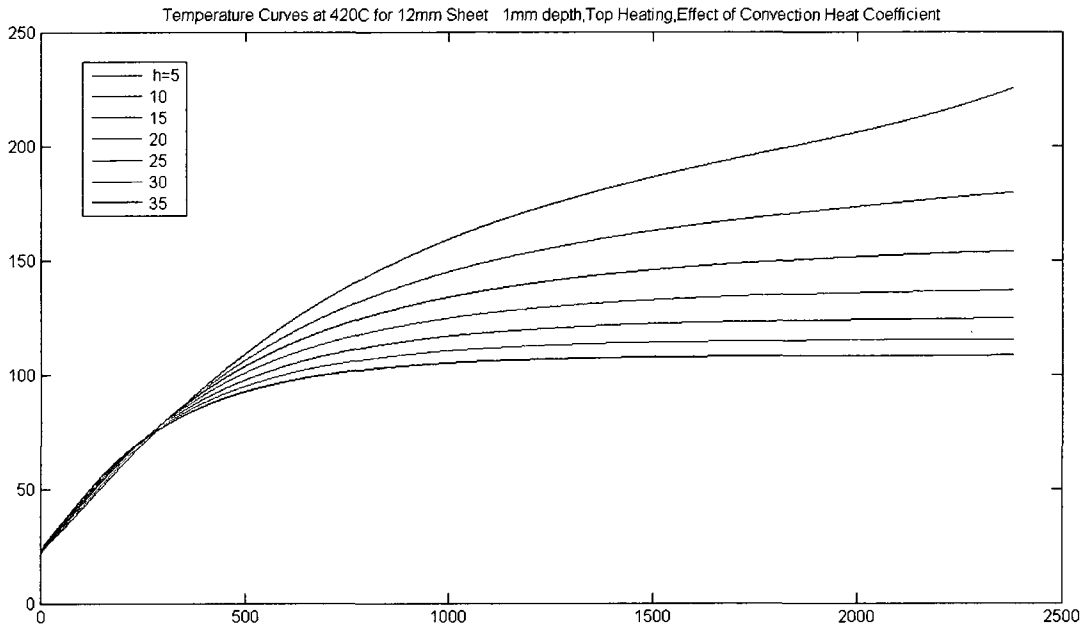


**Figure C-33:** Variation in sheet temperature for different values of convection coefficient.

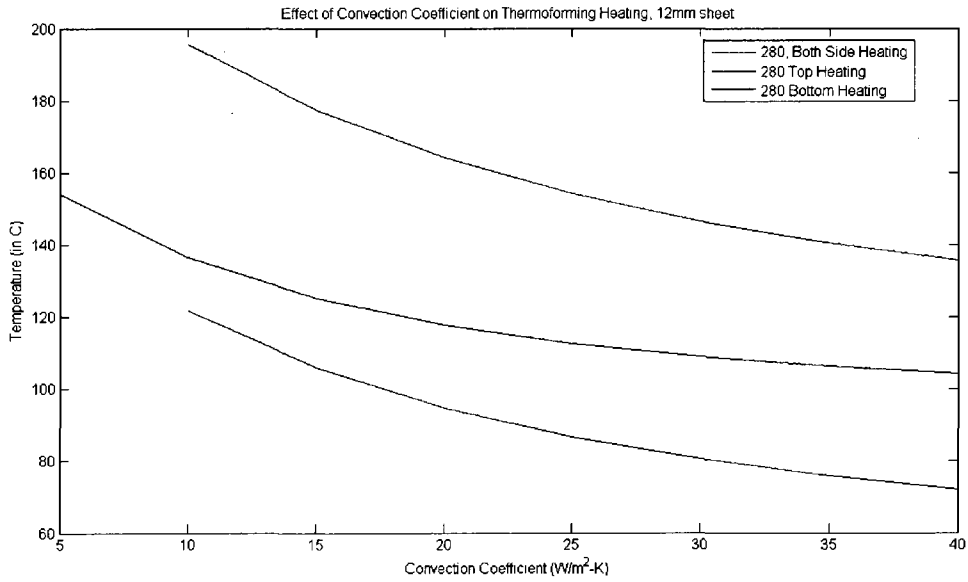


**Figure C-34:** Effect of convection coefficient on sheet temperature for different values of Oven temperatures.

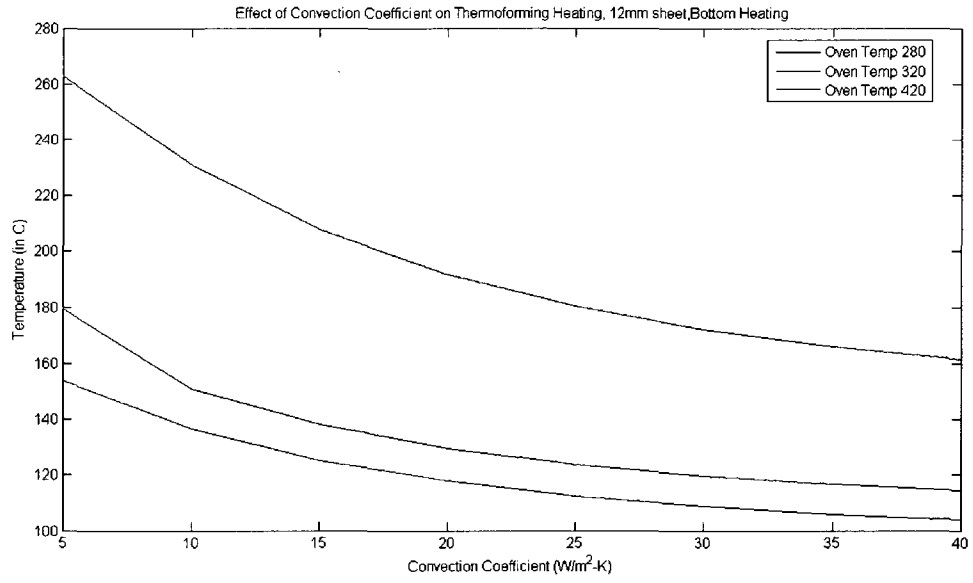


**Figure C-35:** Effect of convection coefficient on sheet temperature for different values of Oven temperatures.